Cape Peninsula
University of Technology

Development of a data collection system for small Unmanned Aerial Vehicles (UAVs) flight

by

YAN ZHOU

Dissertation submitted in partial fulfilment of the requirements for the degree

Master of Technology: Mechanical Engineering

in the Faculty of Engineering

at the Cape Peninsula University of Technology

Supervisor: Mr. Walter. Kohlhofer
Co-supervisor: Prof. Graeme John Oliver
Co-supervisor: Prof. Oscar Philander

Bellville
March 2011

DECLARATION

I, Yan Zhou, declare that the contents of this dissertation represent my own unaided work, and that the dissertation/thesis has not previously been submitted for academic examination towards any qualification. Furthermore, it represents my own opinions and not necessarily those of the Cape Peninsula University of Technology.

Signed **Date**

ABSTRACT

This paper presents the development of a data collection system for a small unmanned Aerial Vehicle (UAV) flight. The following three facets comprise of a UAV system: (1) a UAV aircraft; (2) onboard avionics; and (3) a ground control station subsystem (Taha *et al*., 2010:1). In this project, the UAV aircraft is based on the low-cost autonomous quad-rotator system named "Arducopter Quad", where the onboard avionic system utilizes both an ArduPilot Mega (APM) on-board controller and IMU sensor shield, while the "Mission Planner" software operates as GCS software to gather essential flight data (Xiang & Tian, 2011:176). The approach provides the UAV system structure and both hardware and software with a small UAV data collection system, which is examined throughout the study. And introduce the concept of Arducopter dynamics for better understanding with its flight control.

The study also considers the communication process between the UAV and the ground control station. The radio wave is an important aspect in the UAV data collection system (Austin, 2010:143). The literature review introduced the basis of the radio wave in respect of its travelling speed, and its characteristics of propagation, including how different frequencies will affect radio wave propagation.

The aim of this project was to develop a platform for a small UAV real-time data collection system. The pendulum system was involved to simulate the "Roll" movement of the small UAV, while real-time IMU sensor data was successfully collected at ground control station (GCS), both serial communication and wireless communication, which was applied in the data collection process. The microwave generator interference test proves that the 2.4 GHz XBee module is capable of establishing reliable indoor communication between the APM controller and the GCS.

The work of this project is towards development of additional health monitoring technology to prevent the safety issue of the small UAV. The data collection system can be used as basis for the future research of real-time health monitoring for various small UAVs.

ACKNOWLEDGEMENTS

I wish to thank:

- Mr. Walter. Kohlhofer, my principle supervisor of this research. Guiding me to a significant direction of the research and without his patient guiding the project would not been accomplished.
- Prof. Graeme John Oliver, my co-supervisor of this research. With his help the experimental platform has been established and he showed me some important thoughts of doing this research.
- Prof. Oscar Philander, my co-supervisor. With his achievement in UAV field which help me to get better understanding in UAV telemetry system structure.
- Mrs. Yuan Zhou, my wife. Thanks for her mental support and taking good care of my daily life to help me finish this study.

TABLE OF CONTENTS

LIST OF FIGURES

LIST OF TABLES

GLOSSARY

Abbreviations	Definition/Explanation
2.4 GHz	The frequency used by digital (spread spectrum) radio communication.
APM	ArduPilot Mega is a complete open source autopilot system.
Arduino	An open source embedded processor project.
ArduCopter	Rotary-wing autopilot software for the ArduPilot Mega electronics.
BER	Bit Error Rate
Bluetooth	It is a specification for the use of low-power radio communications in short range.
CLI	Command Line Interface
ESC	Electronic Speed Control. Device to control the motor in an electric aircraft.
EEPROM	Electrically Erasable Programmable Read-Only Memory
FTDI	Future Technology Devices International
GCS	Ground Control Station
I2C	A serial bus, which can connect such as sensor to a microprocessor.
IMU	An inertial measurement unit.
LOS	Line of Sight
LiPo	Lithium Polymer battery. This battery chemistry offers more power and lighter weight the NiMh and NiCad batteries.
Oilpan	ArduPoilt Mega IMU sensor shield. Contains the major on-board sensors (gyros, accelerometers, barometer, etc).
PC	Personal Computer
RAM	Random Access Memory
SCL	Serial Clock
SDA	Serial Data
UAV	Unmanned Aerial Vehicle
WLAN	Wireless Local Area Network
WiFi	A popular technology that allows an electronic device to

	exchange data wirelessly via radio waves.
XBee	It ia a commercial name from Digi International, which is a factor compatible radio modules.
ZigBee	A wireless communication standard, it has longer transmission range than Bluetooth but lower power consumption than WiFi.

CHAPTER ONE
INTRODUCTION

1.1 Introduction

UAV is the acronym for Unmanned Aerial Vehicle, which refers to an ordinary aircraft that can fly without an onboard pilot and is controlled by electronic equipment or flight computer (autopilot), such as radio controlled devices (Bende *et al*., 2008:1373). The aim of this UAV research is to develop a low cost system, which gathers the signals from UAV onboard sensors such as an altimeter, magnetometer, gyros etc. The objectives of this research are to: 1) capture real-time data via an onboard system; 2) send the data to Ground Control Stations (GCS) via a wireless communication system; 3) provide the data to the ground crew to achieve health monitoring.

The research presents methods of flight data collection of UAVs' onboard systems and establishes wireless communication between a UAV onboard system and ground control station. The function of the onboard system is to collect measurement signals, implement real-time monitoring of the UAV's flight status, and to provide support to communicate with the ground control station (Peng *et al*., 2009:2333).

1.2 Background study

Presently, with the development of electronics technology and onboard avionics becoming smaller and smaller, development of a data collection system for small UAVs has become significant research for industrial UAVs. There are three important parts in this research, namely UAV system, data collection system and the wireless transmission process.

1.2.1 UAV system

There are three elements that are required to develop a UAV remote sensing system: (1) a UAV aircraft; (2) onboard avionics; and (3) a ground control station subsystem (Taha *et al*., 2010:1). Figure 1.1 shows an overview of a UAV aircraft system.

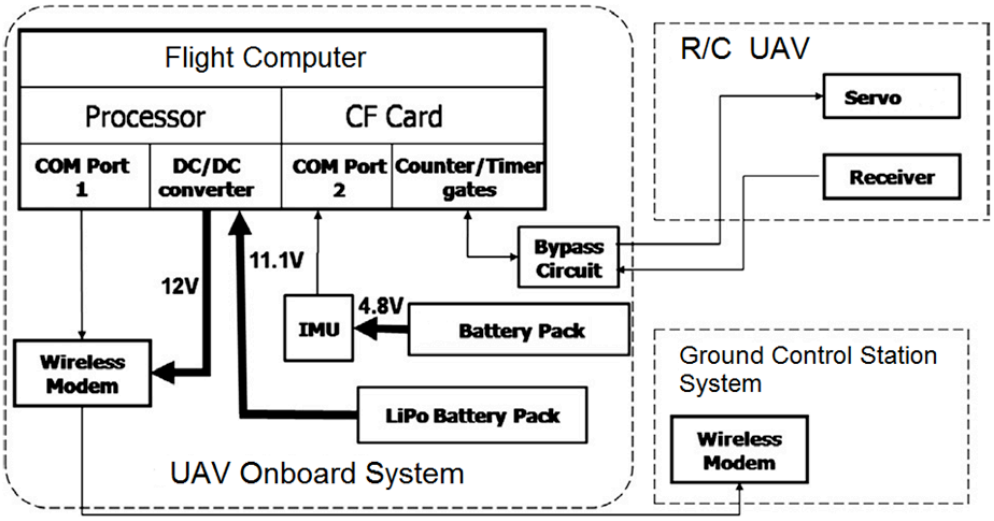

Figure 1. 1: Block diagram representation of working principle of UAV system (Adapted from Taha *et al*., 2010:2)

1.2.2 Data collection system

The data collection system has a high independence for the ground control station because all the sensors for navigation purposes and all flight controls are housed onboard (Xiang & Tian, 2011:174). *"The onboard data collection system is an important role in gathering essential flight data, which contains attitudes, velocities, and angular rates of UAVs and deflections of servo actuators" (*Taha *et al., 2010:2).* A sensor system is mounted on UAVs, which can collect many kinds of data such as chemical, biological, radiological, Pollution, hazel etc.

The ground control station system monitors the flight status of UAVs, and an on board data collection system should provide data transmission utility between the onboard and ground control station (Xiang & Tian, 2011:176). Figure 1.2 shows a model of data flow in the mini-UAV and ground control.

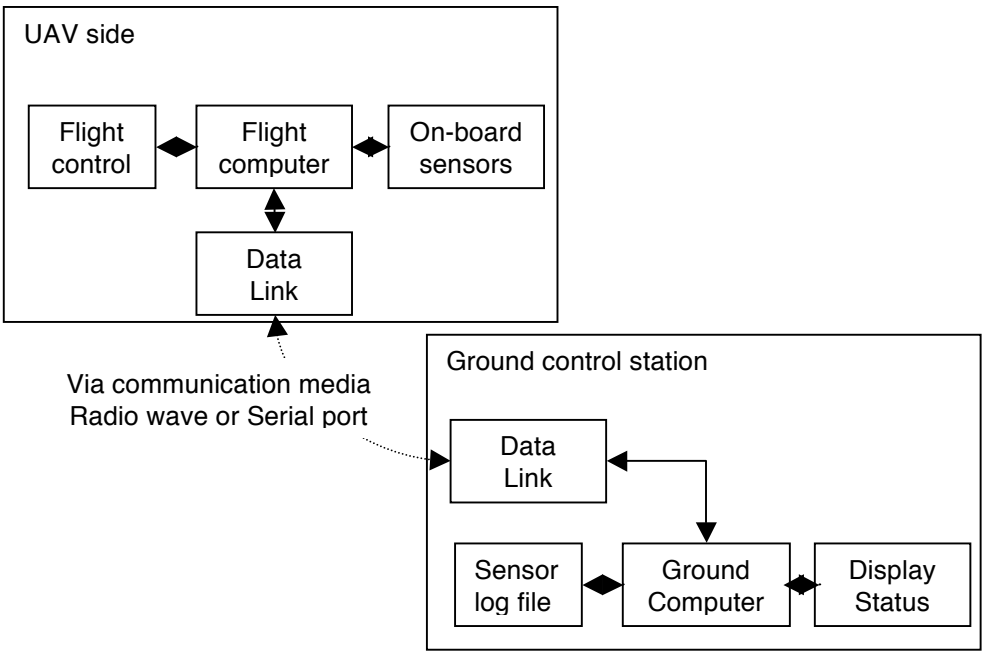

Figure 1. 2: Data flow from UAV side to the ground control station

(Adapted from PÖllänen *et al*., 2008:341)

There are two key systems in the data collection system. The first one is the onboard system, which consists of two major components: the intelligent navigation component and the flight control component (Xiang & Tian, 2011:177). Xiang and Tian (2011:177) state that the responsibilities of the intelligent navigation component and the flight control component are as follows:

- The navigation component: (1) the path planning, which allows the UAV to reach the required waypoints; and (2) the flight condition, which supplies the position and orientation data; and
- The flight control component: (1) to maintain a steady flying platform to achieve the desired operation; and (2) to generate the necessary signal to the onboard servo controller to keep the UAV safe when it is in the air.

The second one is the ground control station system. The ground control station system is an important platform for pilots who need to control UAVs by radio control manually or by sources of data from UAVs. According to Taha *et al*. (2010:4), operation orders are generated and sent to a UAV's onboard system simultaneously and then the UAV's onboard information will transmit to the ground control station system (see Figure 1.3).

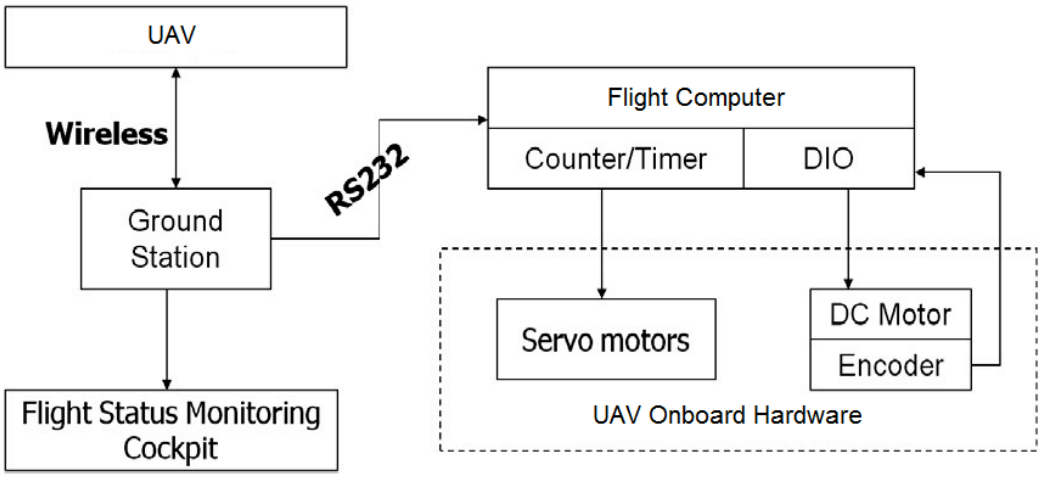

Figure 1. 3: Working principle of the ground control station

(Adapted from Taha *et al*., 2010:4)

Furthermore, Xiang and Tian (2011:178) describe the ground control station system as follows:

- A personal Computer (PC);
- A fully functional wireless modem;
- A flight computer mounted on a UAV; and
- Ground control station software, which allow the user to program waypoint and to monitor the real-time status of a UAV.

The ground control station system includes ground station software, which presents real-time flight conditions by showing the UAVs' position, altitude, and onboard sensors information and so on.

1.2.3 Data collection system for small UAVs

Taha *et al*. (2010:5) state that if you develop a data collection system for small UAVs, you have to consider the weight, dimensions, vibration sensitivity, computational capabilities, power consumption and interfacing capability. Furthermore, the weight and size of the components/hardware for small UAVs should be made as low as possible.

The hardware for a small UAV's data collection system consists of the following parts (Taha *et al*., 2010:5-7):

1) Flight computer system: should be small and light in weight, consume low power, and be compatible with other external devices;

2) Sensor system: the sensor system is related to the output of the UAV's flight status such as attitudes, angular rates or accelerations;
3) Telemetry system: in general, the telemetry system is a pair of wireless modems for data collection purposes. To make sure there is communication between the UAV and the ground control station, the first wireless modem connects with the UAV's onboard system and the flight computer, while the other one should be installed at ground control station system;
4) Power system requirements: refer to power consumption and the range of input voltage of the UAV's onboard device; and
5) Bypass circuit system: the main purpose of this system is to build up a circuit with the function of switching between manual control and automatic control of UAVs.

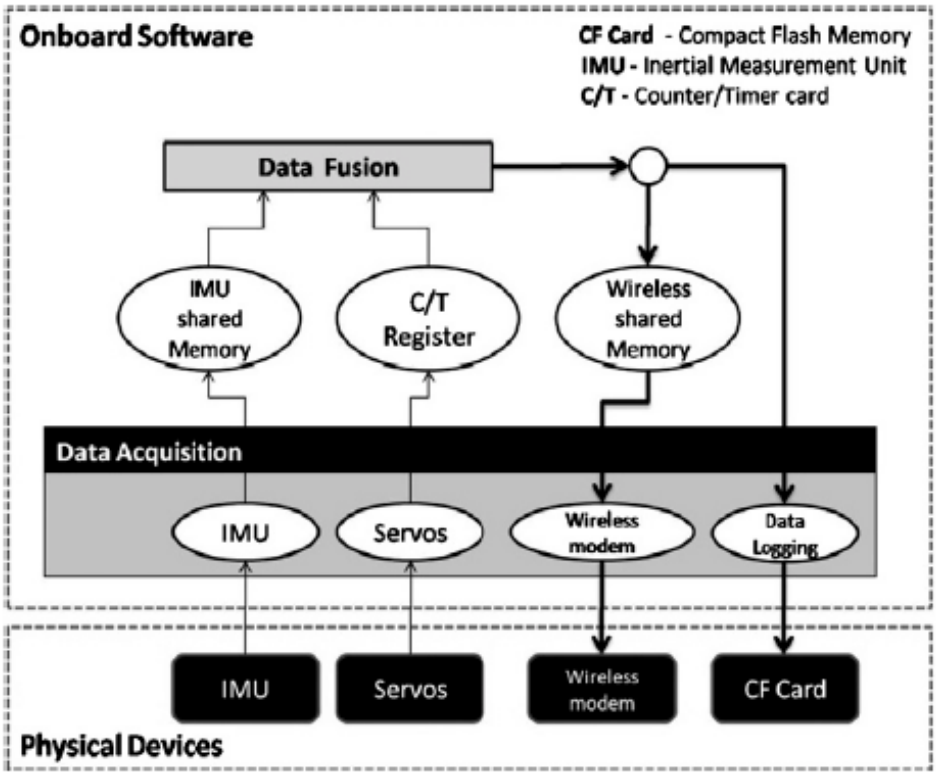

Figure 1. 4: **Architecture of the onboard system of the UAVs**

(Taha *et al.*, 2010:8)

The current research is to investigate an onboard system to collect signals from onboard sensors and to transfer those signals to the ground control station or remote radio controller, which has the ability to read and record data to analyse it.

Both UAV-related hardware and software will be developed in this research, which covers the following (Taha *et al.*, 2010:1):

- Integrated hardware should exhibit compact structure;

- The onboard system should be light weight and have low power consumption; and
- The software should integrate high-level functionalities to allow enough I/O tasks and to influence the onboard hardware in real time.

During the in-flight test, all sensor signals are carried out by the data collection system, the UAVs are operated by a pilot via a radio controlled (R/C) unit and the onboard system records all the UAV's state inputs (joystick inputs from transmitter) and outputs. Taha *et al*. (2010:2) explain inputs and outputs as the following:

- The inputs include the signals to command lateral flapping, longitudinal flapping, heave and yaw of the UAVs; and
- The outputs include the UAV's body velocities in x, y, z directions, angular rates in three axes and Euler angles.

1.3 The research problem

The research problem may be summarized as follows:

- Whether the data collection system is able to collect data from small UAVs:
- Can the data collection system collect accurate data from small UAVs for achieving health monitoring? and
- How data should be collected.

1.4 Research question, sub-questions and objectives

From the research problem, a research question can be concluded as: can a data collection system be developed for small UAVs and how can we develop a data collection system for small UAVs? Thus, there are three sub-questions to assist the research to solve the research question:

1) How does one establish an onboard system for a small UAV flight?
2) Which onboard software should be utilized for flight data collection?
3) How does one communicate between a UAV and the ground station?

Furthermore, the objectives of this research are to:

- Understand the importance of a data collection system for small UAV flight;
- Develop a healthy monitoring system for small UAV flight; and
- Disseminate the results to academics and practitioners.

1.5 Delineation of the research

This research presents the development of data collection for small UAVs for both hardware and software. The end-user will be able to read and record flight status data from ground the control station from a Laptop monitor.

1.6 Research methodology

This is an experimental research project, which should investigate suitable equipment to accomplish the objectives. There are some procedures which should be done as follows:

1) The fight status data gathering process: use six degrees of freedom Inertial Measurement Units (IMUs) with 3 rates sensor gyros and 3 accelerometers. IMUs contain Micro Electro Mechanical Systems (MEMS) gyros and accelerometers, and all the signal measurement electronics are necessary to perform accurately with angular rates of up to +/-300°/s and accelerations up to +/-10g;
2) In flight testing process, to establish the communication between the UAV's onboard flight computer and ground station laptop via hard line connection, which is able to read and record the correct real-time flight data from the ground station laptop: use IMU Demo Test Board to provide a simple PC interface. The board, which comes with PC test software and RS232 cable will display all the output data, and allow selection between different data-frame frequencies and demonstrations. It applies a simplified Attitude/ Heading Reference System); and
3) Once the hard line communication is successful, the real-time wireless communication will apply to the data transmission process, which has the same ability as a hard line connection: use a wireless modem to implement serial data transfer; it operates on a 2.4 GHz Industrial Scientific and Medical (ISM) radio band and serial interface RS232. But there is a RS232 Transceiver to connect with IMUs and the wireless modem, and the RS232 Transceiver is an interface of communication.

1.7 Contribution of the research

Certain objectives should be achieved by this research: 1) the hardware component architecture of the UAV's onboard system should be completed; 2) should discuss the ground control station software scope to display real-time flight data from laptop; and 3) the ground control station should perform a wide range of wireless communication between transmitter and receiver.

After establishing this data collection system, it will be possible to collect more data from another onboard sensor system to provide a variety of information for other fields like mapping, navigation, fire situation monitoring etc.

1.8 Intended program of study

Chapter Two reviews the UAV system, UAV hardware components and UAV ground station software. Chapter Three covers communication literature and also examines data collection methods, and evaluates data collection for UAVs in general.

Chapter Four explains in detail the design of the experimental research approach, while Chapter Five presents and analyses the experimental results, which were collected from small UAVs. Finally, Chapter Six presents and draws conclusions based on the analysis and results.

CHAPTER TWO
MATERIAL AND METHODS

2.1 Background of Unmanned Aerial Vehicles

The development of Unmanned Aerial Vehicles (UAVs) began in the 1950s for military purposes. During the Cold War, many countries conducted research to produce UAVs to adapt to reconnaissance and surveillance (Bendea *et al*., 2008:1373-1374).

Recently, Unmanned Aerial Vehicles (UAVs) became more and more popular than in previous years because of various reasons, for instance, it became widely used in civil and military applications (Paw & Balas, 2010:1).

Certain advantages of UAVs include typically low costs, light mass and low airspeed, which suited information collection purposes. UAVs are also able to fly unnoticed and below the cloud's canopy, which can be accomplished with larger, higher altitude aircrafts and satellites (Xiang & Tian, 2011:174). In some situations UAVs can be handled more easily, safely, cheaply, and efficiently than manned aircraft, since autonomous UAV's do not tire and never lose concentration in the sense of manoeuvring, while this happens naturally with humans (Tariq & Gary, 2003: 14).

According to Peng *et al*. (2009:2333), UAVs can operate in dangerous environments because there is no onboard pilot to control it. Therefore, the above authors believe that this is a huge benefit which reduces risks that human pilots take, while UAVs do the same job as a normal aircraft in terms of manoeuvrability and versatility.

UAVs can fly without onboard pilots, and merely require electronic equipment to control it from the ground. Bendea *et al* (2008:1373) state that the following are advantages of UAV:

- Flight performance. UAVs can manipulate within a wide range of operational altitudes from 100 to over 30,000 m, and the flight endurance is from 1- 48 hours (see Table 2.1). The consequence is that a UAV has an ability to carry out different monitoring facilities; and
- Inexpensiveness. Due to the UAV's design which has variable dimensions, it has a relatively reduced weight frame, and does not require an onboard pilot. Hence, UAVs operate at lower costs than traditional aircrafts.

Table 2. 1: UAV classification – Tactic Group (UAV association)

UAV Categories	Acronym	Range (km)	Climb rate (m)	Endurance (hours)	Mass (kg)
Tactic					
Micro	μ (Micro)	< 10	250	1	<5
Mini	Mini	< 10	150 to 300	< 2	150
Close Range	CR	10 to 30	3000	2 to 4	150
Short Range	SR	30 to 70	3000	3 to 6	200
Medium Range	MR	70 to 200	5000	6 to 10	1250
Medium Range Endurance	MRE	> 500	8000	10 to 18	1250
Low Altitude Deep Penetration	LADP	> 250	50 to 9000	0.5 to 1	350
Low Altitude Deep Endurance	LALE	> 500	3000	> 24	< 30
Medium Altitude Long Endurance	MALE	> 500	14000	24 to 48	1500

(Bendea *et al*., 2008:1373)

UAVs can be operated in complex environments to accomplish tasks such as searches, rescue and emergency disaster responses. But, full scale UAVs require a standard size runway in order to take off and land, and also require a large mobile command station with several operators to control it. Small UAVs can launch almost anywhere, even from your hand, with a single laptop computer or PDA device. Thus, small UAV platforms are relatively safe compared to full scale UAVs. Small UAVs significantly reduce the cost of damage occurring owing to human error or collisions with obstacles (Frew, 2004: 2). Therefore, there is a higher demand for small or mini-size UAV systems (Paw & Balas, 2010:1). The reason is that it is small in size, portability, low costs, and can offer inexpensive, expendable platforms for surveillance and data collection in conditions where large aerial vehicles cannot operate easily. The range of small UAVs is between 15 cm and 1m in size (FU, *et al*., 2008: 614). It is suitable for traffic road monitoring, reconnaissance, searches and mapping rescue positions etc (Taha, *et al*., 2010:1).

2.1.1 Types of UAVs

In addition, compared to fixed-wing UAVs, the helicopter vision with its rotary-wing has better mobility in danger zones, particularly when used for searches and rescue missions. Because of the rotary-wing, UAVs have abilities such as hovering, perpendicularly takeoff and can land in limited launching sites, while still being flexible. Therefore, development of the UAV helicopter has become an increasingly popular research aspect in both academic and industrial fields (Taha *et al*., 2010:1). This is an exclusive ability in rescue missions and aids goods transportation. In effect, the fixed-wing aircraft does not have the ability to accomplish these tasks. As a consequence of most disaster areas, there are problems such as traffic and

communication cut-outs, which do not allow rescuers easy access to execute their tasks (Kowalenko, 2001).

Conversely, searches are performed traditionally on the ground, which means that rescuers take longer to assist those in needs in chaotic and vast environments, while time is always an important factor, which is required to save people's lives. Any kind of small rotary-wing UAVs can easily face such challenges and send first-hand data back to help other rescuers so that they can choose the best way to engage in a rescue mission successfully.

2.2 UAV system architecture

A data collection system for small UAVs consist of an on-board and ground control station (see Figure 2.1), while all sensors for real-time monitoring flight status purposes, and all flight controls are on-board; all flight data is obtained at the ground control station (Xiang & Tian 2011:176).

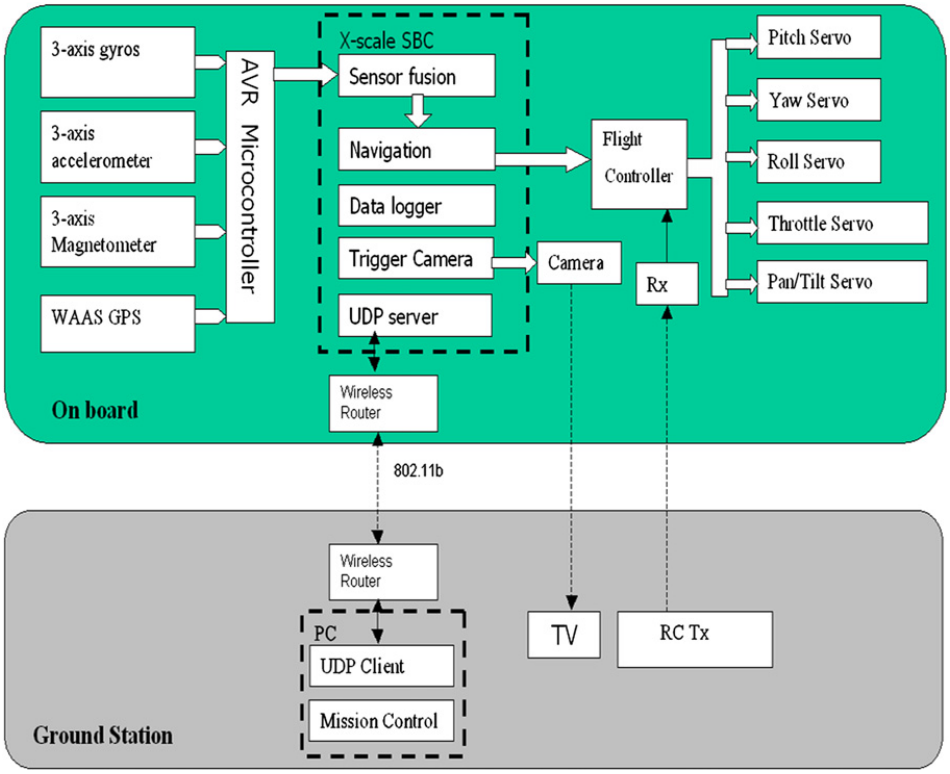

Figure 2. 1: UAV system scheme

(Xiang & Tian 2011:177)

The on-board systems include two major components, namely the intelligent navigation component and the flight control component. The functions of each component are as follows (Xiang & Tian 2011:177):

- The navigation component is for path planning purposes, as well as to allow the UAV to reach the required waypoints. Conversely, the flight status is detected by navigation components such as position and orientation.
- The flight control component is used to maintain stable flying conditions, which allows the navigation system to accomplish the desired position. It generates the control signal to the UAV's on-board servos to keep the UAV safe while it is in the air.

2.3 Hardware components

Xiang & Tian (2011: 177) also mention that the UAV hardware consists of an RC aircraft, camera, an IMU, a GPS, a single board computer, a flight controller, pulse-width modulation, a wireless router and a video transmitter (see Figure 2.2). Once this hardware is installed on a UAV, it is possible to collect a variety of data from UAV.

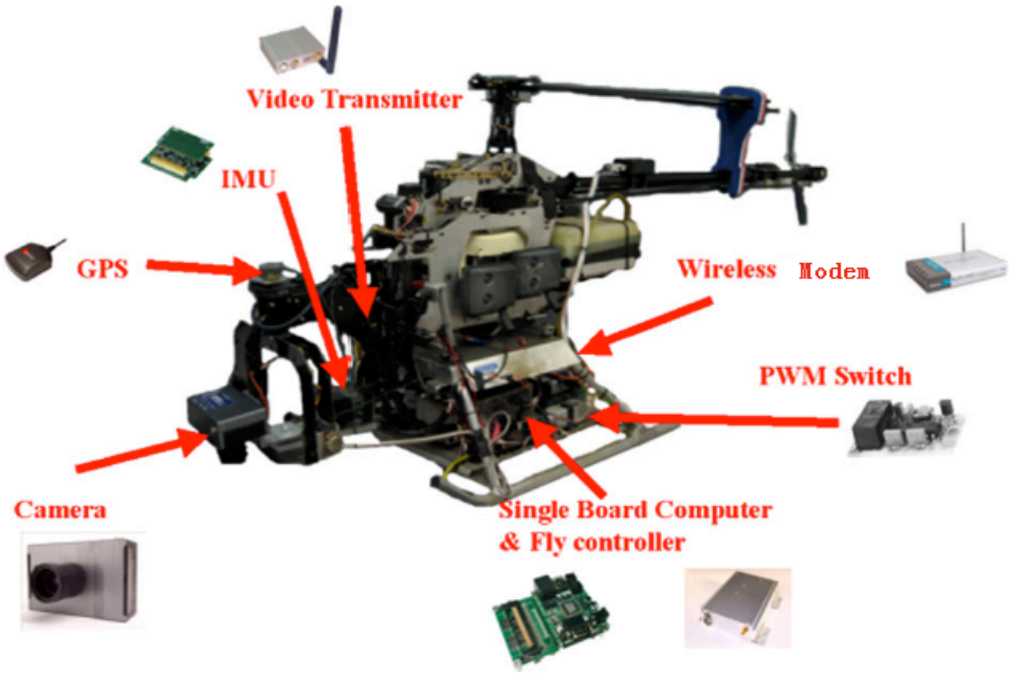

Figure 2. 2: Autonomous sensing image collection system for helicopters

(Adapted from Xiang & Tian 2011:178)

Taha *et al*. (2010:5) point out that on-board hardware components are chosen along with the following considerations:

- The designed on-board system should consume low amounts of electrical energy, since low electrical consumption is equivalent to a light battery pack, and will increase the duration of the operation of the avionic system; and
- All the hardware components should be small in size, whilst considering vibration sensitivity, interfacing capability, computational capability and so on.

According to Taha *et al*. (2010:5) (see Figure 1.1):

- The Lipo battery pack is joined with the DC/DC converter and supplies 12V DC to give every component power of the flight computer;
- The DC/DC converter outputs 12V DC to drive the wireless modem;
- The COM port 2 and Counter/Timer will collect data from the servo actuator deflection and IMU outputs;
- The logged data will be saved on the Compact Flash card, while the data will be received at the ground control station via the wireless modem.

2.3.1 Flight computer system

The flight computer is the core of the UAV on-board system, which should be small and light in weight, and easily interfaced with another subordinate device. Taha *et al*. (2010:5) state that the flight computer system consists of a single computer board, a Counter/Timer card and a DC-DC converter. The authors explain the functions of the computer board, Counter/Timer and DC-DC converter as follows:

- The function of the single computer board is that it contributes enough input and output port for all the sensor units, wireless modem and actuators;
- The function of the Counter/Timer card is to capture the duty cycle of Pulse-Width Modulation (PWM) signals, which come from R/C receiver, and will also breed PWM signals to control the deflections of the servo actuator. The flight computer system plays an important role towards accomplishing autonomous control; and
- The function of the DC/DC converter is to regulate the input power from the battery and supply power to the flight computer.

The flight computer is a central controller for all on-board sensor fusion, for instance, navigation, data logger, camera trigger and communication with the ground control station (Xiang & Tian 2011:177). Those tasks mentioned as above cannot be done without flight the computer.

2.3.2 Sensor system

The major sensors that are used for small UAVs are small, light and have low power consumption. For instance, the UAV's altitude, angular rates or acceleration can be detected by a sensor system, which is designed to use Micro-electro mechanical system (MEMS) technology (Taha *et al.,* 2010:6).

Taha et al. (2010:6) point out the following components, which consist of a sensor system:

- A triaxial gyro (to track dynamic orientation);
- A triaxial accelerometer (along with a triaxial magnetometer to track static orientation);
- A triaxial magnetometer (along with a triaxial accelerometer to track static orientation);
- A temperature sensor (to detect the temperature of a battery); and
- An embedded microprocessor (to process the response of static and dynamic environment data, and to output the calculated data to the host system through a serial port).

2.3.3 Telemetry system

The telemetry systems comprises a pair of wireless modems, which should be compactly designed, light in weight and consume little power (Taha *et al*., 2010:6).

Taha *et al*. (2010:6) assert that "*no configuration is necessary for operating the wireless modem, simply feed the data into one of the pair of modems, then the data is sent out from the other end of the wireless link*". Consequently, there are two wireless modems: one is installed in the UAV and connected to the UAV's flight computer, while the other is installed at the ground control station connected to the ground computer via serial connection.

2.3.4 Power system

The power system is based on power consumption and accommodates a range of input voltage for all the on-board devices. The Lithium – polymer battery is one of the options for a power system because of its light weight, higher power capacity and better life cycle regression rate compared with Ni – Cd, Ni – MH and Li – ion batteries (Taha *et al*., 2010:6).

2.3.5 Bypass circuit

A bypass circuit, which is shown below in Figure 2.3, is required because if the onboard system fails, the bypass circuit will cut the transmission signal between the R/C receiver and autonomous control mode, which guarantees that all the PWM signals from the ground station will directly influence the servos (Taha *et al*., 2010:7).

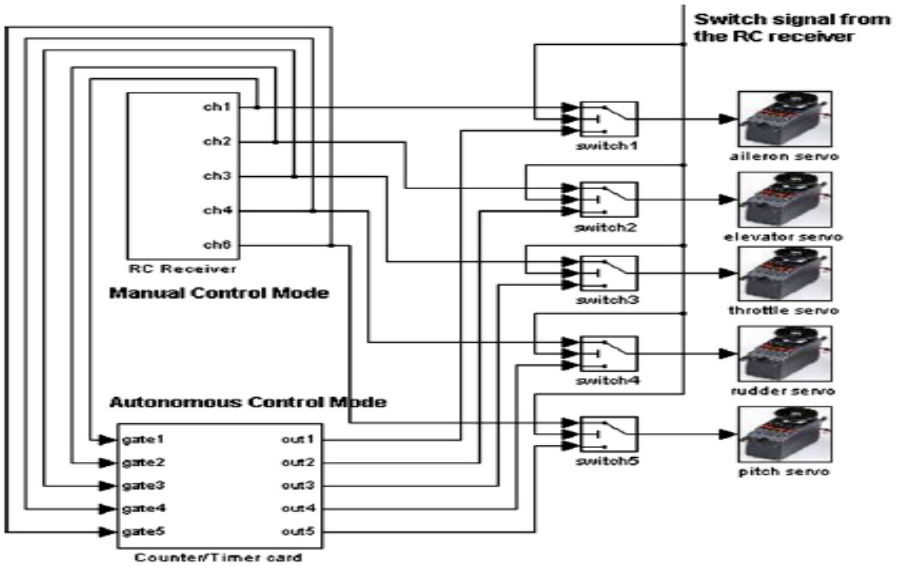

Figure 2. 3: Block diagram of the bypass circuit system

(Taha *et al*., 2010:8)

2.4 Software system

The software comprises two parts, namely an onboard software (See Figure 2.4) system and a ground station (See Figure 2.5). The structure of the software (as shown in Figure 2.6), was designed so that each major component operates as a separate process, under autonomous control, whilst the data hub, onboard sensors, autopilot interface and ground station interface operate all the time (Frew, 2004:6).

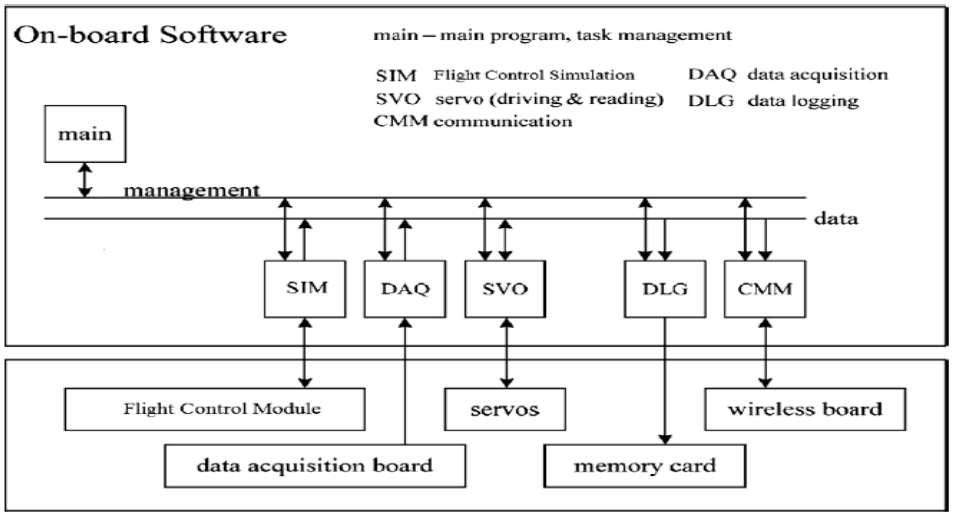

Figure 2. 4: The structure of the onboard software system

(Cai *et al*., 2009:1060)

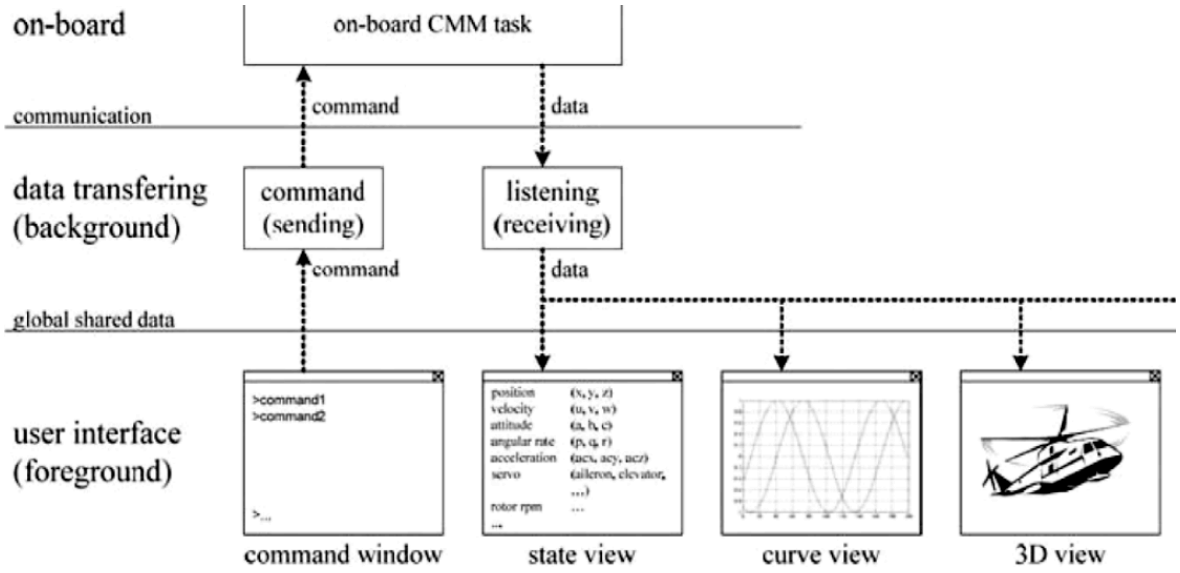

Figure 2. 5: The structure of the ground station software system

(Cai *et al*., 2009:1061)

Taha *et al*. (2010:7-9) also mention that "*the onboard software periodically runs separate processes, which are assigned to the corresponding I/O tasks in order to collect flight data once the data is available, and creates four threads to execute the corresponding tasks for the IMU, servo signal, data logging and wireless communication* ".

And at ground station data from the onboard sensors and autopilot system (for autonomous control) is stored in the shared memory and is later fed into the wireless modem, which is installed at the UAV's onboard system. Hence, the data sets can be received at ground station by wireless modem (Taha *et al*., 2010:7).

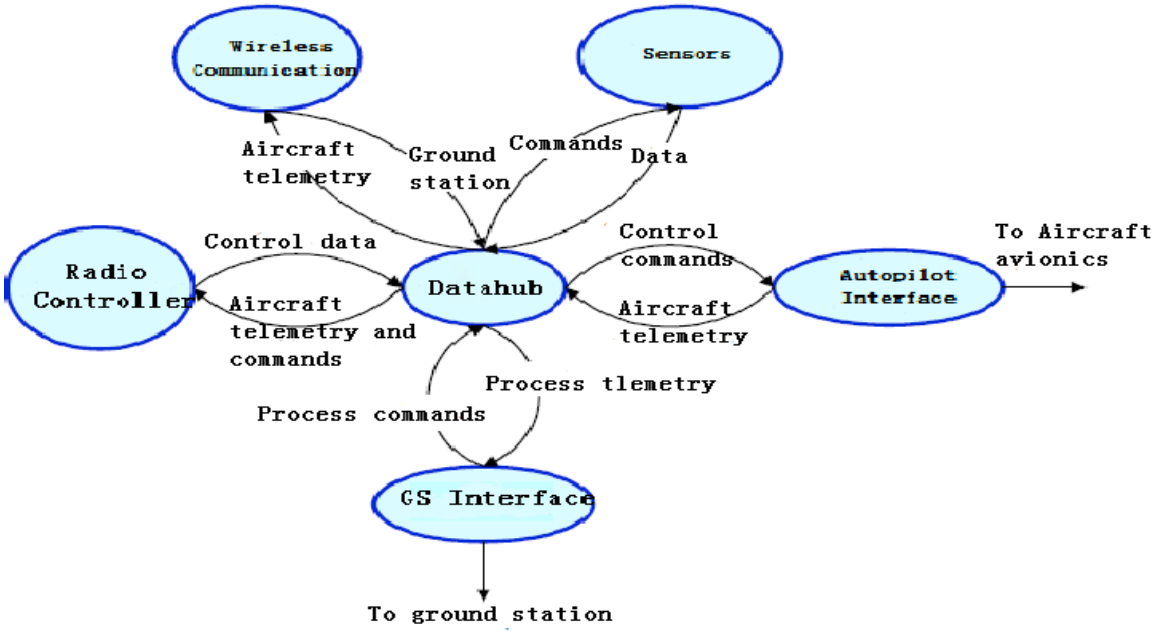

Figure 2. 6: Software architecture

(Adapted from Frew, 2004:5)

2.5 Onboard avionics system

The IMU and GPS sensors are played important role in the onboard avionics system, which provides angular rates, linear accelerations, magnetic fields, airspeed, barometric altitude, GPS positions and velocities measurement data (Paw & Balas, 2010:2).

Paw and Balas (2010:2) state that all sensor data is captured by the flight computer. In the mean time, the flight computer outputs telemetry data via wireless modem, hence, ground control station will be able to receive this telemetry data by wireless modem where installed at ground station. The structure of the avionics system is shown in Figure 2.7.

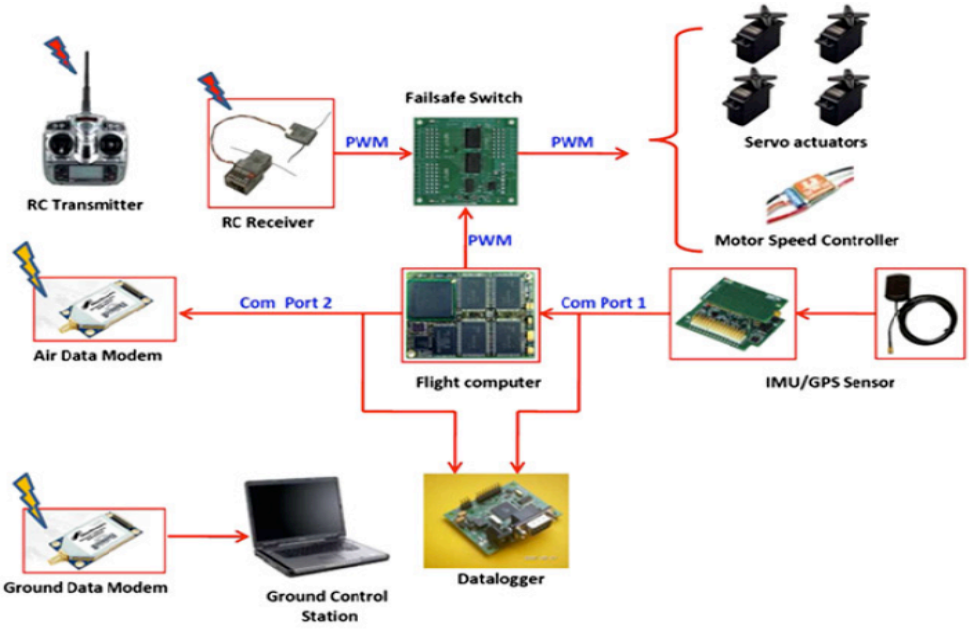

Figure 2. 7: Avionic system architecture

(Paw & Balas, 2010:3)

2.6 Ground control station system

The ground control station is based on a laptop computer with a wireless modem and the ground station software shows the real – time flight status, which, display the UAV's position, altitude, and sensor readings (Xiang & Tian, 2011:178). Via ground station software, the user can easily access the logged flight data to analyse the UAV's condition. Figure 2.8 below shows the ground control station user interface.

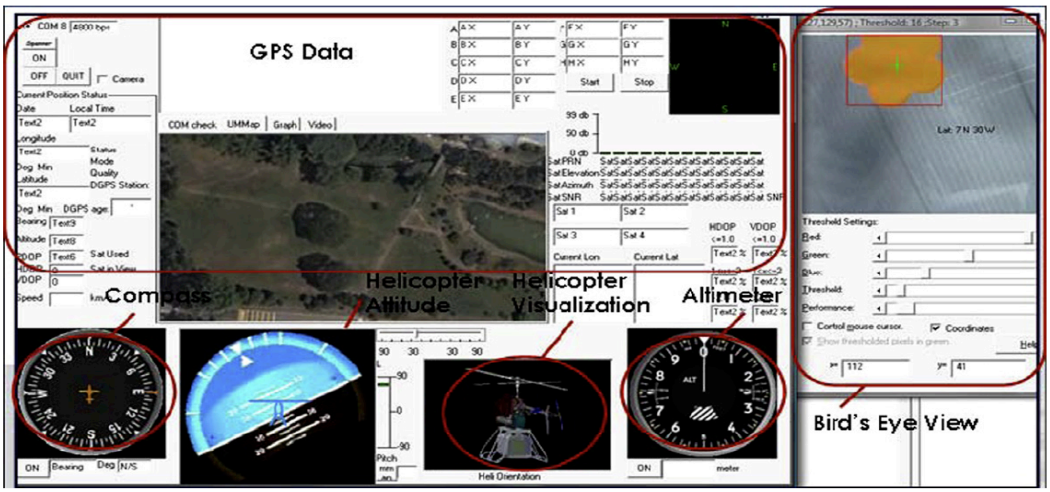

Figure 2. 8: Ground control station software interface

(Taha *et al.*, 2010:8)

2.7 Data collection system specifications

To achieve the UAV data collection system, there are certain specific requirements that should be considered. According to Iscold *et al*. (2008:244), the system should include the following:

- Portability: the UAV aircraft has the limited space and payload weight;
- Easy to operate: the data collection system should be automatic, since the user cannot manage the aircraft and the data collection system at the same time;
- Low – cost: the aircraft may be crushed during the test period. Hence, to avoid an increase in costs, the data collection system should also be cheap; and
- Adaptability: various kinds of aircrafts can be made into UAVs, and involve a variety of fields (aerodynamics, flight mechanics, and so on), while a diversity of sensors can be applied to this data collection system.

2.8 Summary

This chapter introduced basic hardware and software structure of a UAV aircraft, including UAV hardware components, the onboard avionic system, and ground control station system. Based on the findings mentioned above, the process of developing the data collection system for small UAVs are comprises two major parts, namely the UAV onboard avionics system and the other one is ground control station system.

CHAPTER THREE
COMMUNICATIONS

3.1 Overview of communication

Communications in UAV research plays much more of an important role in the overall UAV system. Clot (1999:13) states that there are two major problems of UAV communication, which are: 1) how to get data to and from UAV; and 2) how to operate UAV effectively. Furthermore, a variety of methods rely on the electromagnetic spectrum. Another consideration that should be noted in the communication is what kind of frequencies should be used and how much data will be transmitted.

Communication between the ground control station and the UAV comprises an 'up-link' transmitting command and manipulates command from the ground station to the UAV onboard system, while 'down-link' transmitting, shows the UAV status (Austin, 2010:143).

Austin (2010:143) also notes that there are two fundamental issues to evaluate the performance of communication:

- The 'data rate', which is the amount of data transferred per second by a communications channel and is measured in bytes per second (bps); and
- The 'bandwidth', which is the difference between the highest and lowest frequencies of a communications channel, and is measured in MHz or GHz.

3.2 Communication media

To accomplish communication between the ground control station and UAV may include the following three different media, namely radio, fibre optics or a laser beam (Austin, 2010:143).

Austin also presents characteristics of these three media options, which are described below:

- Laser – the laser method is not too popular currently, since atmospheric absorption limits the range and reduces reliability;

- Fibre-optics – the data transmission use of fibre-optics requires the UAV to fly at low altitude. However, the fibre must be laid down onto the ground, while mobility is a shortcoming of this communication medium; and
- Radio – this is the only system known to be used in communication between the UAV and its controller.

3.3 Introduction of radio

Radio is the one of the most common communication media and can communicate over a distance without any physical connection, while it can be silent and invisible with no limitation of geography. Hence, radio has an advantage to apply to the UAV communication field.

3.3.1 Radio wave

A radio wave is an invisible and silent force field with no limitations of peography that consists of both a magnetic field and an electric field. Frenzel (2010:150) also notes that if we place the following two types of fields into a self-supporting entity, then the electromagnetic field or radio wave will appear:

1) *"A magnetic field is a force generated by a magnet, either a permanent magnet or electromagnet, and current flow in a wire or other conductor produces the magnetic field. Invisible magnetic flux lines emit from the magnet and may influence objects in or near them";* and

2) *"An electric field derives from a voltage, and across two conductors. The attraction of the positive and negative charges across an open space introduces another kind of invisible field that can also influence external objects".*

There is a device called antenna (see Figure 3.1), which can provide both electric and magnetic fields that we refer to as radio waves (Frenzel, 2010:151).

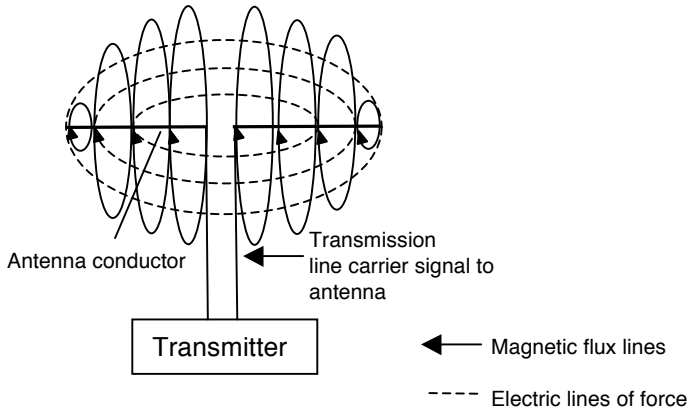

Figure 3. 1: Antenna produces both electric and magnetic fields

(Frenzel, 2010:152)

Frenzel believes that the following aspects will explain how an antenna creates a radio wave:

1) According to Maxwell, "*if you generate a changing electric field, it would, in turn, generate a magnetic field. If the magnetic field is changing and moving forward, it will generate an electric field. The two fields support or generate one another as they change and move outward from the antenna that produces them*" (citied in Frenzel, 2010:151); and
2) The electric field line is always perpendicular with the magnetic field line (see Figure 3.2). And the direction of the radio wave also moves at 90 degrees to both the electric and magnetic field line (Frenzel, 2010:151).

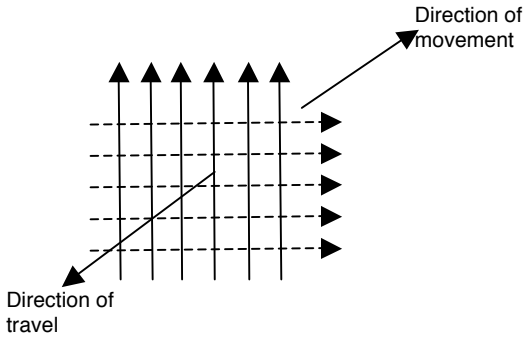

Figure 3. 2: The electric and magnetic field lines are at a right angle to one another and in the direction of radiation

(Frenzel, 2010:152)

3.3.2 Radio wave travelling speed

Radio wave has the same speed as light speed, which is 300,000,000 meter per second, hence, the signal transmission via radio wave is not instantaneous (Frenzel, 2010:152). The difference between the light wave and radio wave is only in frequency and wavelength. However, they are both electromagnetic waves.

The following equations expressed a way to calculate the velocity of propagation or phase velocity of the wave (Paul, 2004:201):

$$v = \frac{1}{\sqrt{\mu\varepsilon}} \quad \text{m/s} \qquad [3.1]$$

where μ = the magnetic permeability

ε = the electric permittivity.

In free space, $\mu = \mu_0 = 4\pi \times 10^{-7}$ and $\varepsilon = \varepsilon_0 \cong (1/36\pi) \times 10^{-9}$, hence the velocity of propagation in free space is

$$v_0 = \frac{1}{\sqrt{\mu\varepsilon}} = \frac{1}{\sqrt{4\pi \times 10^{-7} \cdot (1/36\pi) \times 10^{-9}}} = 2.9979 \times 10^8 \cong 3 \times 10^8 \text{ m/s.} \qquad [3.2]$$

And, if there is a different medium from free space, the relations will be $\mu = \mu_r \mu_0$ and $\varepsilon = \varepsilon_r \varepsilon_0$. The wave velocity of propagation is that the medium relates to the velocity of propagation in free space as

$$v = \frac{v_0}{\sqrt{\mu_r \varepsilon_r}} \quad \text{m/s} \qquad [3.3]$$

Where, μ_r = relative permeability

ε_r = relative permittivity.

3.3.3 Wavelength

Paul (2004:4) states that the wavelength is denoted by λ and is the actual physical length of a radio wave (see Figure 3.3), while the wave must travel to change phase by 2π radians or 360°. Hence, the wavelength and phase constant are associated by

$$\beta\lambda = 2\pi \text{ radians or } \beta = \frac{2\pi}{\lambda} \text{ rad/m or } \lambda = \frac{2\pi}{\beta} \text{ m.} \qquad [3.4]$$

The β is called phase constant and the unit is radians/m

$$\beta = \omega\sqrt{\mu\varepsilon} \quad \text{rad/m} \qquad [3.5]$$

where $\omega = 2\pi f$ and f = the cyclic frequency.

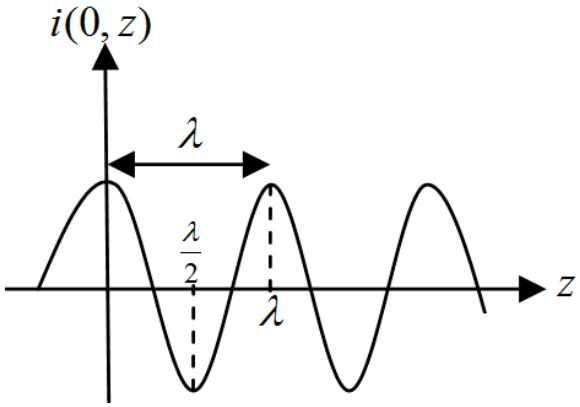

Figure 3. 3: Wave propagation in space and wavelength

(Paul, 2004:5)

From equation 3.1, $v = \frac{1}{\sqrt{\mu\varepsilon}} \Rightarrow \sqrt{\mu\varepsilon} = \frac{1}{v}$

From equation 3.5, $\beta = \omega\sqrt{\mu\varepsilon} \Rightarrow \sqrt{\mu\varepsilon} = \frac{\beta}{\omega}$.

If we combine equations 3.1 and 3.5, it may be an alternative equation as

$$\beta = \frac{\omega}{v} = \frac{2\pi f}{v} \text{ rad/m.} \qquad [3.6]$$

When you place equation 3.4 and 3.6 together, an alternative wavelength equation will be

$$\beta = \frac{2\pi}{\lambda} = \frac{2\pi f}{v} \Rightarrow$$

$$\lambda = \frac{v}{f} \text{ m.} \qquad [3.7]$$

3.3.4 Radio wave propagation

The propagation (see Figure 3.4) is a radio signal, which moves from the transmitter side to receiving side via antenna (Frenzel, 2010:156). If there is no force from outside, the radio wave will travel in a straight line.

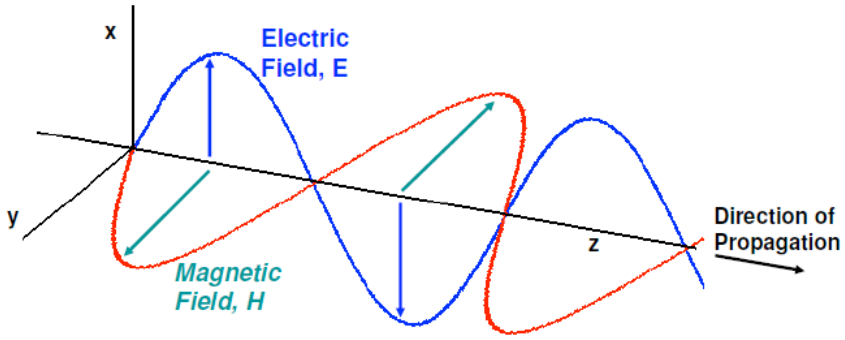

Figure 3. 4: Radio wave propagation schematic diagram

(Jon B. 2009)

However, any kind of obstruction between the transmitting antenna and receiving antenna will block the signal. The radio wave almost has the same characteristics as the light wave. Struzak (2006:45) notes that the radio wave has the following phenomena:

- Reflection: the radio wave will change the original direction when a wave front interacts with dissimilar media. The reflecting object is larger than the wavelength;
- Scattering: the direction of the radio wave is changed when the wave front interacts with the discontinuities medium and after scattering, the wavelength will become smaller compared with the original wavelength;
- Diffraction: the direction of the radio wave propagation changes owing to the process when the radio wave passes through the obstruction;
- Absorption: this is energy transformation, when the incoming energy from the radio wave interacts with the medium material, hence some of the energy will be stored in the medium, which occurs at an atomic level.
- Refraction: the propagation of direction will be changed owing to the radio wave propagation from one medium to another or the same medium with a different refraction index.

It has been claimed (Jon B, 2009) that when the electromagnetic wave propagates away from the transmitting antenna, it takes on a spherical wavefront. When it arrive receiving antenna by the time, the wavefront has a very large radius of curvature and is essentially a plane wave.

3.3.5 Signal strength

The radio wave will become weaker and weaker when it is far away from the transmitting antenna. In fact, the power in the radio wave will decrease because of the squared of the distance between the antenna and the radio signal, which are normally expressed as microwatts (1-millionth of a watt) or nanowatts (1-billionth of a watt) (Frenzel, 2010:152).

3.3.6 Electromagnetic frequency spectrum

Frenzel (2010:153) comments that the "*radio signal applied to the antenna by the transmitter is a sine wave*". Therefore, all sine waves have an amplitude and frequency, furthermore, there are two common and different radio wave communication methods, which are Amplitude Modulation (AM) and Frequency Modulation (FM).

The following aspects comprise differences between AM and FM (Differencebetween.net. 2011):

- AM is more liable to signal distortion and degradation compared with FM;
- AM has a longer transmission range compared with FM;
- AM can be transmitted in mono, which is suggested for talk radio;
- FM is not degraded linearly by distance compared with AM; and
- FM can be transmitted in stereo, which is suggested for music.

Radio transmissions can hold a wide frequency range, and this range is also called electromagnetic frequency (Frenzel, 2010: 153). For different types of communication services, the spectrum is separated into different radio frequency (see Table 3.1).

Table 3. 1: Major segments of the frequency spectrum

Frequency band	Acronym	Wavelength in air	Sample uses
30 kHz to 300 kHz	Low frequencies (LF)	10,000 km – 1000 km	Communication with submarines.
300 kHz to 3000 Hz	Medium frequencies (MF)	1000 km – 100 km	Communication within underground mines.
3 MHz to 30 MHz	High frequencies (HF) or short wave	100 m – 10 m	International broadcasters, radio communication etc.
30 MHz to 300 MHz	Very-high frequencies (VHF)	10 m – 1 m	Television broadcasts, line-of-sight ground to air-craft, communications etc.
300 MHz to 3 GHz	Ultra-high frequencies (UHF)	1 m – 10 cm	Microwave oven, mobile phone, wireless LAN, bluetooth, ZigBee, GPS etc.
3 GHz to 30 GHz	Super-high frequencies (SHF)	10 cm – 1 cm	Satellite television broadcasting, etc.

30 GHz to 300 GHz	Extremely-high frequencies (EHF)	1 cm – 1 mm	Radio astronomy, directed-energy weapon etc.

(Adapted from Frenzel, 2010:153)

For instance, most two-way radio communications for marine, aircraft, mobile and other services, use the spectrum range from 30 MHz to 300 MHz, which is in VHF range.

3.3.7 Difference between lower frequency and higher frequency

There are two essential issues in radio wave transmission: the one is the power of radio frequency, and the other one is radio wave propagation losses. Hence, the following three points conclude the difference between lower frequency and higher frequency (ELPRO Technologies. 2011).

1. Penetrate obstacles

   The radio signal strength will decrease when the radio wave passes through the medium, such as air and concrete wall (see Figure 3.5). If increases the rate of radio frequency, and the rate of attenuation increase. In other words, when radio wave traverses obstacle, the radio strength reduces faster and comes the better effect to pass through obstacle.

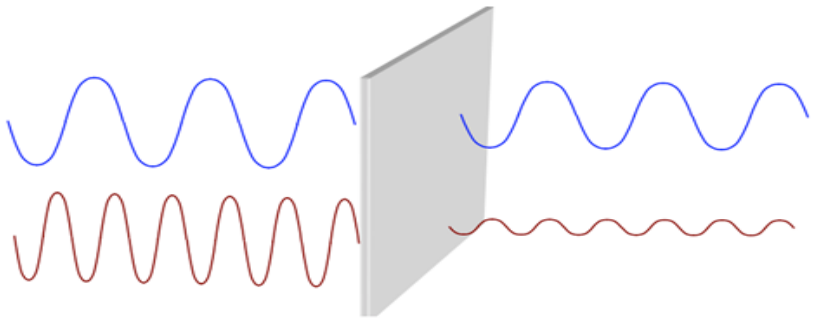

Figure 3. 5: Higher frequency has higher attenuation on penetrating obstacles

(ELPRO Technologies. 2011)

2. Bend around obstacles

   Radio waves will travel in a straight line if there is nothing to interrupt it, and the radio wave can be bended or diffracted when it hits the edge of obstacle, much like a light wave (see Figure 3.6).

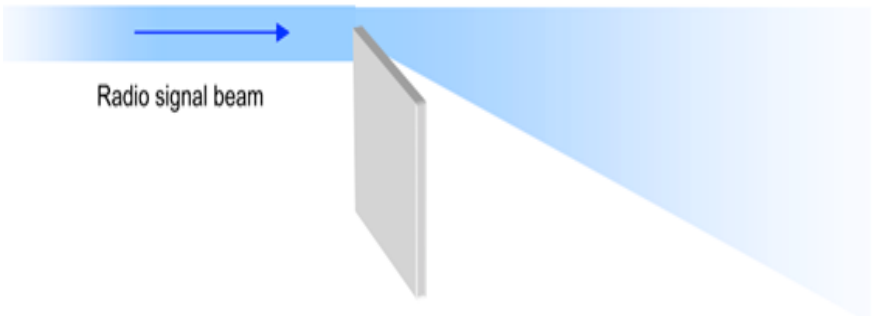

Figure 3. 6: Higher frequencies have less bending than lower frequency

(ELPRO Technologies. 2011)

3. Reflection

   When radio waves interact with a rough surface, the power of radio frequency will be loss. The rough surface will absorb the energy of the radio wave, which means that the reflected signal is weak when incoming radio waves interact with a higher frequency (see Figure 3.7).

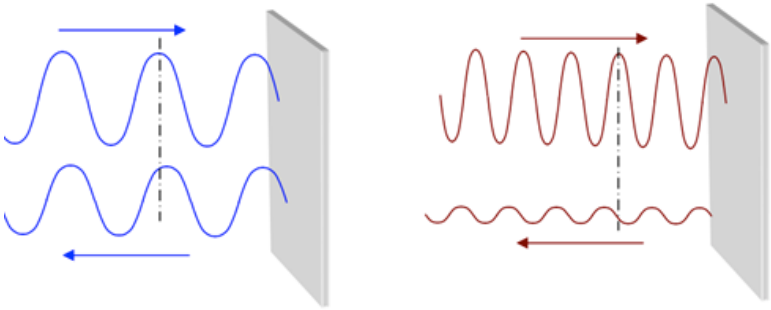

Figure 3. 7: Higher frequencies lose more signal strength on reflection

(ELPRO Technologies. 2011)

From the comparisons mentioned above, the higher frequencies have relatively more spectrums, so channels are wider and allow higher data rates to be transmitted. However, it is not reliable for long distance transmission. Corresponding with the lower frequency, it is more reliable over distance transmission, but can carry less data rates (ELPRO Technologies, 2011).

3.4 Links in radio communication

Radio links in the data collection system is like a bridge, which provides a communication path between the UAV and the ground control station. Strock (1987: 69) states that "*the radio link consists of the radio transmitter, transmitting antenna*

(one or more), receiving antenna (possibly auto-tracking), and radio receiver (one or two)".

Radio link hardware components' functionality is shown below.

I. Radio transmitter – is an electronic device, which assists with antenna to produce the radio wave. The transmitter will generate a radio frequency alternating current, which will be applied to the antenna. Once the alternating current occurs, the antenna radiates radio wave (Wikipedia, 2011a).

II. Transmitting antenna – normally, the transmitter is located at UAV. To ensure proper quality of communication, the location and orientation of antenna is quite important in this case. As mentioned in 3.3.4, the radio frequency propagation is a straight line. It has been claimed (Strock, 1987: 72) that the transmitting antenna must be placed where the signal can be reached by the receiving antenna, and is usually placed on the surface of the UAV, which keeps a line-of-sight at the ground station.

III. Receiving antenna – it has the same principle as the transmitting antenna. The only difference is that the receiving antenna is located at the ground control station and assists the receiver. It requires a good location and orientation to ensure that the signal can be caught by the transmitting antenna.

IV. Receiver – an electronic device consists of a series of amplifiers. Frenzel (2010: 165) claims that the function of a receiver is to boost the weak signal, which is picked up from the receiving antenna, and then added into an output with the originally transmitted information, and maybe also output digital data that can be directly used by a computer.

Frenzel (2010: 145) states that the radio range in the field of Light-Of-Sign (LOS) can be calculated (see Figure 3.8), as shown by the expression below:

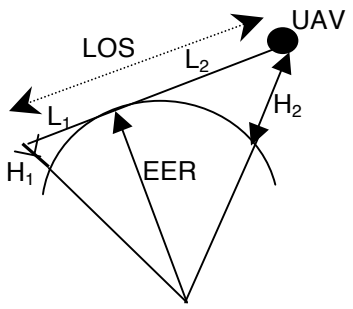

Figure 3. 8: Radio LOS derivation

(Adapted from Frenzel, 2010: 145)

$$L_1^2 = (EER + H_1)^2 - EER^2$$

$$L_1 = \sqrt{(2 \times EER \times H_1) + H_1^2}$$

So, $L_2 = \sqrt{(2 \times \mathrm{EER} \times \mathrm{H}_2) + H_2^2}$

where, H_1 = the heights of the radio antenna;

H_2 = the heights of the UAV; and

EER= Effective Earth Radius may use 8500km for typical radio frequency.

The LOS radio range can be written as:

$$\text{LOS Range} = \sqrt{(2 \times EER \times H_1) + H_1^2} + \sqrt{(2 \times \mathrm{EER} \times \mathrm{H}_2) + H_2^2} \,. \qquad [3.8]$$

3.5 Requirements for development of a data collection system

Typically, data collection systems are normally used in the testing of mobile vehicles, for instance, cars, aircrafts, and submarines etc. It is a special set of communication systems.

Carden, Jedlicka and Henry (2002: 5) state that:

> The data collection system consists of such devices as thermocouple, accelerometers, transducers, filters, signal conditioners, and computers. Different physical variables such as temperature, vibrations, pressures, force and humidity must be measured and converted into an electric signal or message that must be conditioned or amplified and mixed with other signals that are attached to the carrier and those electric signals will transmit to the desired location.

It may also be called a telemetry system, and allows a user to collect data from inconvenient locations, and to transmit this data to a convenient location. According to Strock (1987: 9), the telemetry system is used for collection, transmission and presentation of data.

3.5.1 System outline

An outline of a telemetry system is presented below in Figure 3.9:

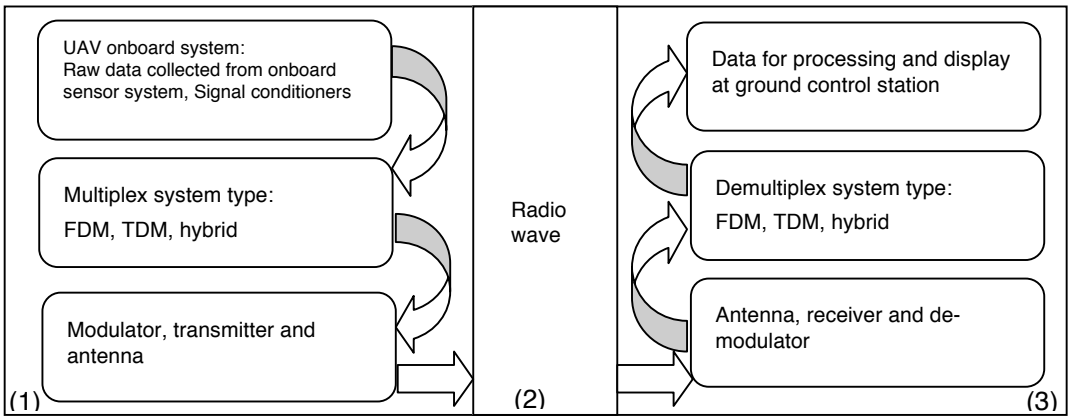

Figure 3. 9: Outline of a telemetry system:
(1) UAV part, (2) Transmission medium, (3) Ground station

(Adapted from Carden, Jedlicka and Henry 2002: 2)

Carden, Jedlicka and Henry (2002: 3) elaborate on the functionality of each part in the telemetry system, which is presented below:

(1) UAV part

a) The first subsystem, the UAV onboard system, is composed of sensors that can be converted from a physical variable into an electrical signal. The signal is weak, and the priority is to boot the weak signal before it is sent to the multiplex system.

b) The second subsystem: The entire sensor's raw data that is collected by the onboard system will be fed into the multiplex system. There are three types of multiplex systems: 1) if data is separated or deposited by the onboard system and fed it into different frequency bins for transmission, which is referred to as Frequency Division Multiplexing (FDM); 2) if the multiplex system separates the data in the time domain, it is referred to as Time Domain Multiplex (TDM) system; and 3) if the system combines both FDM and TDM, it is referred as a hybrid system.

c) The third subsystem: the multiplexed data has been separated in FDM or TDM, and is modulated onto the carrier at the transmitter to drive an antenna.

(2) Radio wave part

When the carrier is modulated with the information, it is propagated to receiving antenna via a medium such as air. To ensure that the sending signal arrives at the receiving antenna, the choice of carrier frequency must be compatible with the antenna. This means that the dimension of the antenna

and the wavelength of the carrier wave must have the same size in terms of range.

(3) Ground station part

a) The modulated carrier is received at the receiving antenna, and then sends it to the receiver, which comprises a radio frequency amplifier and an Intermediate Frequency (IF) amplifier. The modulated carrier is amplified, and then converted into an IF carrier and amplified again.
b) The Demultiplex system will separate the IF carrier data by using Frequency-Division Multiplexing (FDM) or Time Division Multiplexing (TDM) techniques to guide the row sensor data to go to the right channels.
c) The data will displays, record and process in the computer when only the data has been separated and placed into the correct data channel.

With a real-time telemetry system, the ground control station can achieve a real-time analysis, hence the results will instruct the pilot whether there is a need to return to base for safety reasons.

3.5.2 Computer in telemetry system

Generally, computers can serve for constructive purposes in the telemetry application, for instance, it can convert all the binary numbers from the encoder into meaningful engineering unit values and display them (Strock, 1987: 139).

And also, Strock (1987:140) also claims that the computer employed in a telemetry application should have a suitable architecture (see Figure 3.10) for real-time data input, as well as the input ports and controlling software that can carry such data.

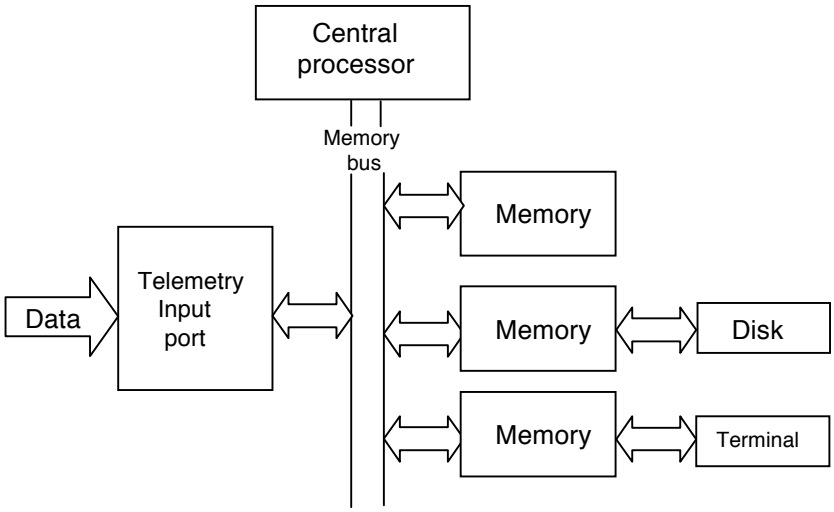

Figure 3. 10: General computer for real-time opration

(Adapted from Strock, 2010: 141)

Data changing occurs too fast under real-time conditions. Hence, Figure 3.12 presents the graphic architecture for a computer in such a system. Strock (1987: 140) notes that: 1) the high-speed processor connects with the high-speed memory and to each secondary device via a “memory bus”, which provides a high-speed data interchange in the system. 2) As long as the device is on the bus, it can communicate with any other device, but the primary condition is that it should be authorized by the central processor.

3.5.3 Software

Telemetry software operates from an end-user’s computer (see Figure 3.11) where it is located at the ground control station. Most data sources represent as “machine language” – ones or zeros (Strock, 2010: 159).

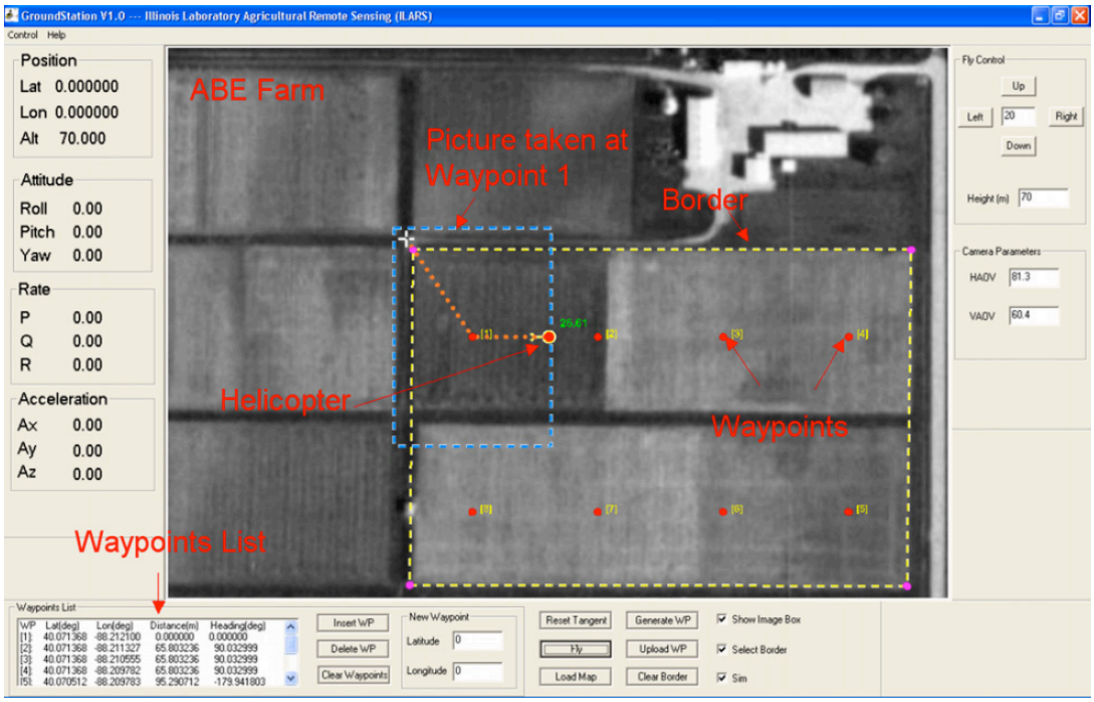

Figure 3. 11: Ground station software

(Xiang & Tian, 2011:179)

Software translates on-off commands to engineering unit values, diagrams, tables and so on. The ultimate goal is that ground station software should provide the UAV's real-time flight conditions such as displaying the UAV's position, altitude, sensor readings, programming waypoint and so on, via the computer monitor.

3.6 Sensor delay

The sensor delay is an issue for both ground control station and onboard sensor system, which ensure gathering the accurate data for analysis purpose. In fact, sensor delay is caused by internal computations, which occur at sensor level owing to factors such as temperature changes, conversion of voltages and transmission delays (Bristeau *et al*., 2010:737).

An investigation conducted by Bristeau *et al*., (2010:737) revealed that "*the magnetometer or the barometer does not show any information (such as time-stamping information) about the delay between the physical measurement and the output value. With such kinds of sensors, data synchronization is almost impossible, but does not include working with analogue sensors*". However, the IMU does provide accurate timing information, and in its output message, which can be considered as a reference clock.

To avoid end-users from experiencing problems, Bristeau *et al*. (2010:737) presents the following solutions:

- When the flight computer receives measurements from the UAV onboard sensors (excluding the IMU), the elapsed time from the latest IMU should also be measured; and
- This elapsed time is added to IMU time and included in the gathered message.

Once this process is complete, a single output message will contain both sensor data and timing detail. This will be a reference for the end-user to estimate the time delay.

3.7 Summary

This chapter briefly introduced some fundamentals of radio communication based on the data collection system. It included aspects such as characteristics of the radio wave, radio communication, structure of the telemetry system and the sensor delay issue. Furthermore, from this chapter it can be concluded that choosing suitable radio frequency rates is key to establishing stable and reliable communication between the UAV and the ground control station in order to calculate the range of LOS.

CHAPTER FOUR
EXPERIMENTAL PLATFORM AND PROCEDURE

4.1 Introduction of UAV platform

The Arducopter Quad (see Figure 4.1) was selected as a UAV platform for this project, because of its low cost, manoeuvrability and stability, and effective performance for photos or videos when it hovers in the air. It also works with remote control operation, and flies at a low speed, with vertical take-off and landing. The most important reason for choosing a Arducopter Quad is because it reduces mechanic complexity, and significantly enhances safety, whilst it also trims manufacturing and maintenance costs down.

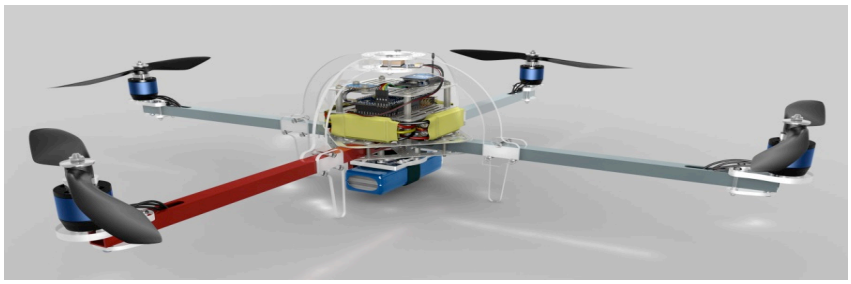

Figure 4. 1: Arducopter Quad

(ArduCopter, 2011)

Altuğ (2002: 72) states that unlike common helicopters that have variable pitch angles, the Quad helicopter comprises four rotors with two pairs of counter-rotating propellers (see Figure 4.2), which are placed at the four corners of the aircraft. The four rotor's pitch angle of the Arducopter Quad is fixed, and in orders to control it, requires lifting to adjust the rotor speed.

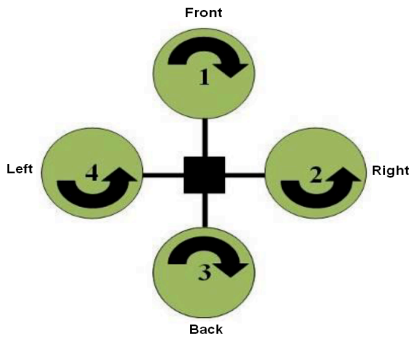

Figure 4. 2: Arducopter Quad's reaction-torque elementary diagram

(Adapted from Rawashdeh *et al.*, 2009: 2)

4.2 The concept of Arducopter dynamics

The reaction-torque of each individual propeller is used to manipulate the altitude, attitude and heading orientation of the quad-copter. According to the basic quad-copter dynamics concept (see Figure 4.3), 1) the quad-copter's altitude is controlled by the speed of four rotors; 2) the yaw of the quad-copter is controlled by changing the rotors speed between the two rotors on one axis and the two rotors on the other axis; 3) the pitch is controlled by changing the relative speed between the front rotor and the back rotor; 3) the roll movement of quad-copter is similar as pitch, and should also change the rotor's relative speed between the left rotor and right rotor.

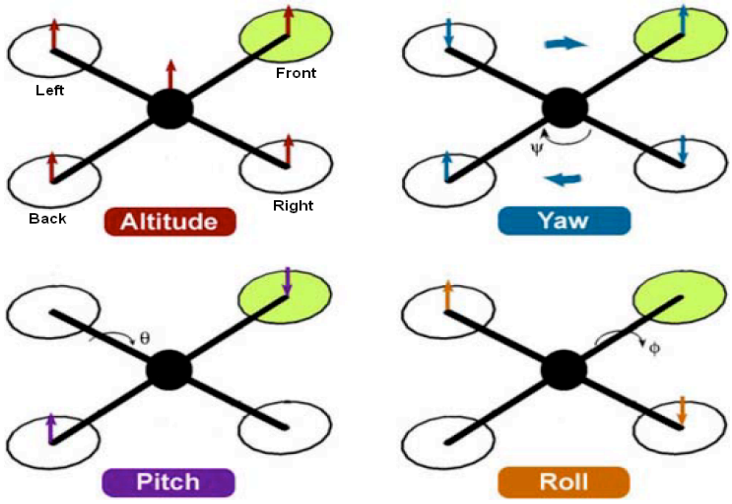

Figure 4. 3: Arducopter Quad dynamics

(Adapted from Raza and Gueaieb, 2010: 248)

4.3 The states equations

The quad copter system, in a six degree of freedom (6 DOF), is for use of different coordinate frames to identify the location and attitude of the vehicle (see Figure 4.4). Raza and Gueaieb (2010: 250) present that: 1) The force and moments will be gathered by the IMU sensor, therefore, the data will be evaluated with reference to the body frame; and 2) The position and speed will be evaluated by using GPS measurements in respect of the inertial frame, which is located at ground station.

Kivrak (2006: 18) claims that:

- This body axis refers to the inertial frame by a position vector (x, y, z), and three Euler angles (ϕ, θ, ψ), which represent pitch, roll, and yaw, respectively, as well as angular rates (p, q, r) around the three orthogonal body axes; and

- The six states include three positions and three linear velocities of the centre of the mass of the quad-copter with respect to an earth fixed reference frame.

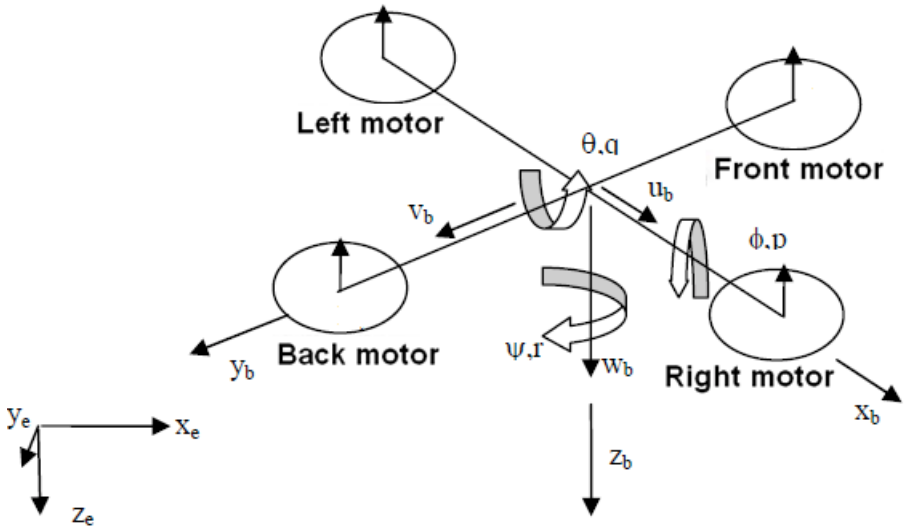

Figure 4. 4: The inertial, body and vehicle frame of reference
(b indicates for body and e indicates for earth)

(Adapted from Kivrak, 2006: 17)

Accordingly, equation 4.1, 4.2 and 4.3 represents the basic rotation matrix in three dimensions, namely:

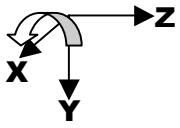

X-axis rotation looks like Z-axis rotation if replaced with:

X-axis with Z-axis

Y-axis with X-axis

Z-axis with Y-axis

$$\begin{aligned} Y' &= Y \times \cos\phi - Z \times \sin\phi \\ Z' &= Y \times \sin\phi + Z \times \cos\phi \Leftrightarrow R_x = \begin{bmatrix} 1 & 0 & 0 \\ 0 & \cos\phi & -\sin\phi \\ 0 & \sin\phi & \cos\phi \end{bmatrix} \\ X' &= X \end{aligned} \qquad [4.1]$$

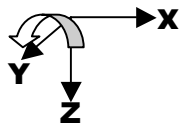

Y-axis rotation looks like a normal 2-D rotation:

$$\begin{aligned} Z' &= X \times -\sin\theta + Z \times \cos\theta \\ X' &= X \times \cos\theta + Z \times \sin\theta \\ Y' &= Y \end{aligned} \Leftrightarrow R_y = \begin{bmatrix} \cos\theta & 0 & \sin\theta \\ 0 & 1 & 0 \\ -\sin\theta & 0 & \cos\theta \end{bmatrix}. \quad [4.2]$$

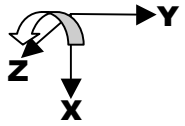

Z-axis rotation looks like a Y-axis rotation if replaced by:

X-axis with Y-axis

Y-axis with Z-axis

Z-axis with X-axis

$$\begin{aligned} X' &= X \times \cos\psi + Y \times -\sin\psi \\ Y' &= X \times \sin\psi + Y \times \cos\psi \\ Z' &= Z \end{aligned} \Leftrightarrow R_y = \begin{bmatrix} \cos\psi & -\sin\psi & 0 \\ \sin\psi & \cos\psi & 0 \\ 0 & 0 & 1 \end{bmatrix}. \quad [4.3]$$

The equation 4.4 represents the resultant transformation matrix, namely:

$$R_x \times R_y = \begin{bmatrix} \cos\theta & \sin\theta \cdot \sin\phi & \sin\theta \cdot \cos\phi \\ 0 & \cos\phi & -\sin\phi \\ -\sin\theta & \sin\phi \cdot \cos\theta & \cos\theta \cdot \cos\phi \end{bmatrix}$$

$$R = R_x \times R_y \times R_z = \begin{bmatrix} \cos\psi & -\sin\psi & 0 \\ \sin\psi & \cos\psi & 0 \\ 0 & 0 & 1 \end{bmatrix} \begin{bmatrix} \cos\theta & \sin\theta \cdot \sin\phi & \sin\theta \cdot \cos\phi \\ 0 & \cos\phi & -\sin\phi \\ -\sin\theta & \sin\phi \cdot \cos\theta & \cos\theta \cdot \cos\phi \end{bmatrix}$$

$$R = \begin{bmatrix} \cos\theta \cdot \cos\psi & \cos\psi \cdot \sin\theta \cdot \sin\phi - \cos\phi \cdot \sin\psi & \cos\psi \cdot \sin\theta \cdot \cos\phi + \sin\psi \cdot \sin\phi \\ \sin\psi \cdot \cos\theta & \sin\psi \cdot \sin\theta \cdot \sin\phi + \cos\psi \cdot \cos\phi & \sin\psi \cdot \sin\theta \cdot \cos\phi - \sin\phi \cdot \cos\psi \\ -\sin\theta & \sin\phi \cdot \cos\theta & \cos\theta \cdot \cos\phi \end{bmatrix}. \quad [4.4]$$

Therefore, by using the transformation matrix R, which is mentioned above, the linear velocities along the body axes can be transformed into an inertial frame (Kivrak, 2006: 19).

$$\dot{x} = \frac{d}{dt}[x, y, z]^T = R[u, v, w]^T \Rightarrow \quad [4.5]$$

$$\begin{bmatrix} \dot{x} \\ \dot{y} \\ \dot{z} \end{bmatrix} = R \begin{bmatrix} u \\ v \\ w \end{bmatrix} \Rightarrow \quad [4.6]$$

$$\dot{x} = \cos\psi \cdot \cos\theta \cdot u + (\cos\psi \cdot \sin\theta \cdot \sin\phi - \cos\phi \cdot \sin\psi) \cdot v + (\cos\psi \cdot \sin\theta \cdot \cos\phi + \sin\phi \cdot \sin\psi) \cdot w$$

$$\dot{y} = \sin\psi \cdot \cos\theta \cdot u + (\sin\psi \cdot \sin\theta \cdot \sin\phi + \cos\phi \cdot \cos\psi) \cdot v + (\sin\psi \cdot \sin\theta \cdot \cos\phi - \sin\phi \cdot \cos\psi) \cdot w$$

$$\dot{z} = -\sin\theta \cdot u + \sin\phi \cdot \cos\theta \cdot v + \cos\theta \cdot \cos\phi \cdot w$$

Use of the transformation matrix T, as shown below, the angular rates along body axes can be transformed into Euler rates (Kivrak, 2006: 19).

$$T = \begin{bmatrix} 1 & \tan\theta \cdot \sin\phi & \tan\theta \cdot \cos\phi \\ 0 & \cos\phi & -\sin\phi \\ 0 & \sin\phi \cdot \sec\theta & \sec\theta \cdot \cos\phi \end{bmatrix}$$

$$\frac{d}{dt}[\phi, \theta, \psi]^T = T[p, q, r]^T \Rightarrow \quad [4.7]$$

$$\begin{bmatrix} \dot{\phi} \\ \dot{\theta} \\ \dot{\psi} \end{bmatrix} = T \begin{bmatrix} p \\ q \\ r \end{bmatrix} \Rightarrow \quad [4.8]$$

$$\dot{\phi} = p + q \cdot \tan\theta \cdot \sin\phi + r \cdot \tan\theta \cdot \cos\phi$$

$$\dot{\theta} = q \cdot \cos\phi - r \cdot \sin\phi$$

$$\dot{\psi} = q \cdot \sec\theta \cdot \sin\phi + r \cdot \sec\theta \cdot \cos\phi$$

Equations 4.6 and 4.8 represent the quad-copter's equations of motion.

4.4 ArduCopter's on-board system's electronics

The complete quad-copter's wiring diagram is shown below in Figure 4.5 and the layout of the electronic system for ArduPoilt Mega flight computer is shown in Figure 4.6.

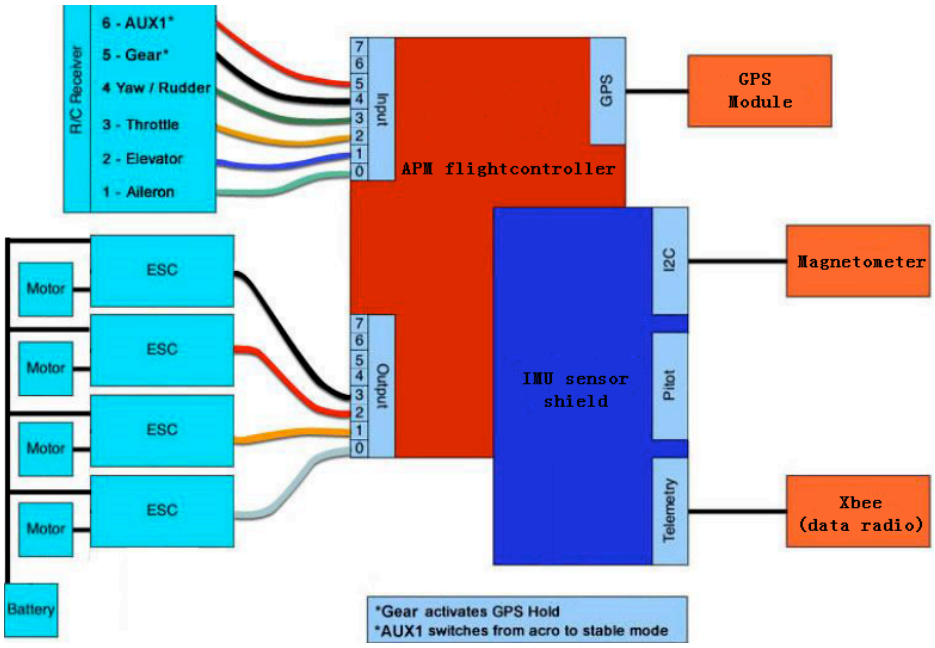

Figure 4. 5: ArduCopter wiring diagram

(ArduCopter, 2011)

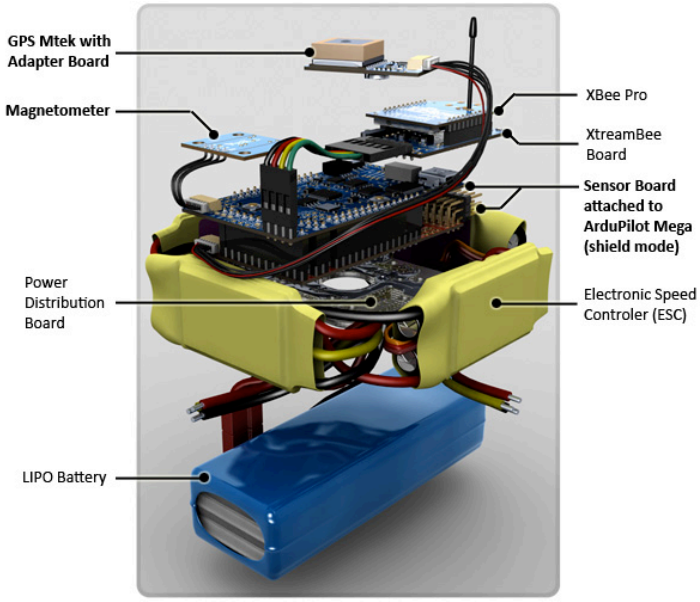

Figure 4. 6: The main electronic components of the ArduCopter

(ArduCopter, 2011)

The platform of the quad-copter UAV is based on the ArduPoilt Mega (APM) board, and the IMU sensor shield (see Figure 4.7):

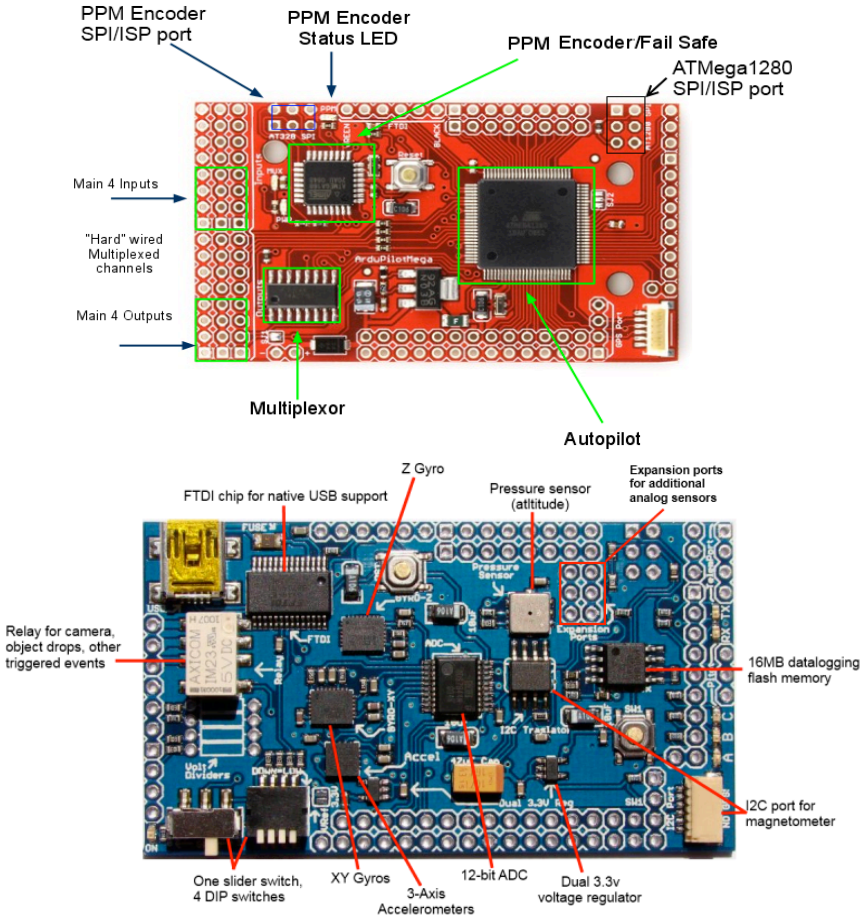

Figure 4. 7: The ArduPoilt Mega (upper) and IMU Sensor shield (lower)

(ArduCopter, 2011)

- The Ardupoilt Mega provides GPS and transmits data via a 900MHz data-link to the ground control station, while it is also intended to meet the requirements of the Surface Mounted Devices (SMD), since the payload should carry a GPS tracker. This device also plays a role as flight computer, which means that all of the input commands from the end user will be processed for the sake UAV flying stability.
- The IMU sensor shield integrates a large selection of sensors, which are required for UAV applications, including three axis of angular rotation and accelerations sensors, absolute pressure and temperature sensor, 16Mbits data logger chip and so on.

Figure 4.8 shows that the final ArduPoilt Mega board and IMU sensor shield once they have been assembled.

Some main features of ArduPoilt Mega and IMU Sensor shield, as shown in Table 4.1 below.

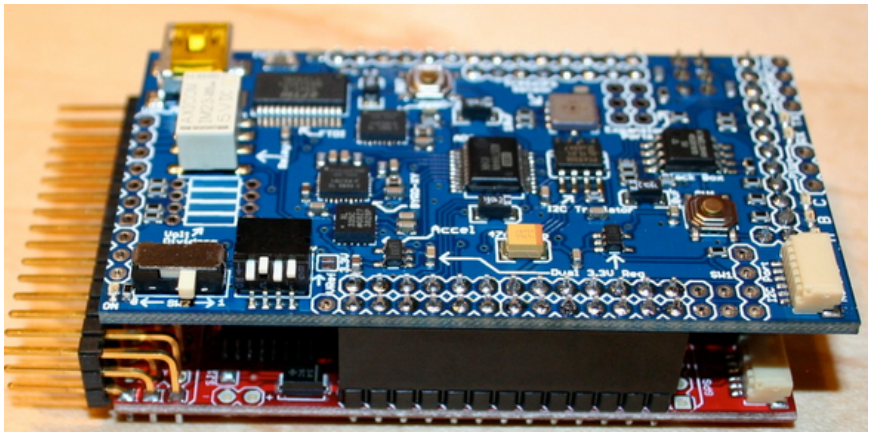

Figure 4. 8: Final ArduPoilt Mega attached with IMU Sensor shield

(ArduCopter, 2011)

Table 4. 1: Main features of APM & IMU shield

APM main features	IMU main features
Based on a 16MHz Atmega1280 processor	Dual 3.3V Regulator for analog sensors
128k Flash Program Memory	Built-in 16MB Data Logger
With a 6-pin GPS connector	Built-in FTDI chip, can be connect with USB.
16 spare analog inputs & 40 digital input/outputs	Modem/OSD port
4 dedicated serial ports for two-way telemetry	I2C Port
Powered by RC receiver or battery	12-bit ADC for better Gyro/Accel/AirSpeed resolution
8 RC channels	0-Bit analog expansion ports

(ArduCopter, 2011)

4.4.1 GPS module

The GPS module (see Figure 4.9) is used for position hold. When the quad-copter moves forward and there is a directional vector, this can be calculated by GPS, which connects with the APM board. It has superior urban performance, as well as USB/UART interface. The specifications of the GPS module can be seen below in Table 4.2.

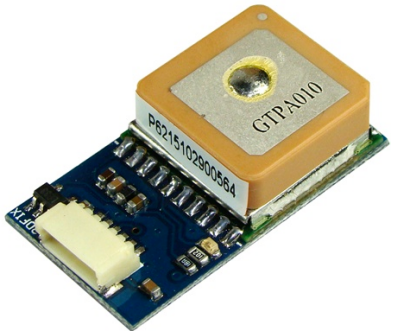

Figure 4. 9: GPS module

(ArduCopter, 2011)

Table 4. 2: GPS module specification

GPS specifications	Technical data
Dimension	16mm x 16mm x 6mm
Sensitivity	Up to -165dBm tracking
Position accuracy	< 3m CEP (50%) without SA (horizontal)
Power consumption	48mA @ acquisition, 37mA @ tracking
Shut-down current consumption	15uA, typical
AGPS function	Support
Maximum update rate	up to 10Hz
Weight	8 g

(ArduCopter, 2011)

4.4.2 Magnetometer

Normally the user manoeuvre quad-copter hovers in the air in one position, hence a magnetometer (see Figure 4.10) is required to be able to correct the drift in the yaw gyro even when quad-copter does not move, since the of GPS module can only calculate a directional vector when it is in a forward motion. The specifications of a magnetometer are provided in Table 4.3 below.

Figure 4. 10: Triple Axis Magnetometer

(ArduCopter, 2011)

The magnetometer is required for absolute heading control, as the GPS module's heading data is noisy when the UAV flies at a low speed or hovers.

Table 4. 3: Triple Axis Magnetometer HMC584

Characteristic	Technical data
Dimension	4.0 x 4.0 x 1.3mm
Cross-Axis sensitivity	0.5 gauss
Measure magnetic strength	Up to ±2 gauss
Power supply	3.3v
Current draw in measurement mode	0.8mA
Output rate	50Hz
Weight	50 mg

(Honeywell, 2011)

4.4.3 Propulsion unit and Electronic Speed Controller (ESC)

The four small and light out-runner brushless motors were chosen as the RCX A2830-12 (see Figure 4.11), while each motor was powered by a three-cell Lipo battery pack with a capacity of 2200mAh.

There are some advantages of using the out-runner electric brushless motor, which are presented below:

- It generates little vibration;
- It makes little noise;
- It will not produce any sparks during the motor run-time, compared with electric brush motor, hence, it greatly reduces jamming signals from the spark; and
- It has a long lifespan.

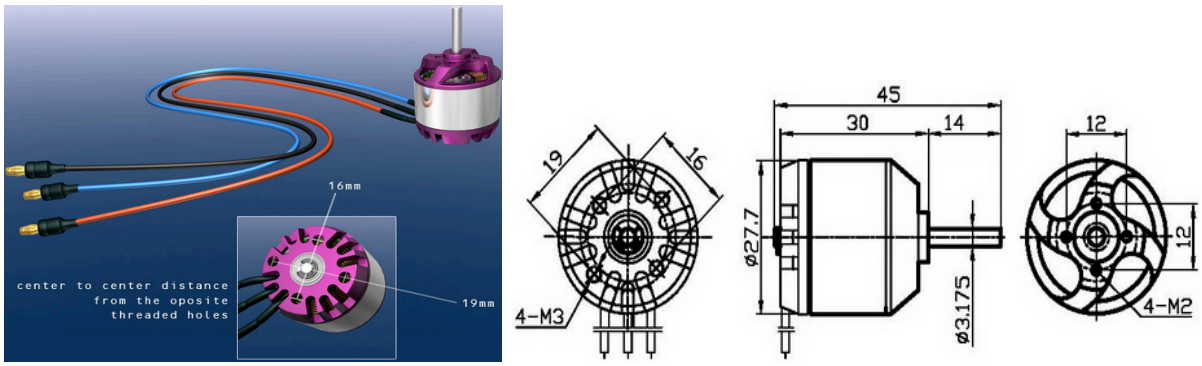

Figure 4. 11: Out runner brushless motor

(MYRCMART, 2011)

The disadvantages of using the out-runner electric brushless motor are presented below:

- It requests heavy batteries; and
- It will reduce the flying time.

The following table, Table 4.4, presents specifications of the brushless motor.

Table 4. 4: RCX A2830-12 850KV out-runner brushless motor

Characteristic	Technical data
Motor size	Φ28*30mm
Shaft size	Φ3.17*30mm
KV (rpm/v)	850
Max power	187w
Battery	2-4Li-Po
Ri (M Ω)	0.136
ESC	30A
Weight	52g

(MYRCMART, 2011)

The brushless motor is one type of 3-phase AC permanent magnet motor. Alternative current is connected to the motor via three wires with three separate square waves (one for each wire to the motor). To change the turning direction, one should swap any two of the three connection wires.

To ensure that the brushless motor performs well whilst running, a qualitative Electronic Speed Controller (ESC) is necessary (see Figure 4.12).

Figure 4. 12: Electronic speed controller

(ArduCopter, 2011)

In fact, the ESC is a square wave generator. The power source of a quad-copter is a Lipo battery, which supplies a direct current. When the DC current flows through the ESC, the output current changes to AC current, and provides power to drive the AC brushless motor (see Figure 4.13).

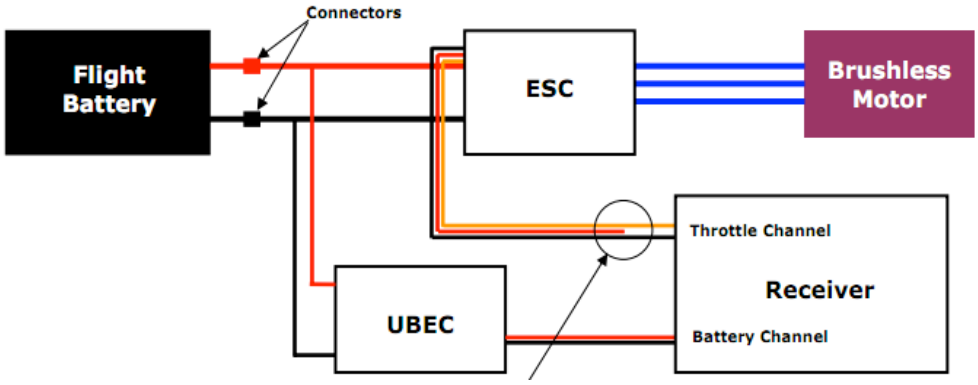

Figure 4. 13: ESC connection diagram

(4max, 2011)

Figure 4.10 shows that the Ultimate Battery Eliminator Circuit (UBEC) is an electronic circuit, which can deliver electric power to other circuitry, and also draws power from the higher voltage main pack, whilst it decreases the voltage to accommodate for the radio receiver and servos. When the red wire of the Throttle channel is broken, one should only use yellow and black wires to connect to the receiver.

To change the spinning speed of the motor, it does not work with changing the input voltage and amps. Increasing or decreasing the wave length of the square wave will obtain the desired speed. The specifications of the ESC are shown below in Table 4.5.

Table 4. 5: Plush 30 Brushless Speed Controllers

Characteristic	Technical data
Cont current	30A
Burst current	40A
BEC mode	Linear
BEC	5V / 2A
Li-Po cells	2-4
NIMH	5-12
Size	45x 24 x 11mm
Weight	25g

(Hobbyking (a), 2011)

4.4.4 Control system

The Arducopter is manually controlled by Remote Control (RC) equipment. It requires at least a 5-channel RC unit, or more is highly recommended such as a Turnigy 9X 9Ch Transmitter and a Turnigy 9X8C-V2 8-channel receiver (see Figure 4.14), which can be used to take control of the quad-copter.

Figure 4. 14: Manual control unit
Turnigy 9x 9Ch Transmitter (left)
Turnigy 9X8C-V2 8-channel receiver (right)

(Hobbyking (b), 2011)

4.4.5 XBee wireless module

In order to establish long range communication between the ground control station and the quad-copter UAV, an additional device such as an XBee wireless module (see Figure 4.15) should be used to extend the capability of the UAV communication range.

Figure 4. 15: XBee wireless module

(ArduCopter, 2011)

Once the XBee wireless module is set up on the Arducopter, the on-board sensor data can be transferred to the ground control station. The end-user can record any data which is required, as well as the data-log from the ground control station. Conversely, the end-user can open the ground station software (should set up the right port number and baud speed), which is capable of showing all the APM data. By using the different frequency range between the RC equipment and the XBee module, is a priority issue for communication purposes. The specifications of the XBee module can be seen below in Table 4.6.

Table 4. 6: XBee-PRO® 802.15.4 (Series 1)

Performance	Technical data
RF data rate	250 kbps
Line-Of-Sight range	1.6 km
Transmit power	+18 dBm
Receiver sensitivity	-100 dBm
Supply voltage	2.8~3.4VDC
Transmit Power Output	10 mW
Frequency band	2.4 GHZ

(ArduCopter, 2011)

4.5 Ground Control Station

The ground control station software is the core, which allows the end-user to be able to monitor and analyse the UAV's flight condition in real-time. Figure 4.16 shows the interface of the ground station control software, which is primarily responsible for navigation and image processing. The software was developed in MS Visual C#. It can be displayed by received real-time avionic data, whilst also allowing the end-user to set the navigation way point.

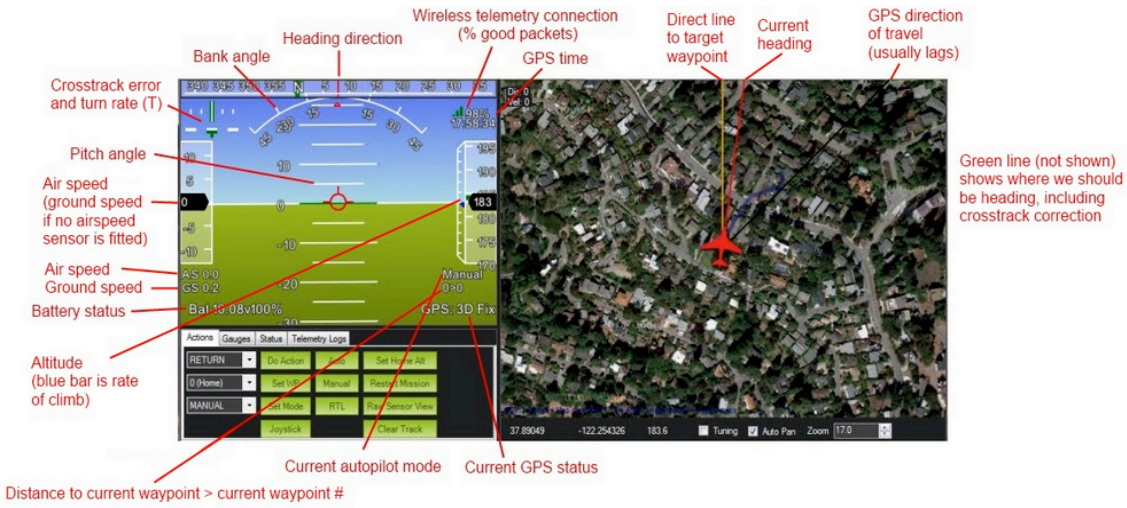

Figure 4. 16: ArduPilotMega (APM) ground control station software

(ArduCopter, 2011)

The PC ground control station receives the data string from the on-board sensor shield via 2.4 GHz XBee wireless transmission. The mission planner has a friendly user interface to accomplish flight path setting up, while viewing various on-board sensor data.

Furthermore, the APM Mission Planner is also able to detect the UAV's orientation, pitch angle, yaw angle, roll angle, altitude and speed etc. Collected flight information can be evaluated by end users at a later stage.

4.6 Summary

This chapter introduced the experimental platform of the arducopter, which has four propellers. This type of helicopter has a better hovering performance than a normal helicopter. The basic concepts of arducopter dynamics were presented, which provide a better understanding of air-movement, and state equations in terms of mathematical methods to describe the basic modelling and control of the arducopter. The chapter also introduced the APM microcontroller, which plays the role of flight computer. It processes raw sensor data into meaningful information and transfers it to ground control station software by the end-user analysis. Chapter Five introduces methods that were used to develop a data collection system for a small UAV.

CHAPTER FIVE
EXPERIMENTAL METHODLOGY

5.1 Overview

To establish communication between the Arducopter and the ground control station is important in the development of a UAV data collection system. End-users at the ground control station use APM mission planner software to gather flight data for further investigation.

This section presents methods that were used for the flight data collection system, including serial port choice, baud rate setting, XBee wireless module installation, data logging etc.

5.2 Serial connection by using a USB cable

The serial port communication (see Figure 5.1) is basically like transferring data one bit at a time, immediately one after another. Therefore, the sensor information passes back and forth between the PC and the arduino mega board, much like using computer language to set a pin high or low, while the corresponding output is like a switch, which controls whether it is on or off. Alternatively, serial port communication can also operate where one side sets the pin, and the other reads it; it is similar to Morse code, which transmits textual information as a serial of on-off tones.

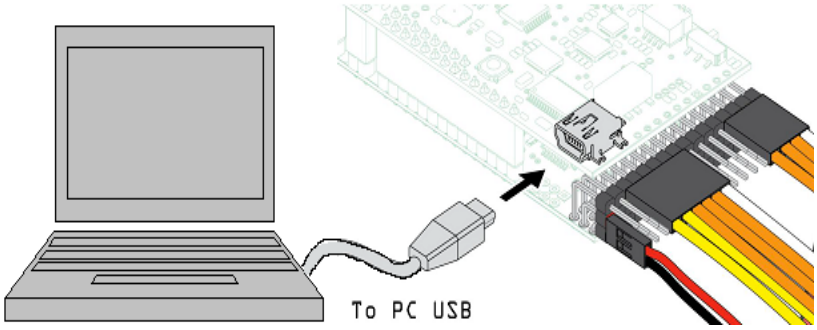

Figure 5. 1: Serial port connection

(Adapted from ArduCopter, 2011)

The driver installation of the serial port is introduced briefly below. Using the one end of a USB cable plugged into the arduino mega board (see Figure 5.2), and the other end of the USB cable to the PC's USB port.

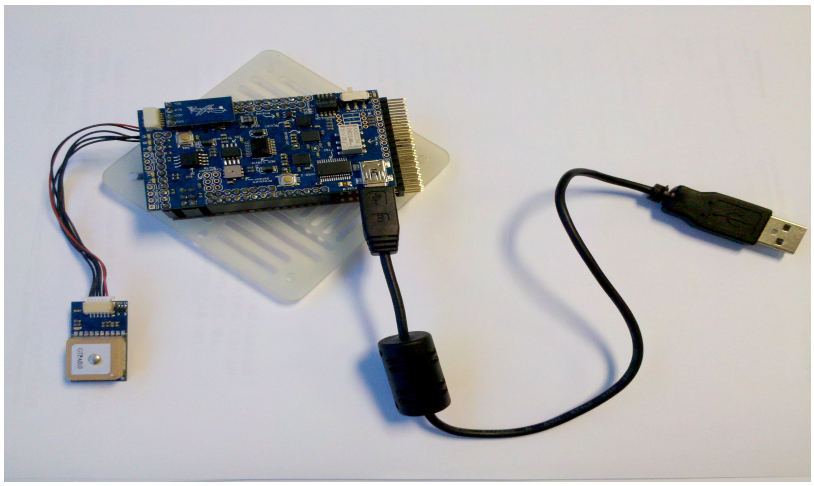

Figure 5. 2: Realistic serial port connection

After a few seconds the “new hardware found” window will appear on the computer screen; click “Browse” to set up the right path to install the hardware driver, which is under the “arduino-0022 folder\drivers\FTDI USB Drivers”, as shown in Figure 5.3 and click the “Next” button to continue.

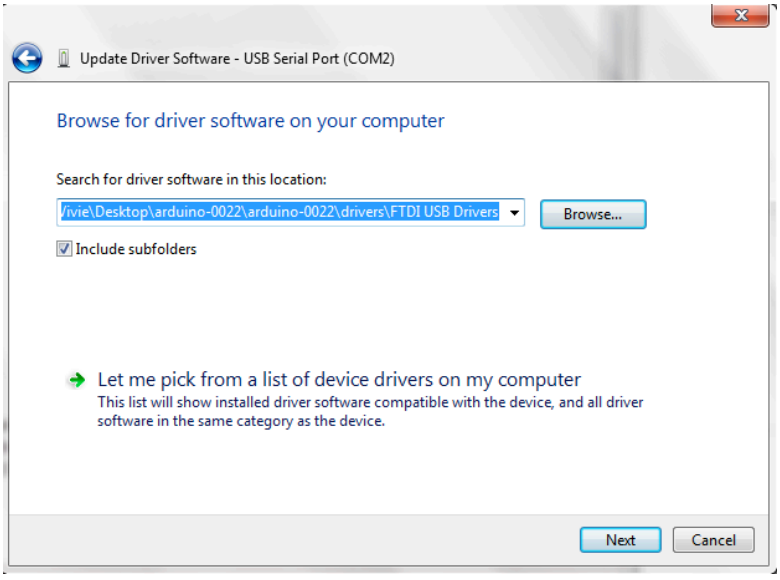

Figure 5. 3: Driver installation for USB serial port

After clicking the “Next” button, Windows will automatically install the driver. The next time that the PC is switched on it will not search the diver again. At a later stage, the in-use serial port will appear on the Windows Device Manager, which is shown in Figure 5.4.

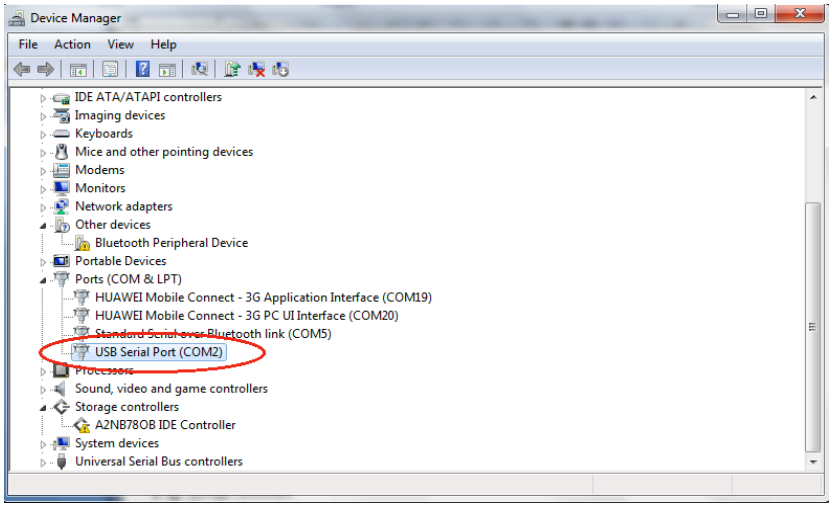

Figure 5. 4: Serial port setting

Before the end-user connects the arduino mega board and the PC via a USB cable, he/she should ensure that the baud rate for the dedicated serial port or different baud rate is selected from the “Port setting option”, as shown in Figure 5.5 below.

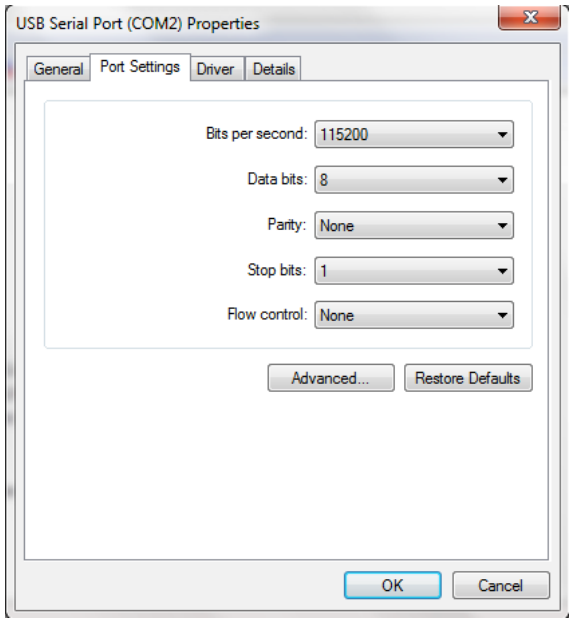

Figure 5. 5: Baud rate setting

Once the number of the serial port and band rate are established, the next stage is to open the ground control station software, which is called the APM mission planner, which is shown in Figure 5.6.

Figure 5. 6: Ardupilot Mega Planner interface

There are three options, which are located in Figure 5.6. The first is the UAV type selection, which uses “ArduCopter2”, followed by the serial port option and the baud rate option, which must be the same as shown above. Following this, click the “connect button”. So that, the ground control station software is able to display the flight information in real- time (see Figure 5.7).

Figure 5. 7: Real-time status of Ardupilot Mega Planner

To select the “Tuning option” from the APM Planner software, the real-time roll, pitch and yaw data will be shown out as real-time, as shown in Figure 5.7.

The on-board raw sensor data can be read and stored in the ground software. There are two ways to monitor and save raw sensor data, which are outlined below.

- Select the raw sensor view option from the APM planner (see Figure 5.8), and at a later stage, click “Save CSV” in order to save the requested data.

Figure 5. 8: Raw sensor data view interface

An advantage of this way is shown by means of a graphical diagram to the end-user, but can only be plotted three-axial of the accelerometer and three-axial of the gyro.

- Another way is by using Command Line Interface (CLI) by choosing the “Terminal” option from the APM planer software (see Figure 5.9) beneath the “Test” command. There are certain options for purposes of on-board flight components testing, such as “PWM”, “IMU”, “GPS”, “Gyros”, and so on.

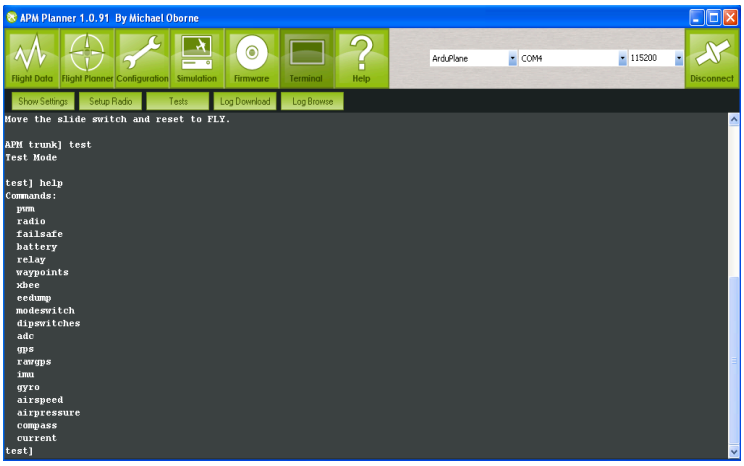

Figure 5. 9: Variety of raw sensor testing under the CLI mode

An advantage of this approach is the variety of on-board raw sensor's data, but end-users should manually download the flight log file, as well as the graph sensor data. Figure 5.10 below shos the data in graph format.

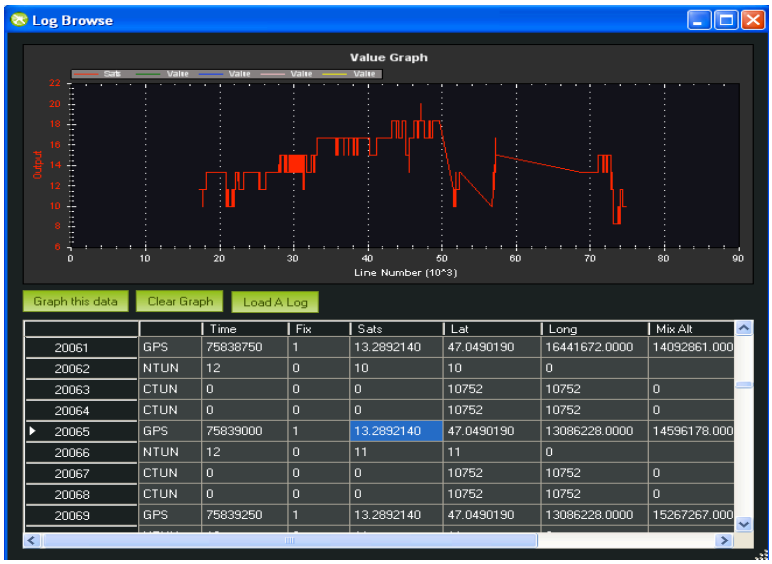

		Time	Fix	Sats	Lat	Long	Mix Alt
20061	GPS	75838750	1	13.2892140	47.0490190	16441672.0000	14092861.000
20062	NTUN	12	0	10	10	0	
20063	CTUN	0	0	0	10752	10752	0
20064	CTUN	0	0	0	10752	10752	0
20065	GPS	75839000	1	13.2892140	47.0490190	13086228.0000	14596178.000
20066	NTUN	12	0	11	11	0	
20067	CTUN	0	0	0	10752	10752	0
20068	CTUN	0	0	0	10752	10752	0
20069	GPS	75839250	1	13.2892140	47.0490190	13086228.0000	15267267.000

Figure 5. 10: Raw sensor data graph

The download log file can be saved in a Microsoft Excel format (see Figure 5.11). Column A shows the sampling time, while column B to column D, respectively, show the value of the accelerometer's X, Y, Z axis (see Figure 5.12 to Figure 5.14), and column E to column G, respectively, show the value of the gyro's X, Y, Z axis (see Figure 5.15 to Figure 5.17).

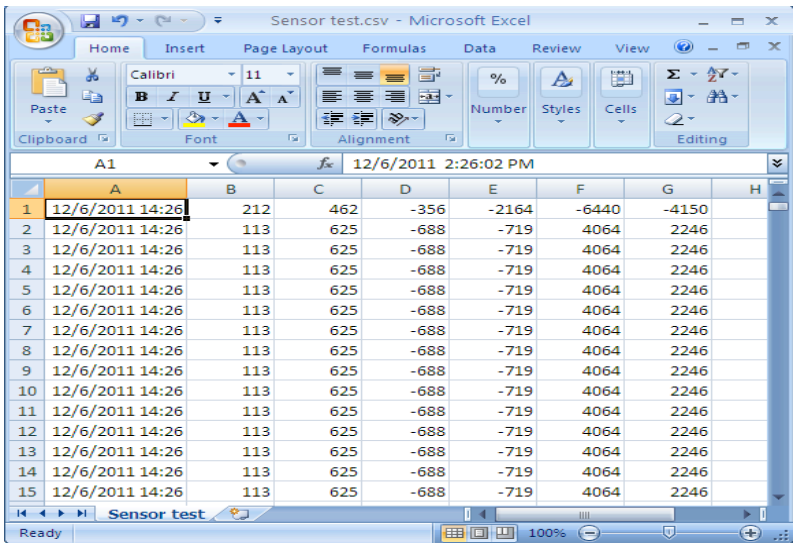

	A	B	C	D	E	F	G
1	12/6/2011 14:26	212	462	-356	-2164	-6440	-4150
2	12/6/2011 14:26	113	625	-688	-719	4064	2246
3	12/6/2011 14:26	113	625	-688	-719	4064	2246
4	12/6/2011 14:26	113	625	-688	-719	4064	2246
5	12/6/2011 14:26	113	625	-688	-719	4064	2246
6	12/6/2011 14:26	113	625	-688	-719	4064	2246
7	12/6/2011 14:26	113	625	-688	-719	4064	2246
8	12/6/2011 14:26	113	625	-688	-719	4064	2246
9	12/6/2011 14:26	113	625	-688	-719	4064	2246
10	12/6/2011 14:26	113	625	-688	-719	4064	2246
11	12/6/2011 14:26	113	625	-688	-719	4064	2246
12	12/6/2011 14:26	113	625	-688	-719	4064	2246
13	12/6/2011 14:26	113	625	-688	-719	4064	2246
14	12/6/2011 14:26	113	625	-688	-719	4064	2246
15	12/6/2011 14:26	113	625	-688	-719	4064	2246

Figure 5. 11: Sample result of raw sensor data in the CSV file

5.3 Methodology

To test and verify data collection accuracy of the on-board sensor shield, the pendulum movement experiment was used in this project. The serial port communication was also involved. The following steps should be accomplished:

1. Establish the pendulum system with the ArduPoilt Mega controller and the IMU sensor shield (see Figure 5.13);
2. Simulate the pendulum system in the Matlab, and plot the linear velocity attenuation and angular displacement;
3. Collect the APM raw sensor reading data via the serial port connection, and plot the pendulum linear velocity attenuation figure;
4. Compare the accuracy of the simulation result and the actual result (serial port connection); and
5. Compare the accuracy of the simulation result and the actual result (wireless connection).

5.3.1 Overview of the pendulum mathematical model

The following are parameters of the pendulum system (see figure 5.12). The cycloid of the pendulum is l; the mass of the pendulum is m; the acceleration owing to gravity is g; the initial time is $t = 0$; the pendulum's linear acceleration is $v(t)$ when $t \geq 0$; the angular acceleration $\omega(t)$; and the angular displacement is $\theta(t)$.

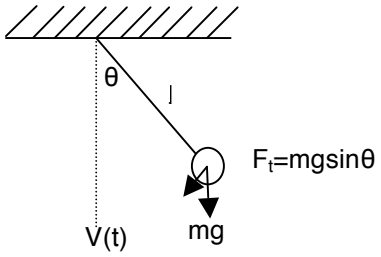

Figure 5. 12: Force analysis in field of gravity

Zhang (2009) presents the following equations:
At the t moment, the tangential force of the pendulum is:

$$f_t(t) = mg\sin\theta(t). \quad [5.1]$$

If there is no air friction in this system, according to Newton's second law, the tangential acceleration is:

$$a(t) = g\sin\theta(t). \quad [5.2]$$

Therefore, the motion of the pendulum's differential equations of motion is as follows:

$$\frac{dv(t)}{dt} = g\sin\theta(t) \quad [5.3]$$

$$\frac{d\theta(t)}{dt} = -\omega(t) = -\frac{v(t)}{l} \quad [5.4]$$

If there is air friction in this system, assuming the resistance is

$$f_r(t) = -kv(t), \quad [5.5]$$

where, $k \geq 0$, which is resistance coefficient, when there is a negative in eq. [5.5], means that the motion of resistance and the pendulum in opposite direction is

$$a(t) = g\sin\theta(t) - \frac{kv(t)}{m}. \quad [5.6]$$

The motion of the pendulum's differential equations of motion is shown below:

$$\frac{dv(t)}{dt} = g\sin\theta(t) - \frac{kv(t)}{m} \quad [5.7]$$

$$\frac{d\theta(t)}{dt} = -\frac{v(t)}{l} \quad [5.8]$$

Using Euler's method, to substitute $dv(t) = v(t+dt) - v(t)$ and $d\theta(t) = \theta(t+dt) - \theta(t)$ into eq. [5.7] and [5.8], obtains the time based recursion equations

$$v(t+dt) = v(t) + (g\sin\theta(t) - \frac{kv(t)}{m})dt \quad [5.9]$$

$$\theta(t+dt) = \theta(t) - \frac{v(t)}{l}dt \quad [5.10]$$

Now the eq. [5.9] and [5.10] can be used in simulation of the pendulum system.

5.3.2 Pendulum system simulation

To ensure that the results are as accurate as possible, the actual pendulum system was also established (see Figure 5.13). In this system the ArduPoilt Mega controller and APM board, as well as the IMU Sensor shield and base plate take the weight of the pendulum system. The following parameters are based on measured value from the experimental platform:

- The cycloid length of the pendulum L=0.7m; and
- Mass of the pendulum m=0.244 kg.

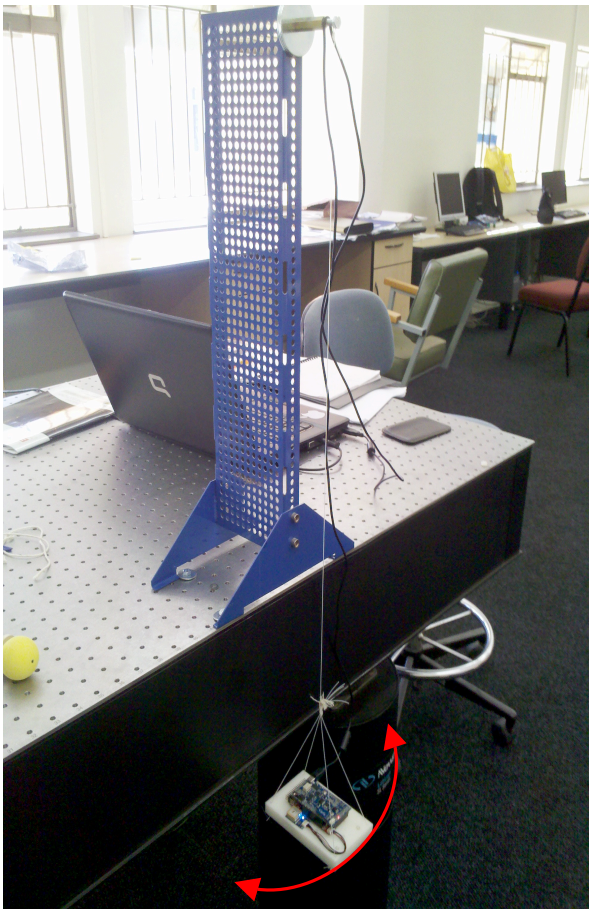

Figure 5. 13: The pendulum system

Figure 5.14 plots the simulation of the attenuation of the pendulum's movement system (the code for pendulum simulation is shown in Appendix A), and assuming that there is resistance from the air (K=0.06), the value of K may be much smaller in reality, with an initial angular setting of θ(0)=3.1. It is close to π, therefore, the initial position of the pendulum approaches maximum point, and hence the obvious non-linear characteristic can be displayed.

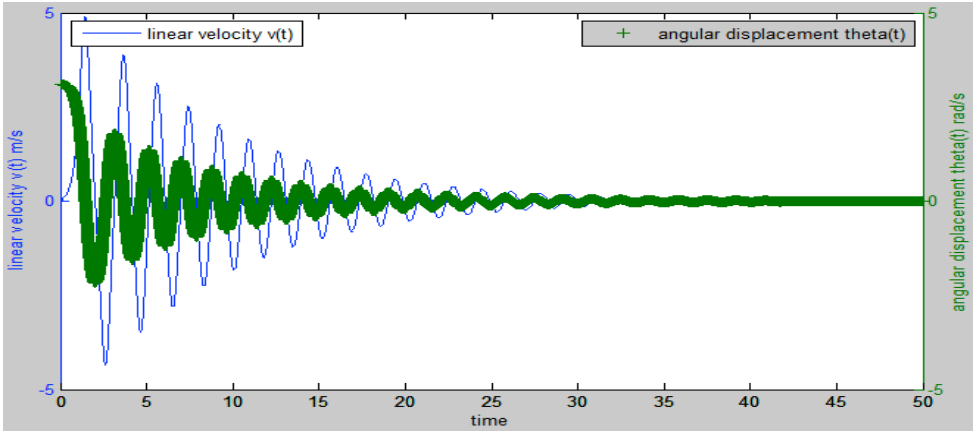

Figure 5. 14: The simulation pendulum system with k=0.06

Figure 5.14 assuming 'θ(0)=3.1', approaching the radian π, therefore, the pendulum almost approaches the maximum point, hence the start-up speed slowly increases, when angular displacement reaches $\pi/2$, and the pendulum reaches maximum acceleration speed. When the pendulum's position is at the lowest point and the angular displacement equals zero, the linear velocity will reach its maximum. If k=0, the linear velocity will reach maximum point when the pendulum's position is at the lowest point.

As mentioned above, if k=0, which means that there is no air friction and no energy loss in the pendulum system, the pendulum swing will continue (see Figure 5.15).

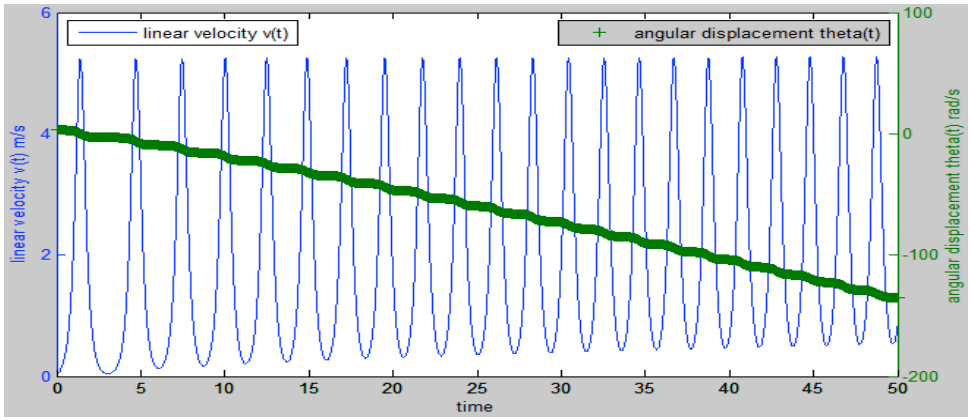

Figure 5. 15: The simulation pendulum system with k=0

Table 5. 1: Simulation with different air damping coefficients in first 20 seconds

Air damping coefficient	Max linear velocity	Min linear velocity	Max angular displacement	Min angular displacement
K=0.06	4.9	0.72	3.1	0.24
K=0.08	4.8	0.29	3.1	0.12
K=0.10	4.7	0.14	3.1	0.06
K=0.12	4.6	0.07	3.1	0.02
K=0.14	4.5	0.035	3.1	0.009

According to Table 5.1, the air damping coefficient is in inverse proportion of both the linear velocity and angular displacement.

5.3.3 On-board IMU sensor data output for pendulum system

Hence, the real-time data collection for the pendulum system has been monitored. Figure 5.16 presents the process of the pendulum system's attenuation.

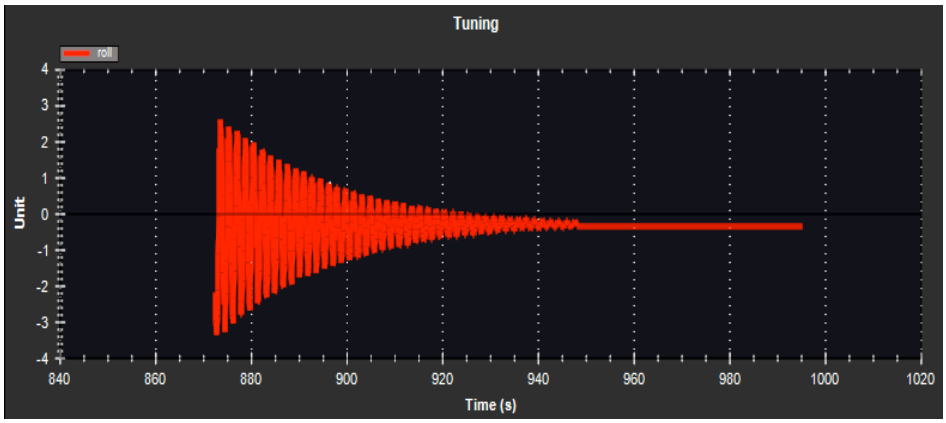

Figure 5. 16: The real-time response of the pendulum system

5.3.4 On-board sensor data reading for pendulum system via MATLAB

Once the raw sensor data is generated, the MATLAB is capable of analysing the sensor information. The procedure is presented below:

1) Find the log file location from the PC, by the default setting, which is under the "Mission Planner\Logs";
2) Open the MATLAB software; go to "File>>Import Data"; and choose the sensor log file;
3) The "Import wizard" window will prompt the end-user, to click "Next", which completes the data import. See Figure 5.17.

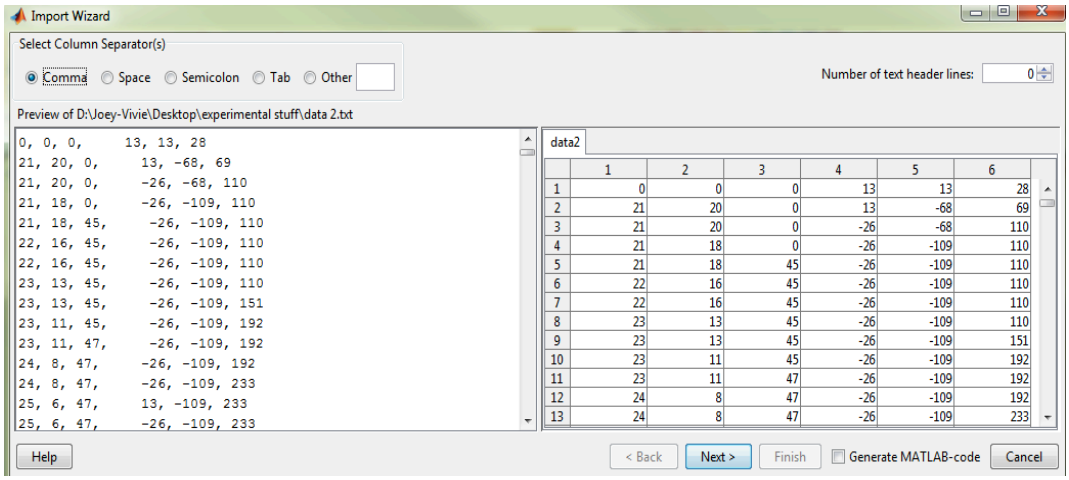

Figure 5. 17: Sample result sensor data import to MATLAB

4) At this point the imported raw sensor data can be found at the “Workspace” window and is named “data” by default. This is shown in Figure 5.18.

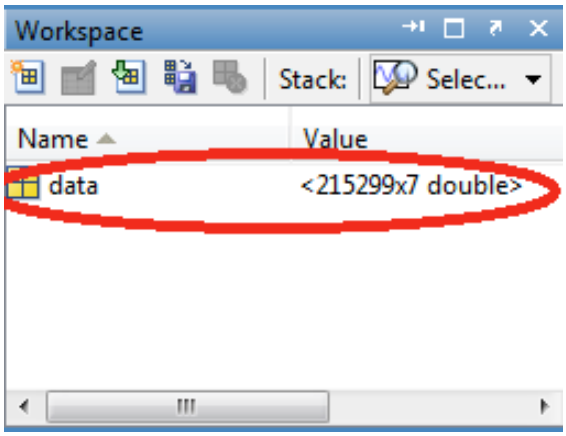

Figure 5. 18: Imported raw sensor data in MATLAB

5) To plot the sample data diagram for the Acceleometer and Gyro in X-axis (see Figure 5.19), the following command should be written:

The Acceleometer

```
>> Acc_X=data(2:size(data,1),1);%to read the first column  data,
                               %from the beginning to the end
>> plot(Acc_X);                %to plot the data
>> title('Accelerometer');     %to write the title
>> xlabel('Testing Time=780Seconds’)       %to name the x label
>> ylabel('X axis');           %to name the y label
```

The Gyro

```
>> Gyro_X=data(2:size(data,1),5);%to read the fifth column data,
                                 %from the beginning to the end
>> plot(Gyro_X);                 %to plot the data
>> title('Gyro');                %to write the title
>> xlabel('Testing Time=780Seconds')  %to name the x label
>> ylabel('X axis');            %to name the y label
```

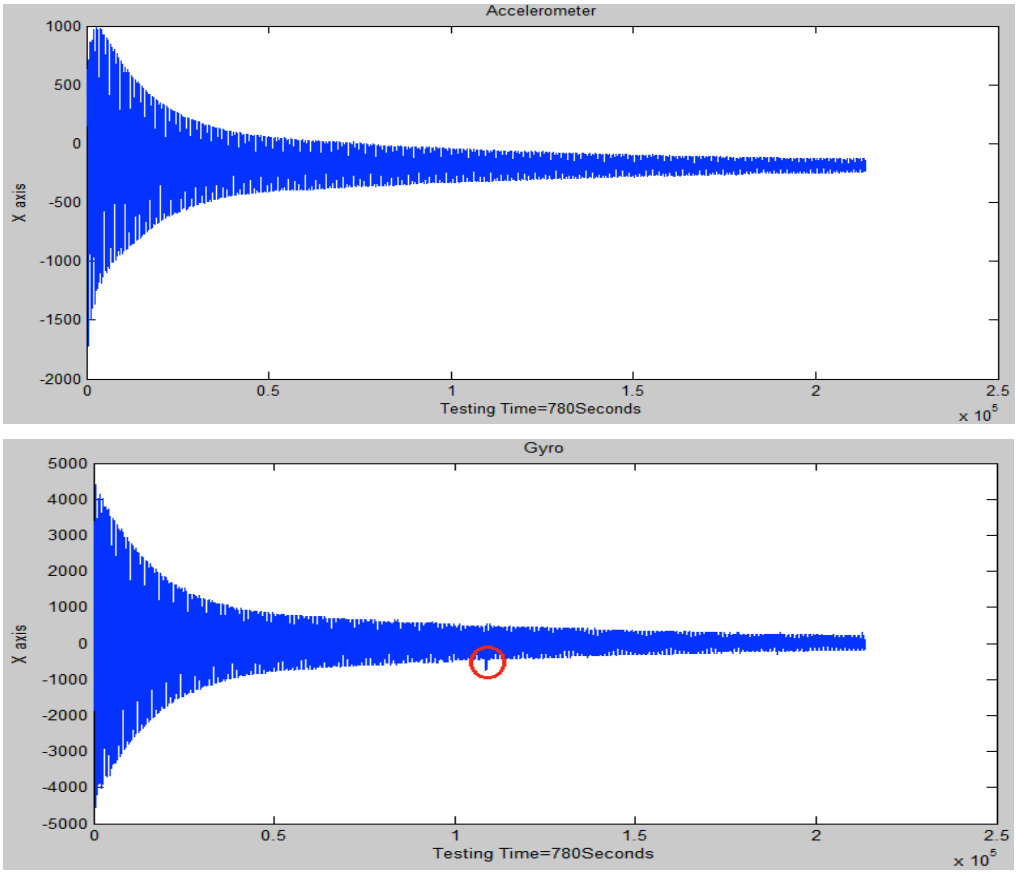

Figure 5. 19: IMU raw sensor data plot
for Accelerometer (Upper) and Gyro (Lower) in X-axis

The accelerometer measures acceleration, which measures the difference between any linear acceleration in the accelerometer's reference frame and the earth's gravitational field vector (Salhuana, 2012). Hence, assuming that the pendulum movement does the 'Roll' movement for the aircraft, and the X-axis of the accelerometer's raw data records, the linear volocity is the 'Roll' movement for the pendulum. Figure 5.19 above (Upper) X-axis shows the raw accelerometer reading of linear volocity attenuation and the (Lower) X-axis shows the raw gyro reading of the angular displacement of the pendulum movement.

During the test, there could be some friction between the communication cable and the pendulum stand. The above marked “red rings” in Figure 5.19 show that the noise was picked up during the real-time data collection procedure, which may be the noise from the “Mini-B” port , cable, or was generated by AMP controller. The answer can be found once the XBee wirelss module is implemented in this experiment.

Since erroneous data was collected, more pendulum data collection tests had to be conducted (minimise the contact between cable and pendulum stand). The following figures represent the sample test result of the real-time on-board data collection.

The running time for the pendulum system is 780 seconds (from pendulum start-up until it is still), and it is without any man-made interruption during the sample test.

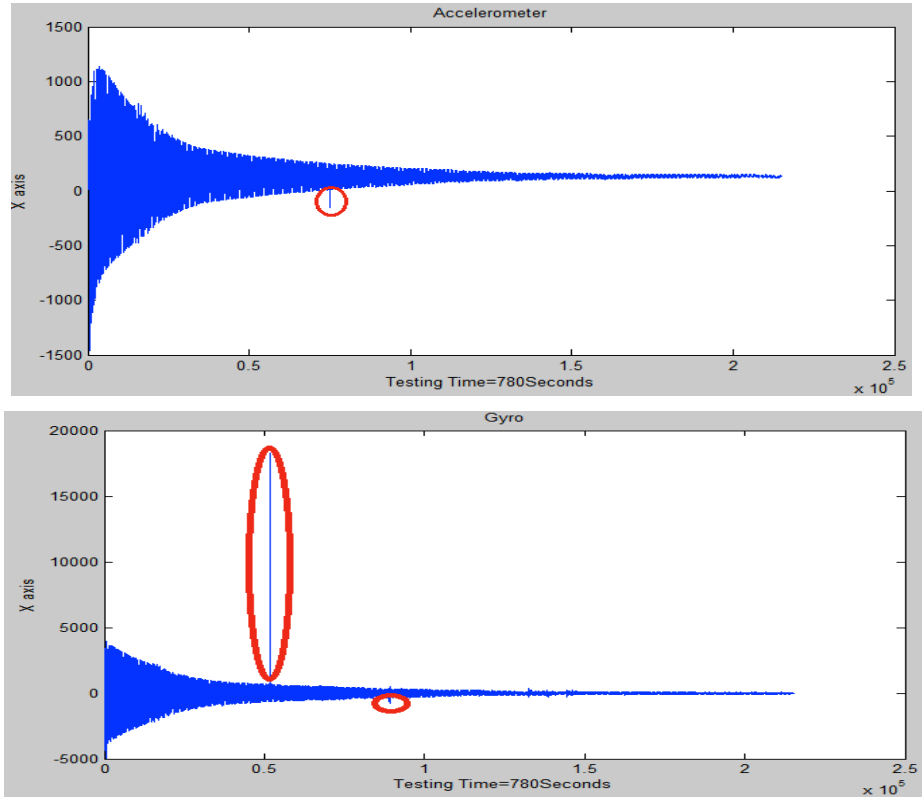

Figure 5. 20: Sample No.1 IMU data plot

Accelerometer (Upper) and Gyro (Lower) in X-axis

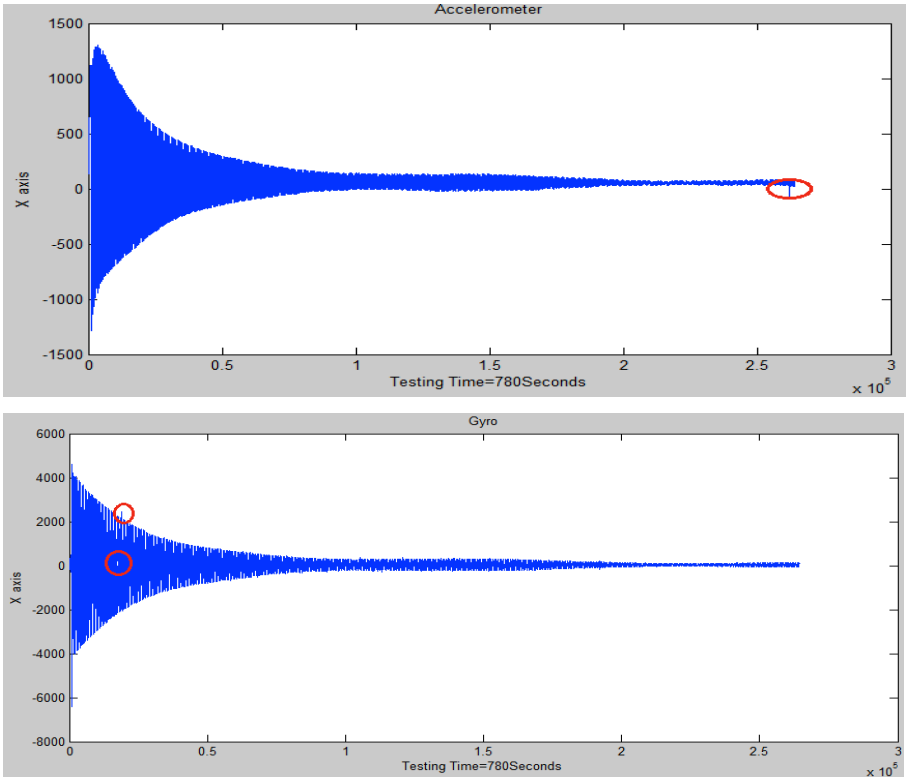

Figure 5. 21: Sample No.2 IMU data plot
Accelerometer (Upper) and Gyro (Lower) in X-axis

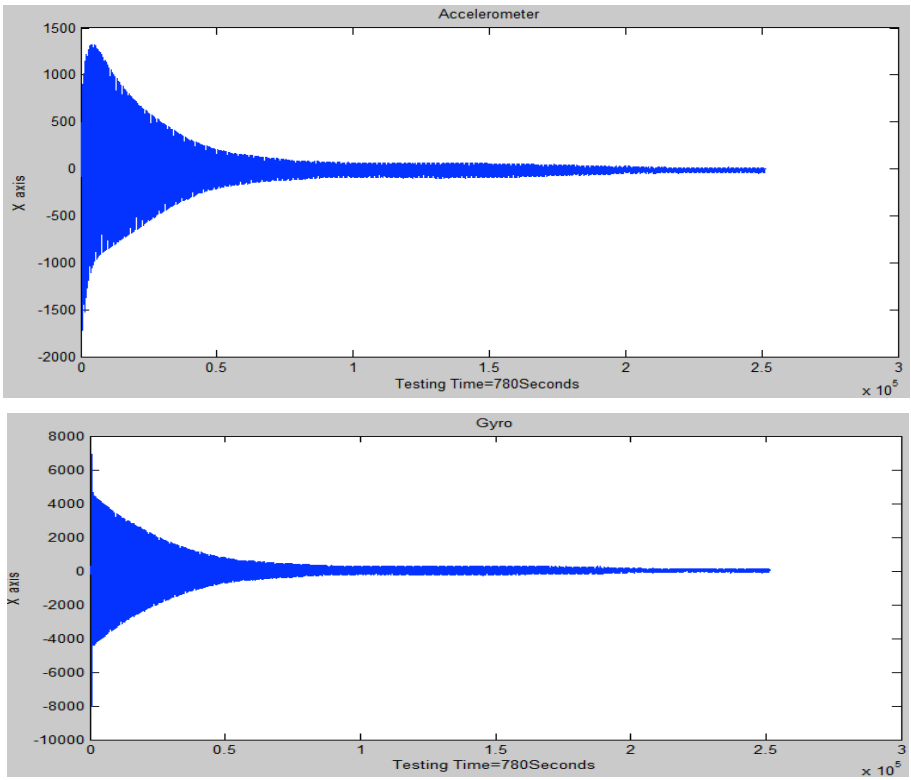

Figure 5. 22: Sample No.3 IMU data plot for
Accelerometer (Upper) and Gyro (Lower) in X-axis

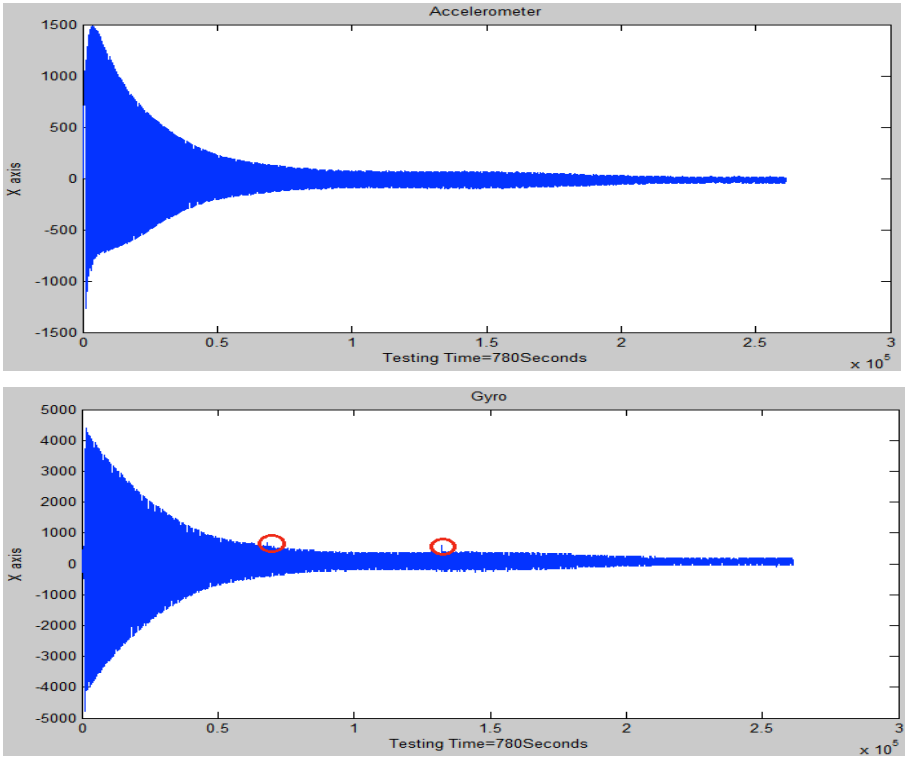

Figure 5. 23: Sample No.4 IMU data plot for Accelerometer (Upper) and Gyro (Lower) in X-axis

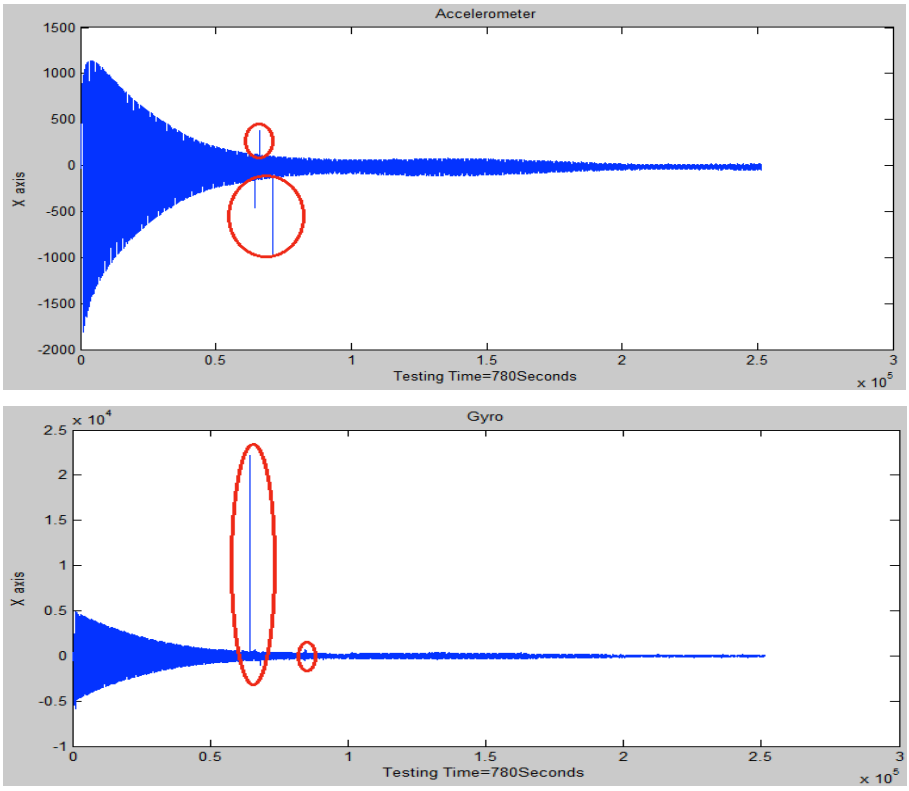

Figure 5. 24: Sample No.5 IMU data plot for Accelerometer (Upper) and Gyro (Lower) in X-axis

Through the 5 times sample test, only Sample No.3 was without any noise. The rest of the sample test results, either produced erroneous data, or data was lost during the data collection process.

The following actual parameters were applied to the Matlab program and compared with the real-time data that was collected:

- The cycloid length of pendulum L=0.7m;
- Mass of pendulum m=0.244 kg;
- Theta0=30.1°;
- Assuming air damping coefficient k=0.006; and
- Simulation time T=780s.

The desired linear velocity and angular displacement is shown in Figure 5.25.

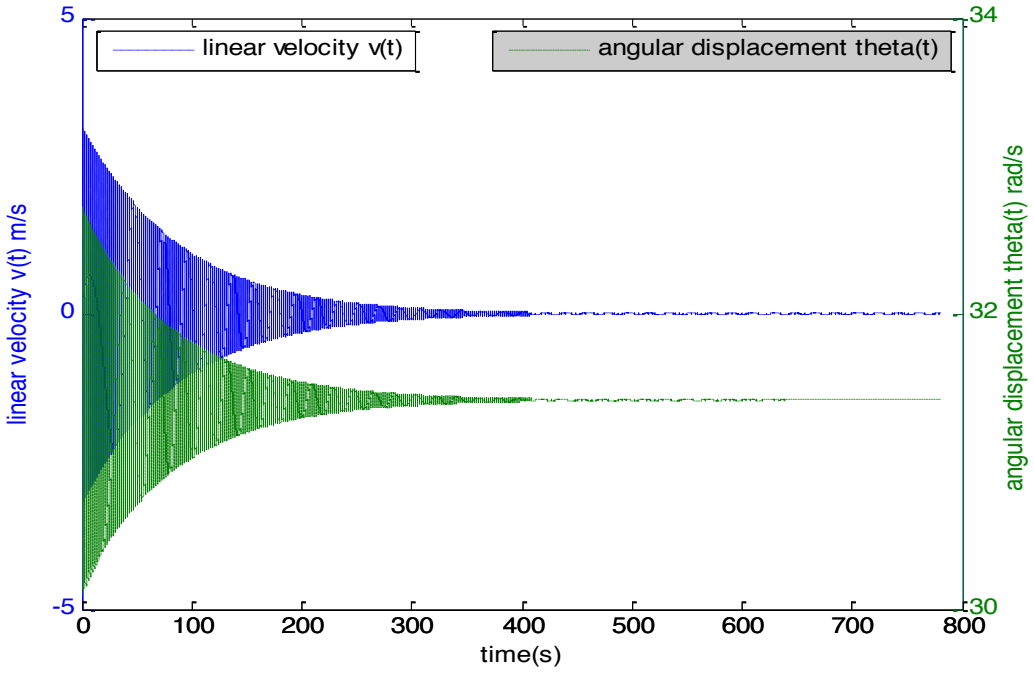

Figure 5. 25: The pendulum desired output with serial communication

The erroneous data, may cause noise to be generated by the serial conection port or the “USB to mini B” cable itself.

To prevent this from occuring, it should be compared with wireless communication.

5.3.5 Basis of the Arduino developing environment

Arduino is a new tool, which is an open-source electronics prototype platform that can make computers sense environment variables and produce meaningful data for end-users. It is based on a simple microcontroller board, and also provides a development environment, which writes individual programs for the chip board. The program language is similar to Java and C language, so making Arduino a physical computing platform establishes the communication between the hardware and software.

Once the program is uploaded to the chip board, Arduino is able to take inputs from a variety of sensors, and take control of it such as LED lights, motors, and so on.

5.3.6 Arduino 0022 open-source software

The software can be downloaded from Arduino's official website. Figure 5.26 below shows the interface of the program's platform.

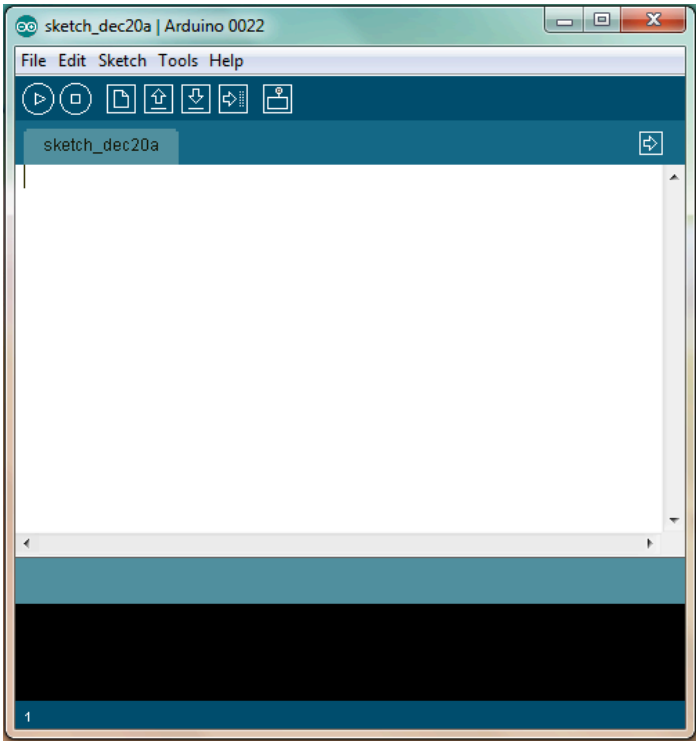

Figure 5. 26: Arduino program interface

In the following step the connection between the Arduino mega board and the Arduino program software would be established.

5.3.7 Arduino 0022 connection with the Arduino mega board

To ensure both the software and hardware, which have contradictory serial communication, the following aspects are always considered: 1) serial port number; 2) bauld ratio; and 3) board speicifications. The procedure is introduced below.

- Select the “Tools” option from the Arduino 0022 program software, and set the board as “ Arduino Mega 2560” as shown in Figure 5.27 below.

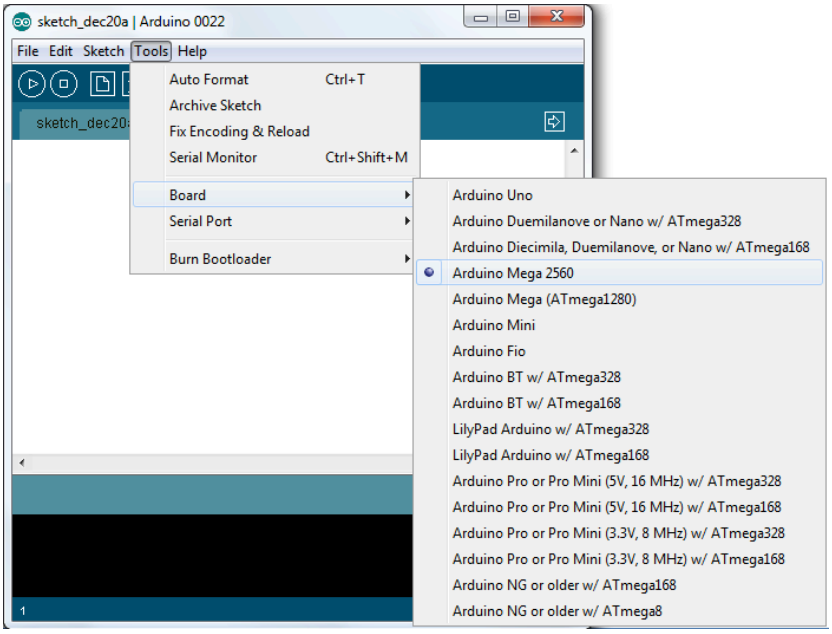

Figure 5. 27: Arduino Mega board selection

- Select the “Tools” option from the Arduino 0022 program software, and set the serial port as the used serial port (see Figure 5.28).

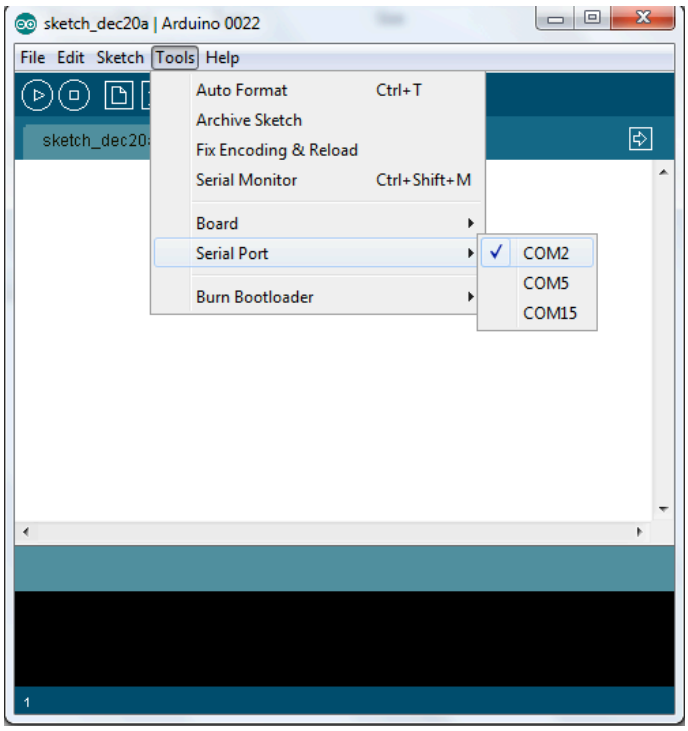

Figure 5. 28: Serial port selection

- To correctly display real-time sensor information, click the “Serial Monitor” option, and set the baud ratio from the software that must match the actual baud rate (see Figure 5.29). Once the following window is prompted, the sensor data can be evaluated by typing certain commands.

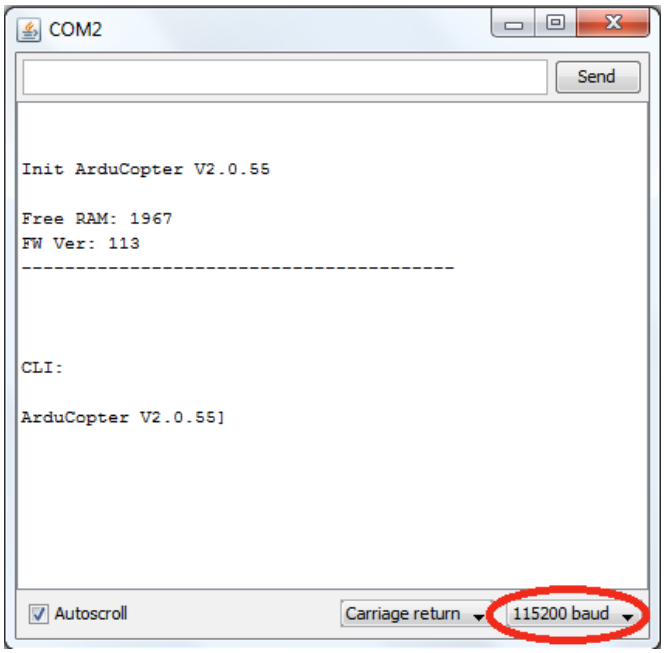

Figure 5. 29: Baud rate setting

5.3.8 Sample data test from Arduino 0022

As mentioned in 5.3.2 above the raw sensor's real-time data is able to show in the "Serial Monitor" window. Therefore, the sample data of the IMU sensor shield and altitude can be displayed, as shown in Figure 5.30 and Figure 5.31:

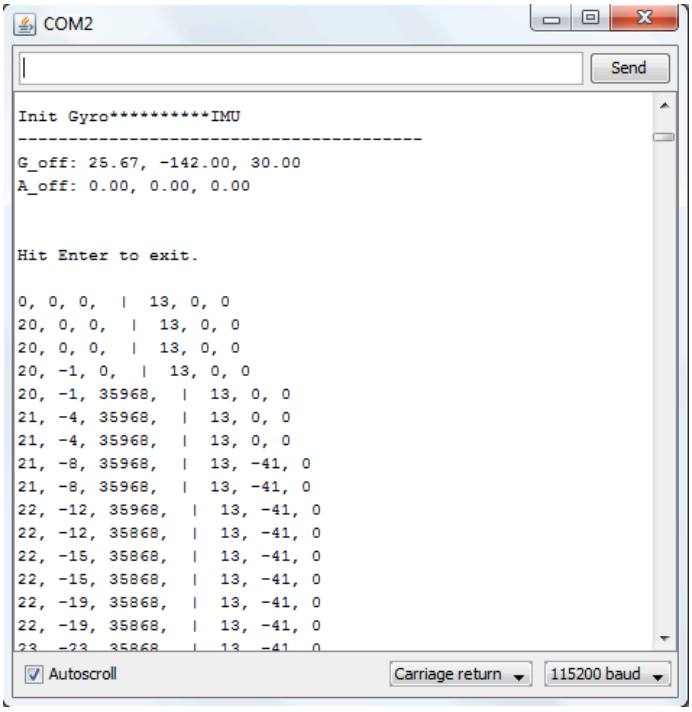

Figure 5. 30: Sample test data of IMU

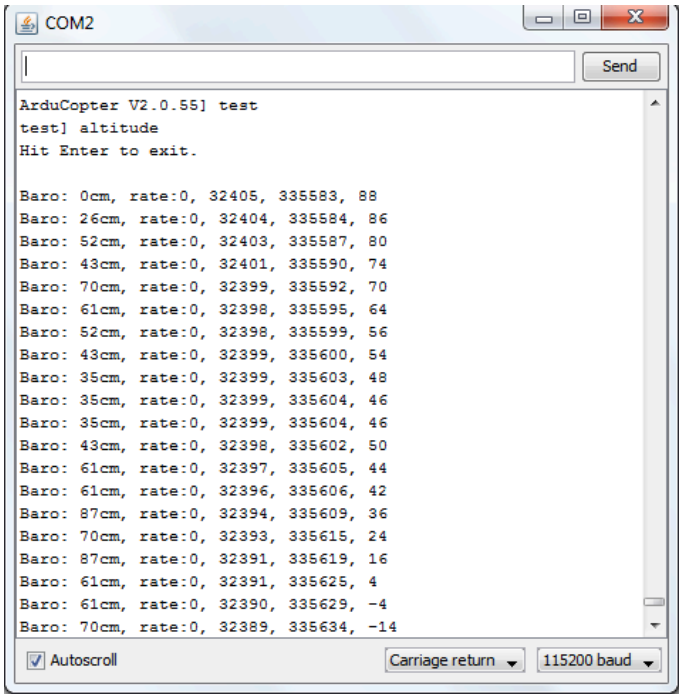

Figure 5. 31: Sample test data of barometer

The sample code for running the IMU sensor (see Appendix B) should be uploaded to the Arduino mega board before the test. Figure 5.32 below shows the gyro and the accelerometer's real-time output value, which is displayed in the "Serial Monitor" window.

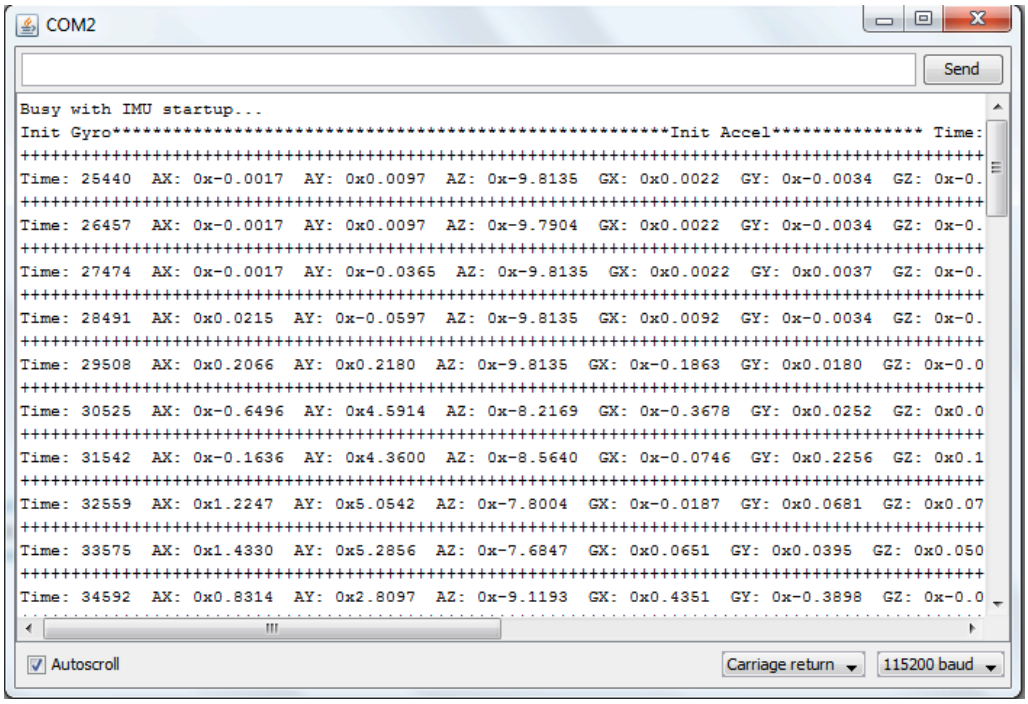

Figure 5. 32: The real-time output data for running the uploaded code of IMU

There are more sample codes for the Arducopter's on-board sensors are not introduced in this chapter (these are available on the Arducopter website).

5.4 The basis of serial bus communication

In this project the serial bus connection plays an important role for communication between the on-board microcontroller and the ground control station. Therefore, some of the basic serial communication types are introduced below.

As this type of communication processes the sending data in one bit at a time, it is done so sequentially via the communication channel or computer bus. However, transmission speed and signal integrity of the serial bus communication will affect its reliability.

In general, the Universal Serial Bus (USB) connection is for communication and power supply between computers and electronic devices (Wikipedia, 2011b); the Serial Peripheral Bus (SPI) connection is to connect with microprocessors and other peripheral chips (Jean & Steve, 2003:6); the Small Computer System Interface (SCSI) connection is most commonly used for hard disks and tape drives, but it can connect a wide range of other devices, including scanners and CD drives (Wikipedia,

2011c); and the I^2C connection is used to attach low-speed peripherals to the motherboard, embedded system, or other electronic device (Wikipedia, 2011d).

The speed of several connectivity methods is shown below in Table 5.2.

Table 5. 2: Speed of some of serial connections (bits/second)

Connection Methods	Data Rate
Universal Serial Bus (USB 1.1)	Low speed1.5Mb/s; Full speed 12Mb/s
Universal Serial Bus (USB 2.0)	High speed 480Mb/s
Universal Serial Bus (USB 3.0)	Super speed 4.8Gb/s
Serial Peripheral Bus (SPI)	Original speed 110kHz
Small Computer System Interface (SCSI) parallel bus	40 MHz
Fast SCSI	8-80 MHz
Ultra SCSI	18-160 MHz
I^2C bus	100 KHz, 400 KHz, 3.4 MHz

(Adapted from Jean & Steve, 2003:5)

5.4.1 The Universal Asynchronous Receiver Transmitter (UART)

The UART is a common slow speed communication standard; the speed is up to 1 Mbits/s. The asynchronous means that the clock information of data is not included in the sending data, therefore, the sender and receiver must arrange timing parameters before engaging with this transmission (Jean & Steve, 2003:6).

Jean and Steve (2003:6) also state the following aspects: 1) the purpose of the UART is to convert bytes from the computer's parallel bus to a serial bit-stream; 2) for instance, there is a terminal, which connects with the PC for use by an end-user who wishes to send a command or character, hence the UART transmitter of the terminal will receive those commands or characters. Thereafter, the transmitter processes its byte onto the serial line one bit at a time with a specific transmitting rate; and 3) in the end, the UART receiver takes all of the bits and rebuilds the (parallel) byte to place it in a buffer. Figure 5.33 shows how the UART indicates, which data should be sent.

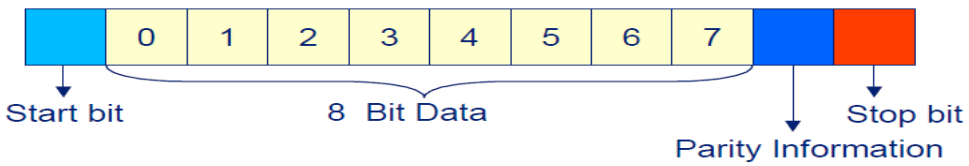

Figure 5. 33: The "Start bit" and "Stop bit"
presents the UART data's transmitting status

(Jean & Steve, 2003:6)

5.4.2 The Universal Serial Bus (USB) overview

The USB is a standard, which connects PCs to peripherals. Jean and Steve (2003:9) state categorically that there are some advantages of using the USB, which are described below:

- Hot pluggable;
- Supported by 99% of PCs;
- Up to 127 devices can be connected together;
- USB interface is commonly used
  - USB to serial port; and
- Data transfer rates up to 12 Mbps.

The USB is a simple piece of hardware and transceiver, which compares with another communication bus. It is a synchronous transmission, but can be a higher power consumption (Jean & Steve, 2003:9).

5.4.3 The I2C bus

The I^2C bus (see Figure 5.34) is also called the Inter- integrated circuit bus. It is a serial bus that allows multiple low speed peripherals such as sensors that are connected to a microprocessor. It is a popular communication protocol with low-bandwidth, and short-distance in an embedded system.

It comprises two physical wires, namely the Serial Data (SDA), and the Serial Clock (SCL), while the working voltage is +5 V or +3.3 V (Wikipedia, 2011d).

In this project the I^2C bus synchronized all the data transfer between the magnetometer and the “Oilpan”.

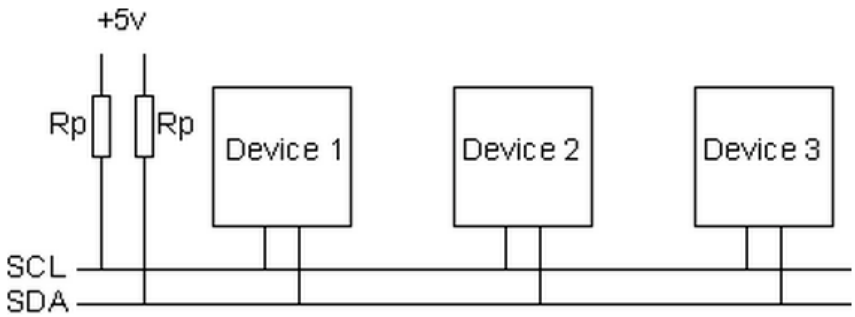

Figure 5. 34: The lay out of the I^2C Bus

(Robot-electronics, 2011)

Figure 5.38 shows that the SCL and SDA lines are connected to all devices on the I^2C bus. To make the circuit work, a third wire to the ground or 0 volts is required. There may also be a 5volt wire power, which is distributed to the devices.

Robot-electronics (2011) states that *"both SCL and SDA lines are "open drain" drivers. What this means is that the chip can drive its output low, but it cannot drive it high. For the line to be able to go high, you must provide pull-up resistors to the 5v supply. There should be a resistor from the SCL line to the 5v line and another from the SDA line to the 5v line.*" Therefore, Figure 5.38 presents only one set of pull-up resistors for the entire I^2C bus, and not for each device. The resistor Rp will pull the line up to +5V Vcc when there is no I^2C device pulling it down.

5.5 Wireless connection with APM mission planner

For wireless communication purposes, the XBee module was considered for this project. The module has minimal power demand, and also provides reliable data delivery between the UAV and the ground control station.

The test environment was indoors, and the longest distance in the lab was about 10 metres. The transmission range of the 2.4 GHz XBee module ensures that the two modules are able to receive each other's data successfully during the test.

The key features of 2.4 GHz XBee wireless module are shown in Table 5.3 below.

Table 5. 3: Specification of the XBee modules

Performance	XBee
Indoor range	Up to 30m
Outdoor RF LOS range	Up to 90m
Transmit power output	1mW
RF data rate	250,000 bps
Serial interface data rate (Select from software)	1200 bps – 250 kbps (or another baud rates)
Receiver sensitivity	-92 dBm (1% packet error rate)
Supply voltage	2.8-3.4v
Operating frequency	2.4 GHz
Operating temperature	-40 to 85℃
Communication interface	UART

(ArduCopter, 2011)

5.5.1 Hardwire connection with APM

The ArduCopter (2011) shows that when you connect the XBee wireless module with its adapter to the APM sensors shield (see Figure 5.35), the adapter should be in "Master" mode ("Master" and "Slave" - the reverse of the TX and RX pins).

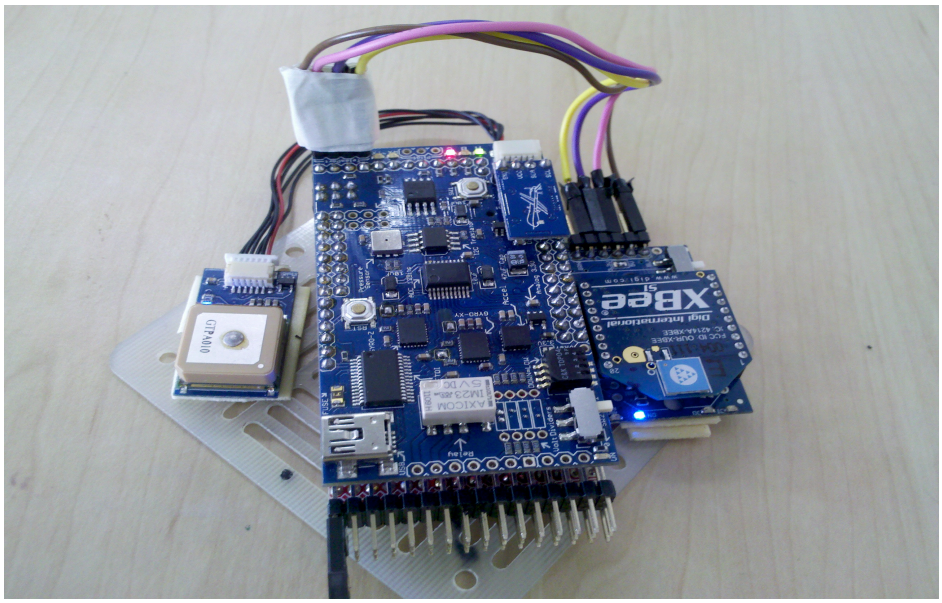

Figure 5. 35: XBee wireless module connection with APM & IMU sensor shield 2.4 GHz XBee module (RHS) and GPS (LHS)

5.5.2 Connection at ground control station

At the ground control station, the XBee adapter connects to the laptop's USB port via a USB to a mini B cable (see Figure 5.36).

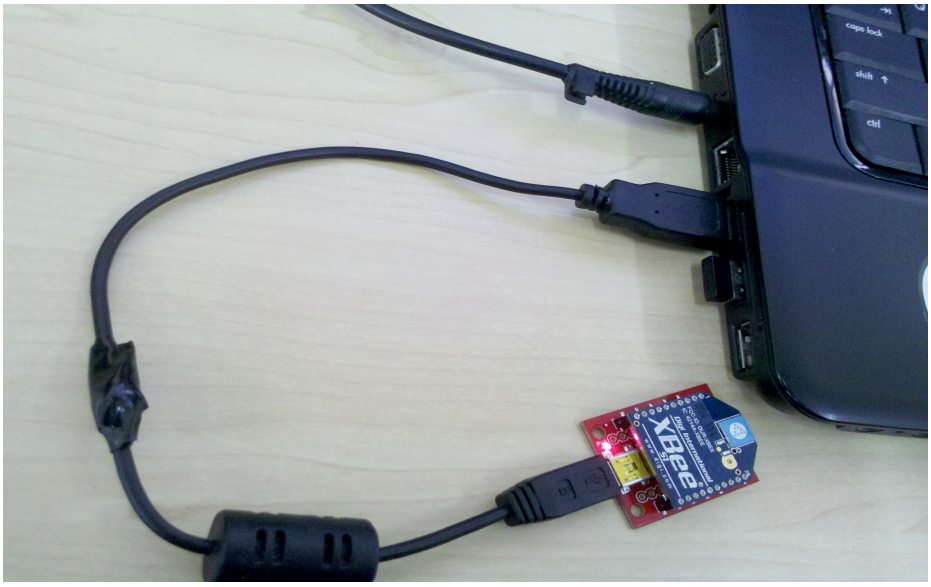

Figure 5. 36: XBee module attached with XBee Explorer board connection with laptop via USB to mini B cable

5.5.3 Setting up XBee module

Before establishing a connection between two XBee wireless modules, there should be configuration.

- Download and install the XBee configuration software Digi X-CTU and attach the first XBee module to XBee explorer board.
- The COM port will show in the Com port window and the baud rates of the XBee module is defaulted by 9600 Baud. To test the connectivity between the XBee module and the XBee explorer board, so click the “Test / Query” button (see Figure 5.37).

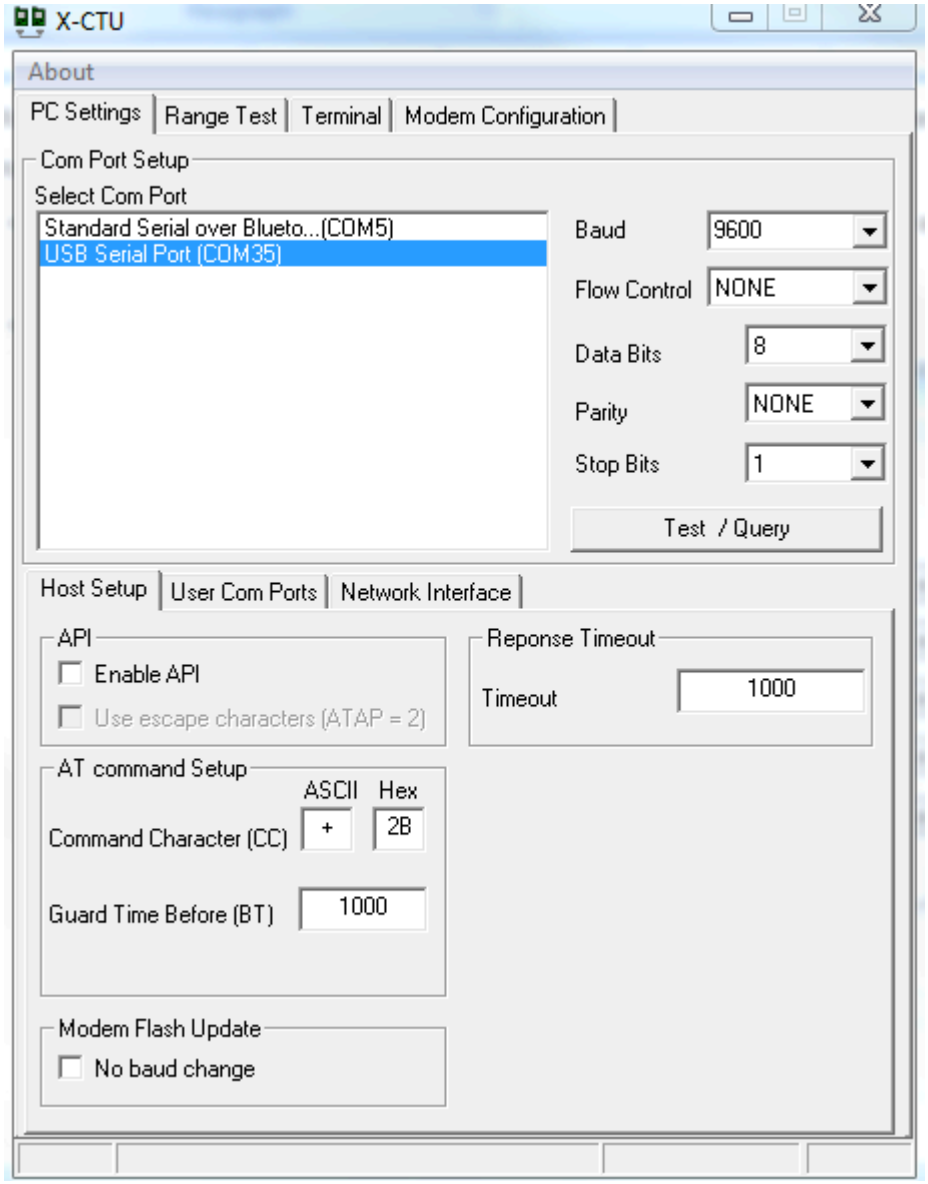

Figure 5. 37: XBee configuration software, X-CTU interface

- Click the “Read” button to display the current XBee module’s specifications.
- Choose the “Modem Configuration” button to program the Xbee modules. Because the address is different for each XBee module, assuming that the network topology is in point-to-point mode, here the second Xbee module’s address should be placed into first XBee module’s destination address, whilst placing the first Xbee module’s address into second XBee module’s destination address (see Figure 5.38).

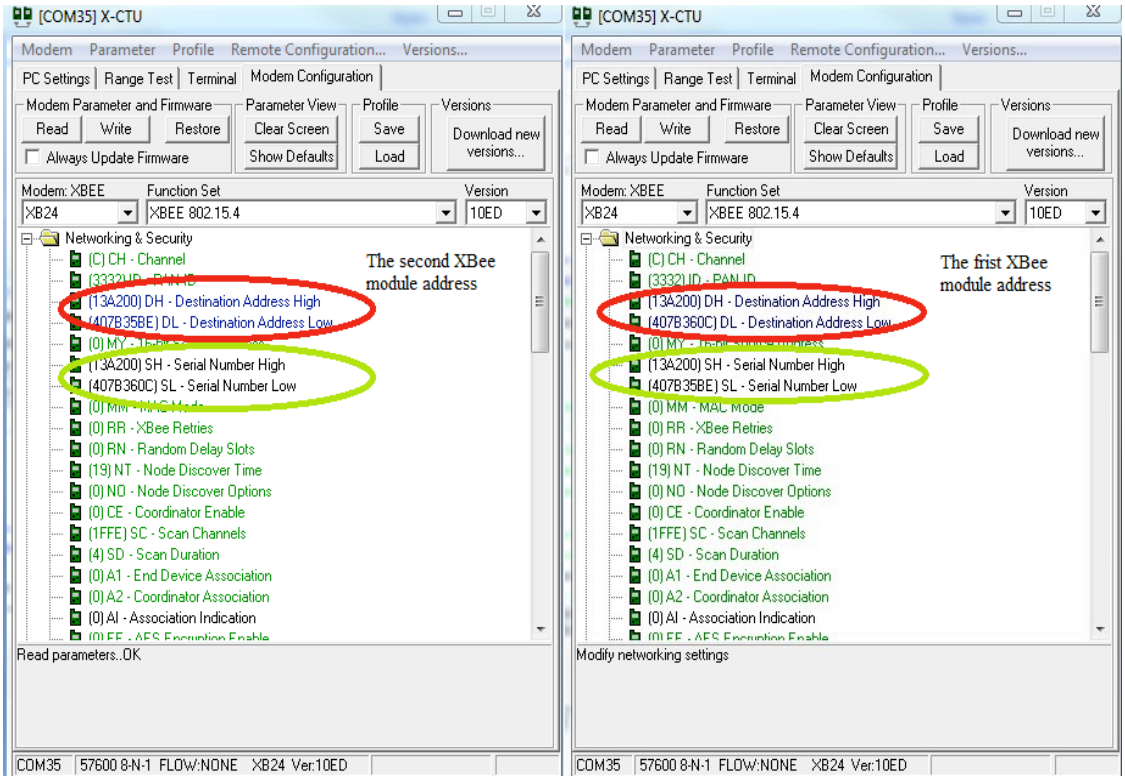

Figure 5. 38: XBee address configuration

- The test was conducted to choose the effective baud rates for the XBee modules. Selection of the maximum band rate for both 2.4 GHz XBee modules is 57600 bps. Otherwise, XBee modules cannot communicate with each other. Communication cannot be established over this baud rate (see Figure 5.39).

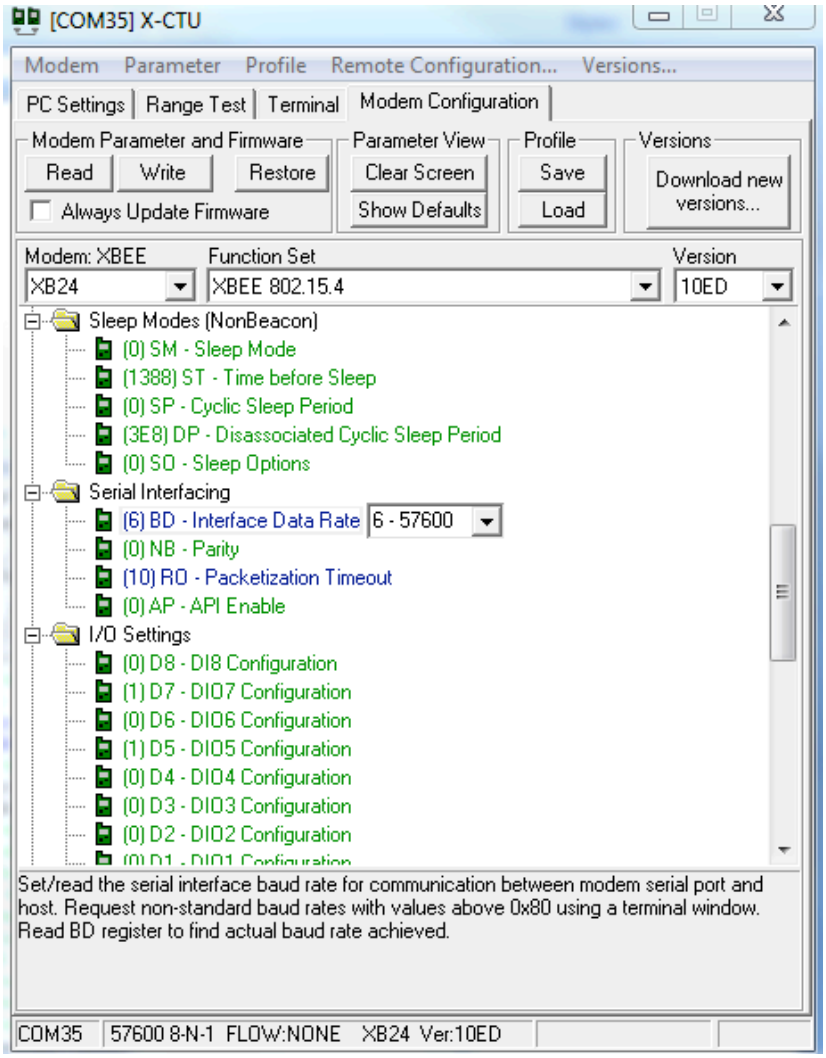

Figure 5. 39: XBee Band rate configuration

- Once all the settings have been completed, click the “Write” button to save all the configurations.

5.5.4 Setting the Ardupilot Mega Mission Planner

Following the physical wire connection, carefully choose the matched XBee port from the ground software (see Figure 5.40), and refer to Chapter 5.2 for more detail.

Figure 5. 40: XBee wireless module serial port selection

Hence, the capability of long range communication is implemented via the 2.4 GHz XBee module.

5.6 Wireless data collection for pendulum system

The APM board, IMU Sensor shield, base plate and Lipo battery, and so on assume the weight of the pendulum system (see figure 5.41). The following parameters are measured value form on the experimental platform:

- The cycloid length of pendulum L=0.7m;
- Mass of pendulum m=0.478 kg;
- Theta0=30.1°;
- Assuming air damping coefficient k=0.006; and
- Simulation time T=780s.

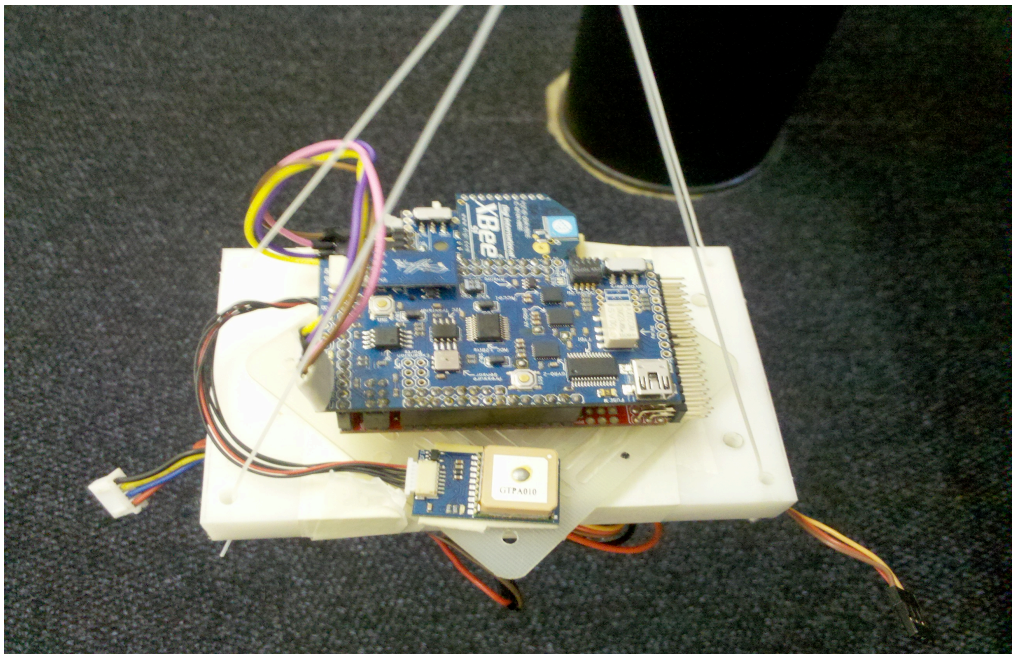

Figure 5. 41: Experimental platform with wireless communication

The desired linear velocity and angular displacement for the pendulum system is shown in Figure 5.42 (the parameters of the pendulum simulation can be modified from Appendix A).

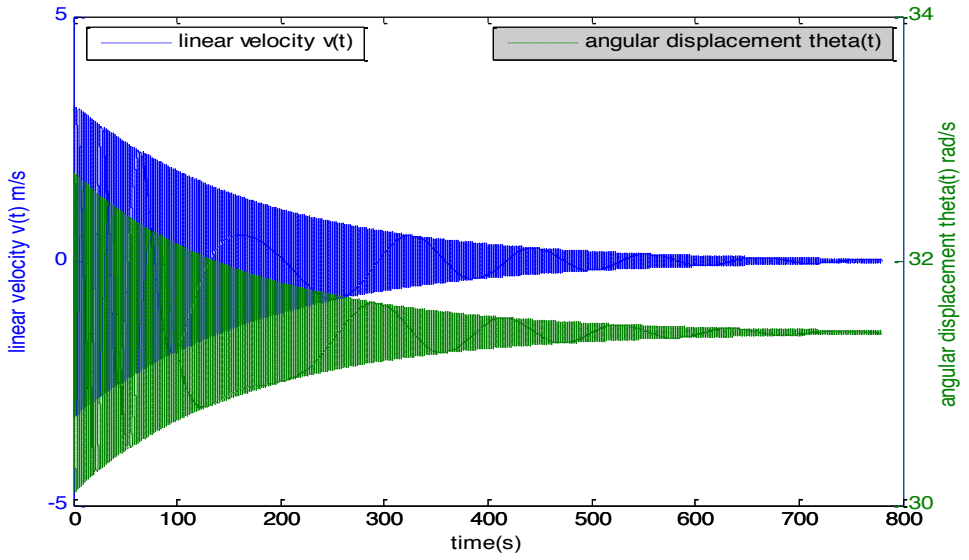

Figure 5. 42: The pendulum's desired output with wireless communication

When wireless communication has been implemented between the APM controller board and the ground control station, real-time raw IMU sensor data collection for linear velocity and angular displacement of pendulum system can also be obtained. The following wireless transmission tests prove that the collected data shows the process of pendulum damping. Figures 5.43 to 5.49 represent seven data collection experiments that were accomplished. The first five tests were conducted without any interference, while the rest of the data collection tests experienced interference from the microwave oven.

When human hands are physically used to release the pendulum from its initial position, it is difficult to keep the pendulum's movement along the pendulum's X-axis. Therefore, the desired test results and the actual test results are two distinct results. The raw sensor data only records the voltage change of the specific sensor such as accelerometer, gyroscopes, barometer and magnetometer and so on.

The following output results were found from the Mission Planner. Because the Mission Planner does not support the real-time raw sensor value reading, the Arduino code was developed and combined with "PUTTY" serial monitoring software to accomplish the real–time data collection purpose (see Appendix A).

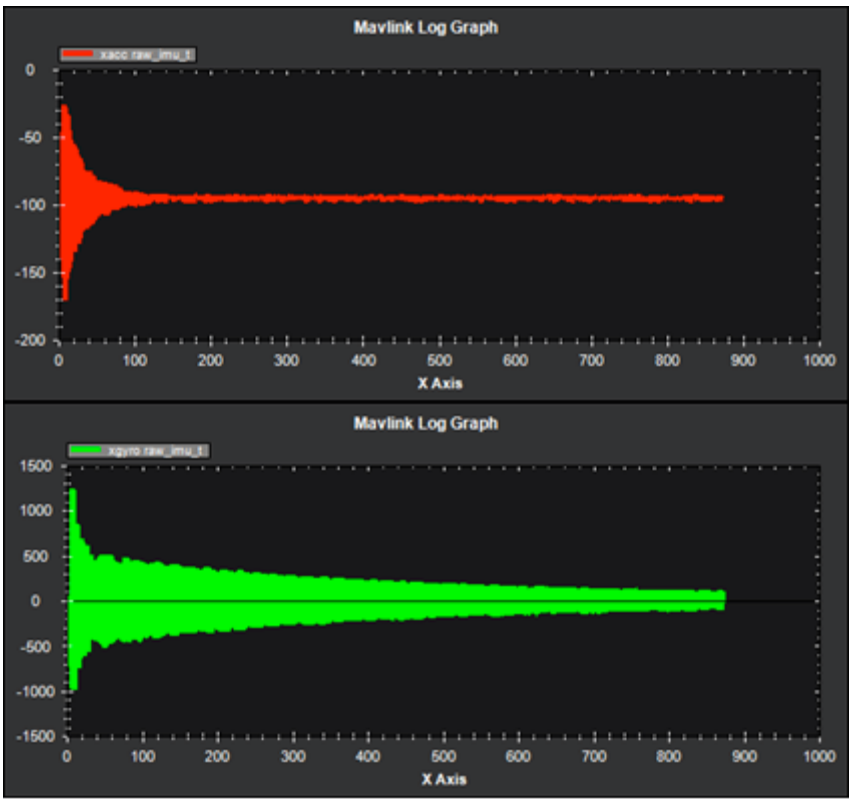

Figure 5. 43: The 1st pendulum test output with wireless communication Accelerometer (Upper) and Gyro (Lower) in X-axis

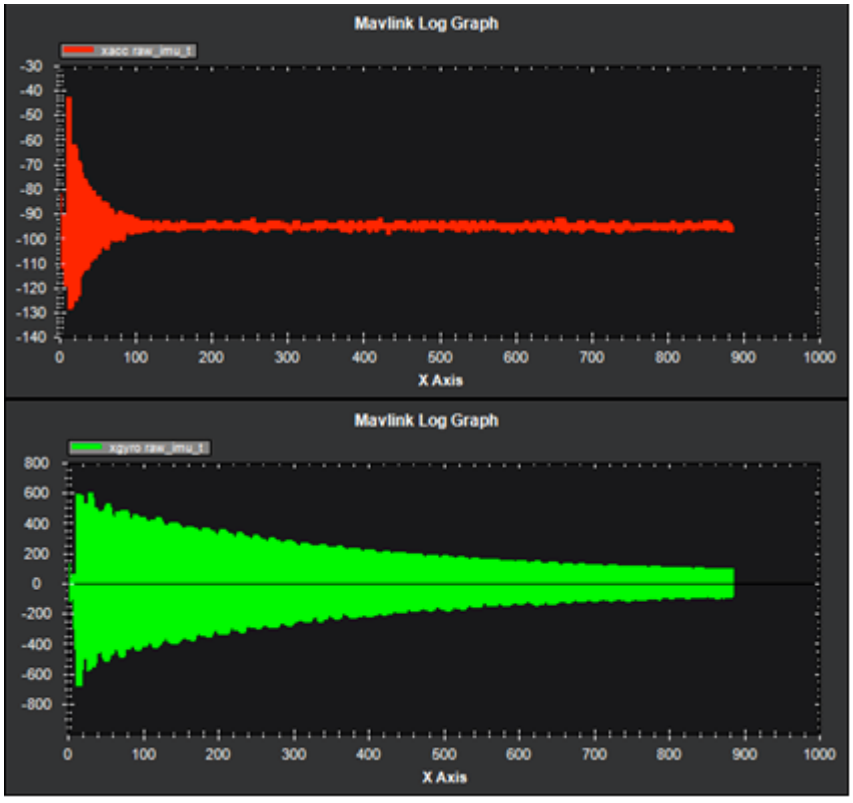

Figure 5. 44: The 2nd pendulum test output with wireless communication Accelerometer (Upper) and Gyro (Lower) in X-axis

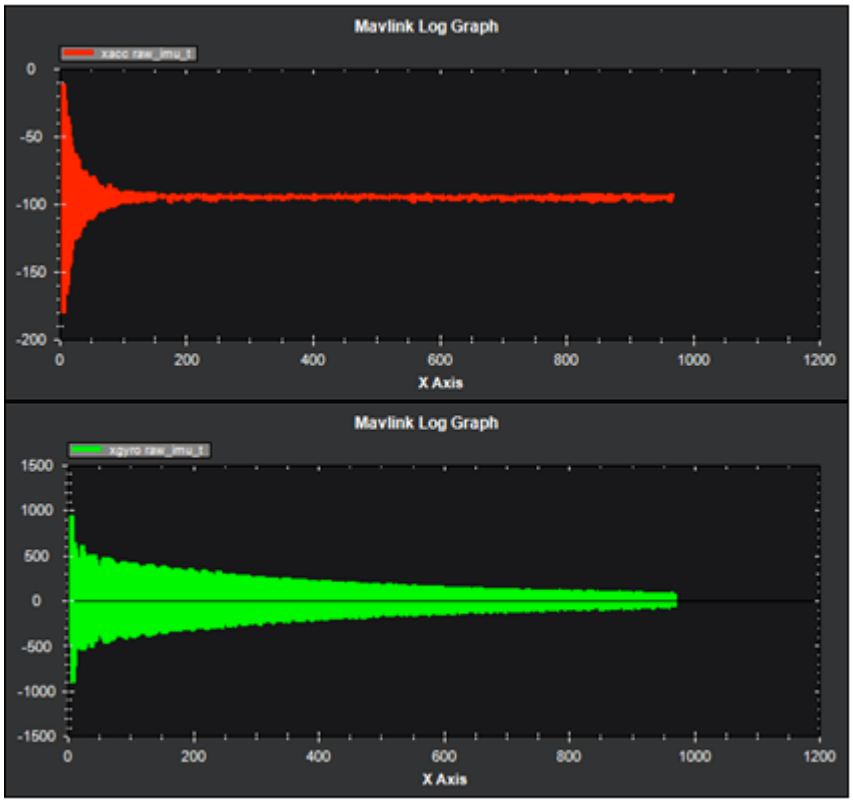

Figure 5. 45: The 3rd pendulum test output with wireless communication Accelerometer (Upper) and Gyro (Lower) in X-axis

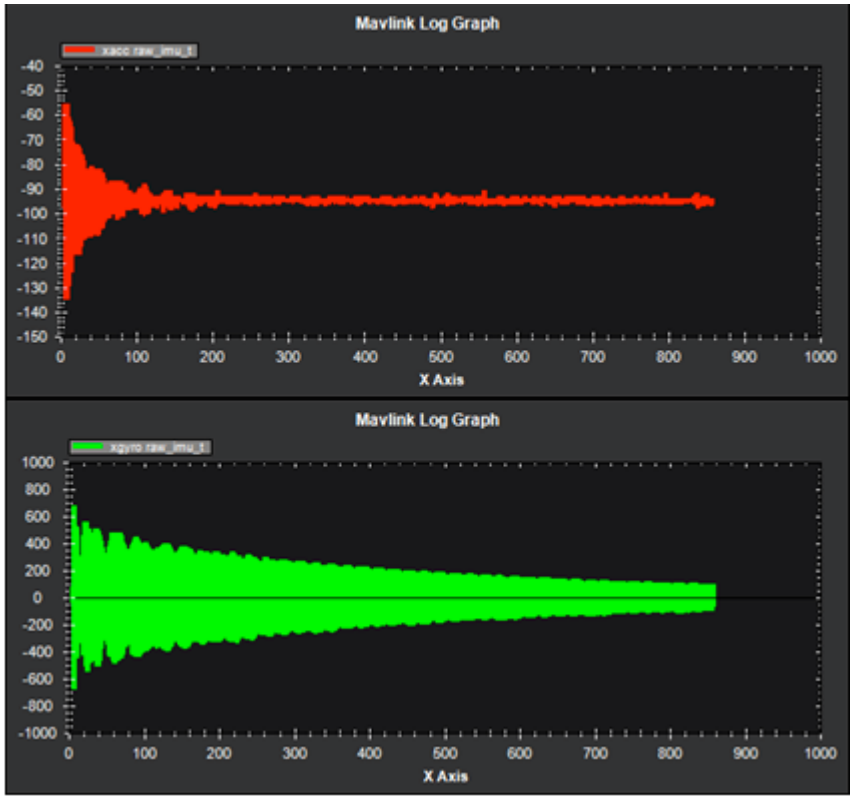

Figure 5. 46: The 4th pendulum test output with wireless communication Accelerometer (Upper) and Gyro (Lower) in X-axis

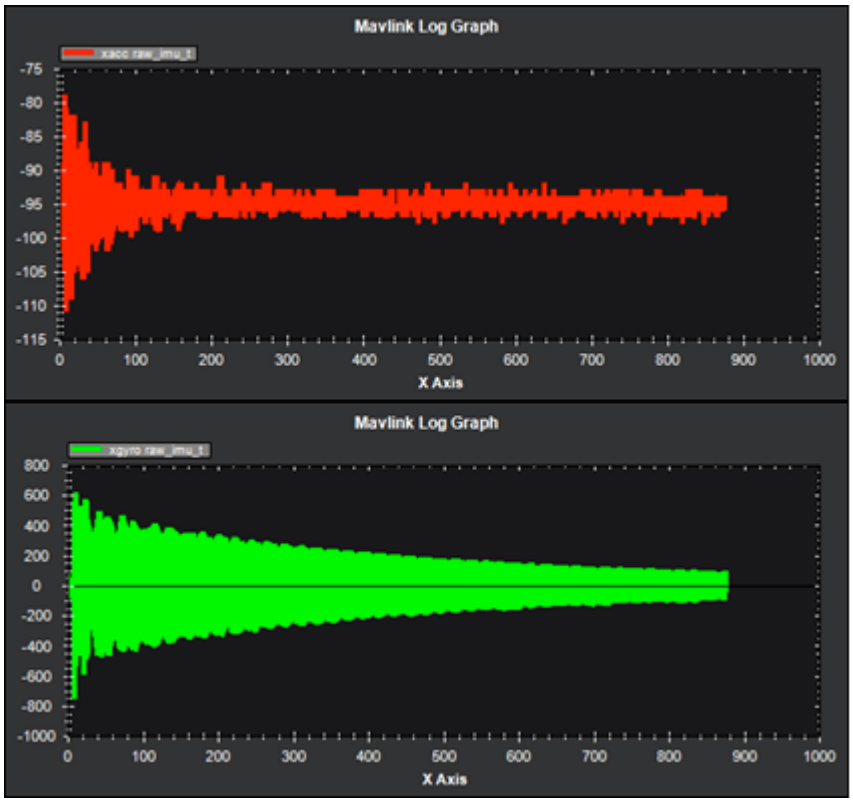

Figure 5. 47: The 5th pendulum test output with wireless communication Accelerometer (Upper) and Gyro (Lower) in X-axis

It should also be mentioned here: the laptop is used to collect raw sensor data from the IMU sensor and it always be connected with the IEEE 802.11 wireless local area network (WLAN), which operates at a 2.4 GHz frequency band. May there is a potential interference source. And the Xbee wireless module provide the 30m operation range in this test.

Besides the above-mentioned, there was no other interference during the data collection process for the above tests. In the actual test, the pendulum vibrated when it did the 'X-axis roll' movement, which caused friction to increase because of the weight of the pendulum, and generated a vibration source for the cycloid of the pendulum. The accelerometer's X-axis output presented the vibration signal in the pendulum damping process. It also distinguished the gyro's X-axis raw data from the desired pendulum outputs.

From the data that was collected from the pendulum movement, irrespective using of a serial connection or a wireless connection, the test output illustrated that the IMU sensor functioned as expected when measuring dynamic accelerations and angular

displacement. The test also showed that the 2.4 GHz XBee module did not conflict with the WLAN interface.

5.6.1 2.4 GHz XBee module interference test

Testing the reliability of the XBee module's data transmission under interfering conditions was a significant part of this project.

The interference source for the XBee modules should also work in the same conditions, which is on a frequency of 2.4 GHz. Moreover, most household microwave ovens are marked as "Rated frequency 2450MHz", which operates at the same frequency range as the XBee modules. Also, the power of a microwave oven is 1350W, which is much stronger than the 1mW XBee modules.

The indoor interference test was implemented under the LOS condition, and the percentage of signal strength was obtained from the GCS software. The microwave oven was placed at a testing range of 10 m, the XBee module, which was mounted on the APM board side was 110 cm and the GCS height was 70 cm. Table 5.4 below shows the signal strength of the 2.4 GHz XBee module in a specific indoor range.

Table 5. 4: Signal strength test for the 2.4 GHz XBee modules

The distance between AMP board and GCS	Signal strength without microwave generator interference	Signal strength with microwave generator interference
2m	99%	90%
4m	98%	82%
6m	97%	68%
8m	94%	62%
10m	90%	59%

Table 5.3 shows that the signal strength was decreased by an increase in the distance between the AMP board and the GCS. If there is an interference source close to the GCS, and it operates at the same frequency range as 2.4 GHz, it will certainly affect the quality of data collection. Through this test, even though there is a signal strength drop from the microwave interference, the communication between the APM controller and the GCS was not lost in this indoor test.

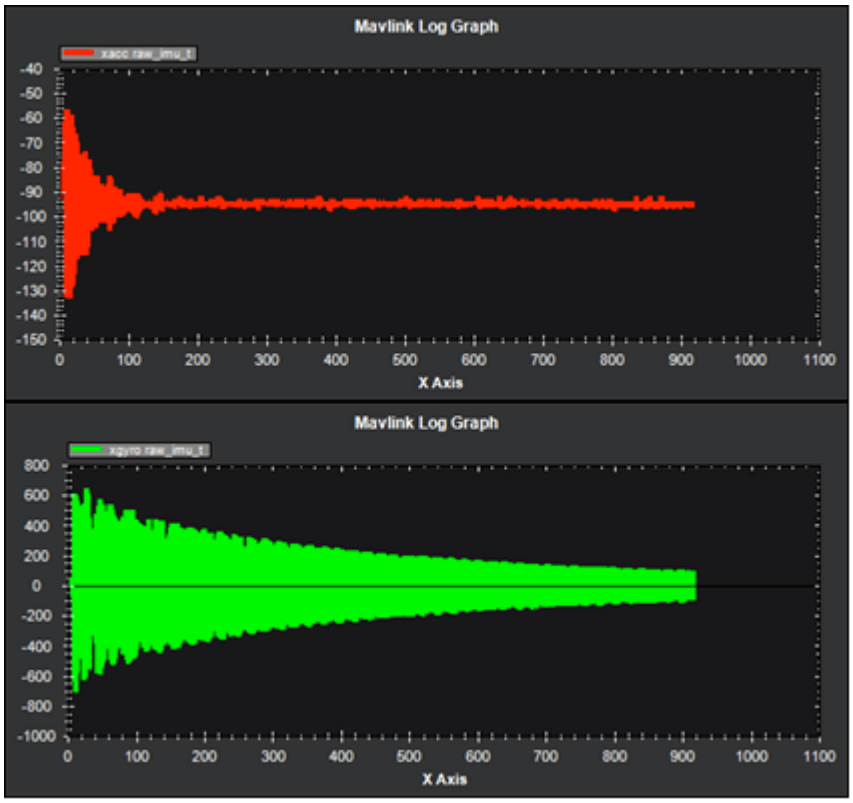

Figure 5. 48: The 1st pendulum test output with interference Accelerometer (Upper) and Gyro (Lower) in X-axis

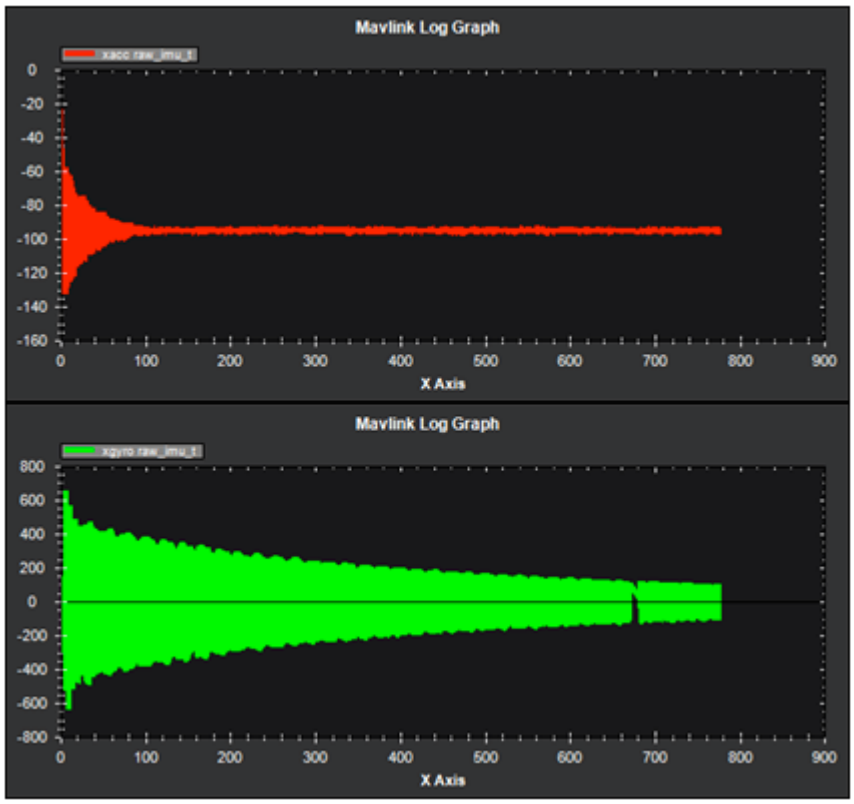

Figure 5. 49: The 2nd pendulum test output with interference Accelerometer (Upper) and Gyro (Lower) in X-axis

During the test, the microwave oven was switched at four times higher in terms of the level of power, while the distance between the microwave oven and the GCS was within 2 meters, and the WLAN connection was also switched on.

The test result (see Figure 5.48 and Figure 5.49) illustrated that under the interference conditions, the XBee module was still able to transmit data correctly without any communication lost.

5.7 Comparison between wireless data collection and serial data collection

The data collection experiment was done with both the serial connection and the wireless connection, and the damping process of the pendulum system was recorded. Certain differences were noted, which are presented below.

- The raw sensor reading value was not the same compared with Figure 5.20 and Figure 5.43.
- The data that was collected by the serial port connection was much more accurate than the wireless connection. Because of the contact between the “USB to the mini B” cable and pendulum stand, the vibration was absorbed from pendulum (see Figure 5.25 and Figure 5.42).
- There was no noise signal during 2.4 GHz XBee wireless communication. However, serial communication has huge potential to collect noise (should be from the USB cable or physical connection port, the proof can be fond in Figure 5.24).
- Serial communication had no time delays (see Figure 5.19 lower) when using 2.4 GHz XBee wireless communication, but had a 50Hz time delay (about 20ms). All the collected test results showed that the time delay can be ignored.

The next chapter explains the above aspects.

5.8 Difference between wire and wireless communication

The main difference between wire and wireless communication is a physical connection when using a serial cable to communicate between the APM board and the GCS (see Figure 5.50), while the communication media comprised cable. The other used two XBee modules with each one mounted on the UAV side and the GCS side (see Figure 5.51), while the communication media comprised radio wave.

The wire communication:

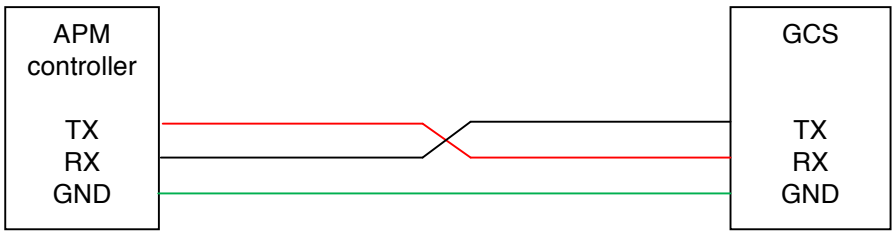

Figure 5. 50: Serial connection scheme

Advantages of wire communication:

- Using a serial port connection with the APM board, the maximum baud rate can reach 115200 bps.
- There is no time delay when using serial communication if data is sent from device A to device B (sending data and receiving data can occur at the same time).

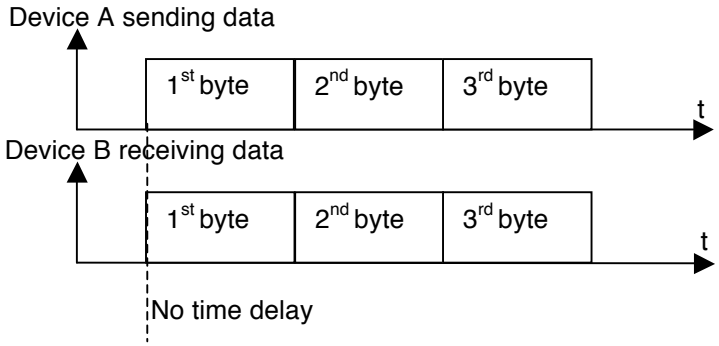

Figure 5. 51: No time delay for wire communication

Disadvantages of serial communication:

- The noise signal can be generated from the cable or connection port.
- Via “USB to mini B” cable communication it is impossible to apply to a UAV flight to achieve flight mission.

The wireless communication:

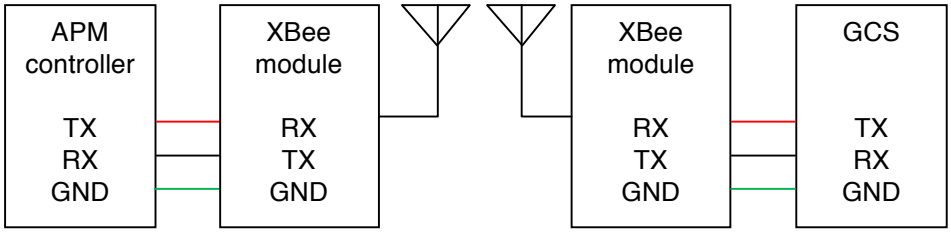

Figure 5. 52: Wireless connection schematic

Advantages of wireless communication:

- There is no physical connection to restrict the movement of the UAV.
- The communication range can be extended by choosing different XBee modules such as the XBee Pro module.

Disadvantages of wireless communication:

- It has time delay when sending real-time data back to the GCS. The data is buffered in the DI buffer until confirm the stop bit is there and then the data is packetized and transmitted (Digi, 2009:11).

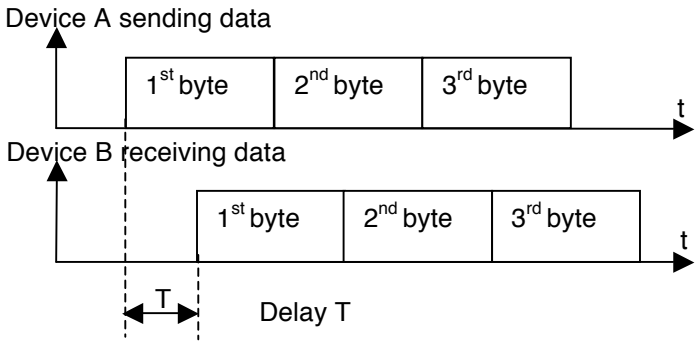

Figure 5. 53: Delay timing for wireless communication

- The communication can be interrupted by other devices, which operate at a similar frequency band.

5.9 Summary

This chapter described details of all the major procedures of how to gather on-board raw sensor data, which was displayed at the ground control station via serial communication and 2.4 GHz wireless communication. These included, utilizing the ground PC software ‘Mission Planner’ and the open source software ‘Arduino 0022’ to collect the sample output data of IMU sensor from UAV on-board sensor shield, while it also introduced the Arduino developing environment of uploading the source code or modifying the source code to drive on-board IMU sensor. The chapter also introduced the basic concept of bus communication, and outlined the differences between wire and wireless communication.

The pendulum system was described in this chapter, as well as use of the serial connection and the wireless connection to collect the IMU sensor raw data to illustrate the damping process of the pendulum system. The output results showed that using the 2.4 GHz XBee module as transmission media for the UAV telemetry system is capable of collecting reliable on-board sensor data.

CHAPTER SIX
DATA COLLECTION BASIS

6.1 Characteristics of data collection system

The data collection system comprised devices such as an accelerometer, gyros, barometer, microcontroller, and so on. Many kinds of physical variables were measured and converted into an electrical signal. The procedure for sending data should be done before information is sent to the required location such as signal amplification and mixes with other signals that are attached to the carrier.

As mentioned above, there was a general process for obtaining data from the UAV on-board sensor system.

The project is sought to choose on-board sensors and UAV hardware components, which would effectively obtain the real-time flight data. The following aspects are basal issues of this UAV data collection project, as presented below.

6.2 Internal UAV communication

According to the APM main board, the autopilot is based on an ATmega1280 processor, which is a low- power CMOS 8-bit microcontroller, and also has a system clock speed of 16 MHz (Atmel, 2012). Table 6.1 shows the difference between the ATmega1280 and the ATmega640/1281/2560/2561in their family.

Table 6. 1: Comparison between ATmega1280 and ATmega640/1281/2560/2561

Device	Flash	EEPROM	RAM	General Purpose I/O pins	16 bits resolution PWM channels	Serial USARTs	ADC Channel
AT mega 640	64 KB	4 KB	8 KB	86	12	4	16
AT mega 1280	128 KB	4 KB	8 KB	86	12	4	16
AT mega 1281	128 KB	4 KB	8 KB	54	6	2	8
AT mega 2560	256 KB	4 KB	8 KB	86	12	4	16
AT mega 2561	256 KB	4 KB	8 KB	54	6	2	8

(Atmel, 2012)

Table 6.1 shows that us the ATmega1280 has a 128KB Flash program memory, which is to store codes (also 4KB is used for the boot loader) , 8KB RAM, 4KB EEPROM, which can be used to read, and is written by the EEPROM library.

The ATmega1280 provides four hardware UARTs for Transistor-Transistor Logic (TTL 5V) serial communication. It is capable of communication with computers, microcontrollers or other Arduino devices (Arduino, 2012).

6.3 Communication in the data link

Establishing a data link is a major demand to ensure that the UAV's information can be received by the ground control station. In other words, the data link consists of two subsystems: 1) Air Data Terminal (on the UAV side) and; 2) the Ground Data Terminal (on the ground control station side). Herewith, the sensor data stream and the UAV's control data contain data link communication (see Figure 6.1).

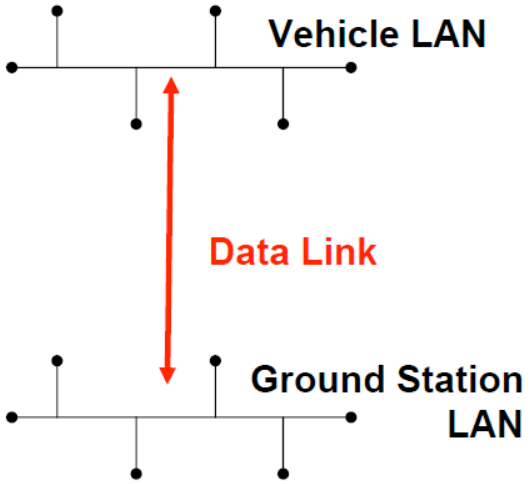

Figure 6. 1: UAV communication network layout

(Adapted from Gerardo 2009:4)

The AudruCopter's on-board sensor shield, which provides the source of collecting various flight data, can be obtained through the radio 'data link', which comprises up-link (provides control of UAV flight path and commands to its payloads), and radio down-link (provides both a low data rate channel to acknowledge commands and transmits UAV's real-time status information, and may have a high data rate channel for payload data such as video and radar). Baiotti *et al*. (1999:3) assert the following thoughts concerning data link communication, which were considered for this project:

- Operation range;
- Low-bit-error on data link;
- Low intercept ability; and
- Limited size and low power consumption.

Firstly, in theory, to increase the operation range of UAV, receiver sensitivity should be increased in order to gain a higher configuration antenna at the ground control station and on both sides of UAV, or by increasing the transmitted power (Baiotti *et al*., 1999:3). The higher gain antenna obtains an antenna radiation pattern. It is a focused radio wave beam with narrow beam width, which allows more power to be transmitted to the receiver direction; in other words, it increased the receive signal strength; If the higher gain antenna is applied on the receiving antenna side, it will capture more of the signal from the transmitting side (Wikipedia, 2011e).

In practice, increasing the transmitted power is a popular method to enhance the UAV operating range. It requires a steady platform that should be installed during the UAV in flight operation (also see Chapter 3, 3.4).

The other critical issue of the UAV data link is the Bit Error Rate (BER). Wikipedia (2011f) states that "*it is the number of bit errors divided by the total number of transferred bits during a studied time interval. BER is a unitless performance measure often expressed as a percentage*."

To ensure that the ground control station receives meaningful and analysable raw sensor data, the data link should reduce the BER to allow end-users to gather effective sensor data.

Breed (2003) claims that the way to reduce the BER is to minimize the "Noise" in the radio signal transmission, which reduces the bandwidth, but the limitation is to abandon the desired transmission bit rate, or by using higher power transmission to increase the energy per bit, which it will interfere with other systems.

The equation below presents the probability of error (POE). It is proportional to E_b/N_o, which is a form of signal-to-noise ratio (Breed, 2003).

$$POE = \frac{1}{2}(1 - erf)\sqrt{E_b/N_o} \qquad [6.1]$$

erf is error function

E_b is the energy in one bit, the unit is Joules and

N_o is the noise power spectral density (noise power in a 1 Hz bandwidth), and the unit is Joules per second .

The energy per bit E_b can be determined by dividing the carrier power by the bit rate. The error function erf is different for each of the various modulation methods.

Therefore, to obtain better transmission results with low BER, these factors should be balanced for optimization E_b/N_o .

It is important to keep the intercept low during the data link in transmission process, especially on a battlefield where the data link may be attacked by hostile forces' electronic warfare threats. Hence, to provide more protection should be provided for the data link. To generate an authentication code, resistance deception should be employed such as using a secure code in spread-spectrum transmission, or by some of the techniques that provide resistance to jamming (Torun, 2012).

The data link should use components that are of a small size, light weight and low power consumption such as XBee wireless modules (see Chapter 4, 4.4.5); it will enhance the endurance of the UAV (also see Chapter 1, 1.2.3).

6.4 Ground control station characteristics

The ground control station is the operational control centre for entire UAV system. It provides data storage, processing of onboard sensor data, displaying of real-time flying way points, and so on.

Torun (2012:2) states that the ground control station comprises the following:

- The system architecture of the ground control station should be upgraded without restructuring the entire system in future;
- The UAV control system's attributes should be flexible to adapt end-users and mission variation;
- The UAV control software can be maintained and displays appropriate status results;
- The ground control station can be deployed and easily transported;

- Provides the function of upload way point coordinates and onboard payload operation via system data link as direct ground connection;
- Provides monitoring payload and telemetry data in real-time, and all the data can be recorded for future analysis and processing;
- All the payload output data can be displayed as diagram and exploited; and
- Can display more than one payload data from the same monitor, simultaneously.

Conversely, the ground control station is also able to adapt to a variety of computer platforms, programming languages, operating systems, and so on.

6.5 Summary

This chapter presents the core characteristics of the data collection system. It was an essential part of this project, which comprises the UAV internal communication, data link communication and ground station communication. The above-mentioned provides a general outline to establish the UAV data collection system.

CHAPTER SEVEN
CONCLUSIONS AND OBSERVATION

7.1 Project conclusion

The purpose of this project was to review some significant components of a small UAV data collection system. It presented the Ardupilot Mega hardware, ground software 'Ardupilot Mega Planner', and specified sensors that were used to obtain raw data collection. Two different data transmission methods were used to obtain real-time flight data, namely serial port transmission and XBee wireless module transmission.

An experimental Arducopter Quad was used to develop and test the accuracy of a data collection module for a small UAV. Flight tests were conducted, which demonstrated the accurate and effective flight control of the ArduPoilt Mega computer (UAV flight computer). The UAV onboard system was introduced in Chapter 4, which provided a better understanding of how to establish it. The Arduino code of the ArduPoilt Mega computer was used to continuously request data from the on-board sensor shield. In the mean time, the flight computer processed and logged the collected data, and transmitted it to the ground control station. To obtain communication between the UAV and the ground control station, via a serial cable connection or a wireless module connection, flight information was displayed at ground control station. This project presented a clear layout to develop a data collection for the UAV, which was shown in Chapters 3 & 6.

For a basic test we recorded gyroscopic data from the on-board sensor. The sample test result shows that the module that was installed on the Arducopter Quad is capable of monitoring and recording the on-board sensor data in real-time. The recorded flight data can be used for future analysis by end -users.

Summarily, data link communication was a fundamental part of this project. Good communication between the UAV on-board system and the ground control station ensured safety and effectiveness consummate a small UAV data collection system.

This data collection system may be applied to all types of model aircraft, while both hardware and software can be upgraded for different requirements.

The following is a summary of the project's contributions, which can provide a better understanding to someone who has an interest in small UAV data collection fields.

- The basic hardware and software structure of a small UAV aircraft was evaluated, which included the basic functionality of UAV hardware components, the onboard avionic system components, and the ground control station system.

- In the communication media phase, some fundamentals of radio communication were also introduced: radio wave, radio communication, structure of the telemetry system, and the sensor delay issue.

- The basic concept of Arducopter dynamics was presented, which mathematically presented Arducopter's air-movement, and stated equations presented mathematical methods to describe the basic modelling and control for the Arducopter.

- The APM microcontroller was briefly introduced, as well as freeware ground control station software, which displayed the raw sensor data in real-time, and the Arducopter's on-board electronics specifications.

- On-board sensor testing was shown, while Matlab was used to analyse recoded data.

- The open source programming language, Arduino, was modified so that output data could be monitored via the serial monitor function of the Arduino software.

However, certain aspects were not achieved:

- The extra sensor payload for achieving UAV healthy monitoring purpose; and

- The video camera was not used for surveillance and reconnaissance applications.

Comparing the Arducopter Quad flight system structure with other small UAV flight systems, all comprise of an on-board system, communication system and the ground control station, but the Arducopter Quad flight system was of a smaller size and more compact design.

Work done by Xiang and Tian (2011) and Taha *et al*. (2010) present that the transmission method for a small UAV's data collection system comprises three main systems, which are: the manual flight control system can use a 35 MHz or 72MHz frequency band; the telemetry and command data link system can use a 900MHz frequency band; and the video link system can use a 2.4GHz frequency band.

7.2 Observation

The data collection system was applied for the Arducopter Quad helicopter, which gathers UAV flight status information. Thus, a low cost, light weight, MEMS flight control system was used, including on-board sensor, flight computer and a 2.4 GHz wireless transmission system. The ground control software that was used, included the auto altitude hold, display GPS navigation and setting the fly way point.

The following faults were generated during the ground test:

- Communication problem

  The APM controller, via the serial port connection to the ground control station software, should have been able to communicate with the 'Mission Planner' effectively most of the time, but it did freeze the laptop while downloading the raw sensor data from on-board data logging flash memory. After uploading the latest ArduCopter firmware to the APM, the problem seemed to have been solved. The fault may have been with firmware.

- Air/Ground communications

  The issue that was considered here was the frequency bands shortage of VHF and UHF. Clot (1999) states that: a) The same frequency used more than once in world wild wireless communication may cause conflict between the two Designated Operating Coverage (DOC) areas. b) Using the A/D convertor to transfer commands to the digital communication system will improve this situation, but the transmission time delay will occur. This is caused by air and ground processing systems, especially in multiplexed situations.

The UAV data collection system has not been used in a real aircraft till now, thus the full capability of the ArduPoilt Mega on-board system was not tested. Therefore, more work should still be done in this field.

7.3 UAV's potential in future

In the future, the small UAV flight data collection system may face various sensor payloads to achieve a healthy aircraft monitoring system. Conversely, the on-board microcontroller or flight computer should be equipped with a high speed processor and a large flash program memory, which is compatible with different sensor payloads.

The small UAV has huge growth potential in several fields, but the following practical issues should be considered:

- Reduction of the hardware and software costs;
- Extended payload range;
- Air vehicle's weight, volume and power consumption;
- Air vehicle's spare interfaces with an avionics system;
- Increase the data-link's bandwidth capabilities;
- Enhance the capability of operating a UAV's on-board sensor via a ground control station; and
- Flight computer resource's reserved capabilities for memory, timing, and so on.

In conclusion, the small UAV system has great potential for many applications, which require accurate data collection systems to satisfy flight data analysis for end-users' future use. In this project, the on-board sensor's sample results were obtained by the GCS. For future research, the blade flapping measurement system can be based on this data collection system, where the idea would be to apply the piezoelectricity film sensor to the rotor blade, and to identify whether the helicopter's rotor blade in health condition or not. And displayed in real-time state will be possible.

REFERENCES

4max. n.d. How to wire up a UBEC with an ESC that has a built in BEC. [online]. Available from: http://www.4-max.co.uk/pdf/How2wireupaUBEC.pdf. [Accessed 30 September 2011]

Arduino, 2012. *Arduino Mega.* online]. Available from: http://arduino.cc/en/Main/ArduinoBoardMega. [Accessed 2 February 2012]

ArduCopter. n.d. *ArduCopter instructions.* [online]. Available from: http://code.google.com/p/arducopter/wiki/ArduCopter?tm=6. [Accessed 16 September 2011]

Atmel. 2012. *8-bit Atmel Microcontroller with 64K/128K/256K Bytes In-System Programmable Flash*. [online]. Available from: http://www.atmel.com/dyn/resources/prod_documents/doc2549.pdf. [Accessed 29 January 2012]

Altuğ, E., Ostrowski, J. and Mahony, R. 2002. Control of a Quadrotor Helicopter Using Visual Feedback. *International Conference on Robotics & Automation*, 0-7803-7272-7/02: 72-77.

Austin, R. 2010. *Unmanned Aircraft Systems: Their Design, Development and Deployment*. US: John Wiley & Sons, Inc.

Baiotti, S. Scazzola, G, L. Battaini, G & Crovari, E. 1999. *Advances in UAV Data Links: Analysis of Requirement evolution and implications on future equipment.*[online]. Italy: Marconi Communications S.p.A. Available from: http://ftp.rta.nato.int/public//PubFulltext/RTO/MP/RTO-MP-044///MP-044-B10.pdf. [Accessed 22 December 2011].

Bendea, H., Boccardo, P., Dequal, S., Giulio Tonolo, F., Marenchin, D. & Piras, M. 2008. LOW COST UAV FOR POST-DISASTER ASSESSMENT. *The International Archives of the Photogrammetry, Remote Sensing and Spatial Information Sciences*, XXXVII(B8): 1371-1379.

Breed, G. 2003. Bit Error Rate: Fundamental Concepts and Measurement Issues. *High Frequency Electronics.* Available from: http://www.highfrequencyelectronics.com/Archives/Jan03/HFE0103_Tutorial.pdf. Accessed 23 December 2011].

Bristeau, p., Dorveaux, E., Vissière, D. & Petit, N. 2010. Hardware and software architecture for state estimation on an experimental low-cost small-scaled helicopter. *Conrtol engineering practice*, 18: 733-746.

Cai, G., M, C., B., Lee, T. & Dong, M. 2009. Design and implementation of a hardware-in-the-loop simulation system for small- scale UAV helicopters. *Mechatronics*, 19: 1057-1066.

Carden, F., Jedlicka, R. and Henry, R. 2002. *TELEMETRY SYSTEM ENGINEERING*. [online]. Norwood: ARTEC HOUSE, INC. Available from: http://books.google.com/books?id=3LK44UI0YCEC&printsec=frontcover#v=onepage&q&f=false. [Accessed 22 August 2011].

Clot, A., 1999. *COMUNICATION COMMAND AND CONTROL.* [online]. Belgium: RTO AVT Course. Available from: http://ftp.rta.nato.int/public//PubFulltext/RTO/EN/RTO-EN-009///EN-009-02B.pdf. [Accessed 5 September 2011].

Digi. 2009. *XBee®/XBee-PRO® RF Modules*. [online]. US: © 2009 Digi International, Inc. Available from: http://www.sparkfun.com/datasheets/Wireless/Zigbee/XBee-Datasheet.pdf. [Accessed 27 September 2011].

Differencebetween.net. n.d. *The Difference Between AM and FM.* [online]. Available from: http://www.differencebetween.net/technology/the-difference-between-am-and-fm/ . [Accessed 16 August 2011].

ELPRO Technologies. n.d. *Performance of Different Frequency Bands 2.4 GHz vs 900/869 MHz.* [online]. Australia: Available from: http://www1.crouse-hinds.com/wirelessio/PDF/White%20Paper/white_paper_frequencies.pdf. [Accessed 11 August 2011].

Frenzel, L. 2010. *Electronics Explained: The New System Approach to Learning Electronics*. US: Elsevier Science.

FU, X., ZHOU, Z., XIONG, W. & GUO, Q. 2008. MEMS-Based Low-Cost Flight Control System for Small UAVs. *TSINGHUA SCIENCE AND TECHNOLOGY*, 13(5): 614-618, October.

Gerardo, P. 2009. UAV *Data Link Design for Dependable Real-Time Communication*. [online]. Available from: http://www.slideshare.net/GerardoPardo/uav-data-link-design-for-dependable-realtime-communications. [Accessed 21 January 2012].

Hobbyking(a). n.d. *Plush 30 Brushless Speed Controller*. [online]. Available from: http://www.hobbyking.com/hobbycity/store/uh_viewitem.asp?idproduct=2164. [Accessed 30 September 2011].

Hobbyking(b). n.d. *Turnigy 9X 9Ch Transmitter w/ Module & 8ch Receiver.* [online]. Available from: http://www.hobbyking.com/hobbyking/store/uh_viewItem.asp?idProduct=8992. [Accessed 04 October 2011].

Honeywell. n.d. *3-Axis Digital Compass IC HMC584.* [online]. Available from: http://www.sparkfun.com/datasheets/Sensors/Magneto/HMC5843.pdf. [Accessed 29 September 2011].

Jean, M. & Steve, B. 2003. *AN10216-01 I^2C MANUAL*. [online]. Available from: http://ics.nxp.com/support/documents/interface/pdf/an10216.pdf. [Accessed 20 December 2011].

Jon B, H., 2009. Radio-*Frequency Electronics: Circuits and Applications*, 2nd ed. US: Cambridge University Press.

Iscold, P. 2008. Low-cost flight test system for light aircrafts. *Aircraft Engineering and Aerospace Technology: An International Journal*, 80(3): 243-252.

Kivrak, A. 2006. *Design of control system for a quadrotor flight vehicle equipped with inertial sensor*. [online]. Turkish: ATILIM UNIVERSITY. Available from: http://www.acikarsiv.atilim.edu.tr/browse/156/168.pdf. [Accessed 7 September 2011].

KOWALENKO, K. IEEE Future Technology Session. n.d. *UAV Technology to Aid in disasters*. Available from: http://www.ieee.org. [Accessed 14 February 2011].

MYRCMART. n.d. *RCX A2830-12 850KV Outrunner Brushless Motor.* [online]. Available from: http://www.myrcmart.com/rcx-a283012-850kv-outrunner-brushless-motor-airplane-free-mounts-p-3723.html. [Accessed 29 September 2011].

OCW. n.d. *Autonomous Navigation of a Quadrotor Helicopter Using GPS and Vision Control*.[online]. Available from: http://ocw.mit.edu/courses/mechanical-engineering/2-017j-design-of-electromechanical-robotic-systems-fall-2009/projects/MIT2_017JF09_sw1_milstone.pdf. [Accessed 19 September 2011]

Paul, C. 2004. *Electromagnetics for Engineers: With Applications to Digital Systems and Electromagnetic Interference.*USA: John Wiley & Sons, Inc.

Paw, Y.C. & Balas, G.J. 2010. Development and application of an integrated framework for small UAV flight control development. *Mechatronics*, 9: 1-14.

Peng, K., Cai, G., Chen, B.M., Dong, M., Lum, K.Y., & Lee, T.H. 2009. Design and implementation of an autonomous flight control law for a UAV helicopter. *Automstics*, 6: 2333-2338.

PÖllänen, R., Toivonen, H., Peräjärvi,K,. Karhunen, T., Ilander, T. & Lehtinen, J. 2008. Radiation surveillance using an unmanned aerial vehicle. *Applied Radiation and Isotopes,* 11: 340-344.

Rawashdeh, O., Yang H., AbouSleiman, R. and Sababha, B. 2009. MICRORAPTOR: A LOW-COST AUTONOMOUS QUADROTOR SYSTEM. *ASME,* DETC2009-86490: 1-8.

Raza, A. & Gueaieb, W. 2010. *Intechopen.* [online]. Canada: University of Ottawa. Available from: http://www.intechopen.com/articles/show/title/intelligent-flight-control-of-an-autonomous-quadrotor. [Accessed 7 September 2011].

Robot-electronics. 2011. *Using the I2C Bus*. [online]. Available from: http://www.robot-electronics.co.uk/acatalog/I2C_Tutorial.html. [Accessed 20 December 2011].

Salhuana, L. 2012. Tilt *Sensing Using Linear Accelerometers*. [online]. USA: Freescale Semiconductor. Available from: http://www.freescale.com/files/sensors/doc/app_note/AN3461.pdf. [Accessed 4 April 2012].

Struzak, R. 2006. *Radio-wave propagation basics*. [online]. Italy: The Abdus Salam International Centre for Theoretical Physics ICTP. Available from: http://wireless.ictp.it/school_2006/lectures/Struzak/RadioPropBasics-ebook.pdf. [Accessed 16 August 2011].

Taha, Z., Tang, Y.R. & Yap, K.C. 2010. Development of an onboard system for flight data collection of a small-scale UAV helicopter. *Mechatronics*, 9:1-13.

Tariq, S & Gary, B. 2003. *SOFTWARE- ENABLED CONTROL*. Canada: John Wiley & Sons, Inc.

Torun, E. n.d. *UAV Requirements and Design Consideration*. [online]. Turkey :Technical & Project Management Department, Available from: http://ftp.rta.nato.int/public//PubFulltext/RTO/MP/RTO-MP-044///MP-044-B04.pdf. [Accessed 3 February 2012].

W. Frew, E. 2004. Flight Demonstration of Self-directed Collaborative Navigation of Small Unmanned Aircraft. *America Institute of Aeronautics Astronautics*, 9: 1-14.

Wikipedia. 2011a. *Transmitter*. [online]. Available from: http://en.wikipedia.org/wiki/Radio_transmitter. [Accessed 19 August 2011].

Wikipedia. 2011b. *USB*. [online]. Available from: http://en.wikipedia.org/wiki/Usb. [Accessed 20 December 2011].
Wikipedia. 2011c. *SCSI*. [online]. Available from: http://en.wikipedia.org/wiki/SCSI. [Accessed 20 December 2011].

Wikipedia. 2011d. *I2C*. [online]. Available from: http://en.wikipedia.org/wiki/I2C. [Accessed 20 December 2011].

Wikipedia. 2011e. *High-gain antenna*. [online]. Available from: http://en.wikipedia.org/wiki/High-gain_antenna. [Accessed 28 December 2011].

Wikipedia. 2011f. *Bite error rate*. [online]. Available from: http://en.wikipedia.org/wiki/Bit_error_rate. [Accessed 23 December 2011].

Xiang, H. & Tian, L. 2011. Development of a low – cost agricultural remote sensing system based on an autonomous unmanned aerial vehicle (UAV). *BIOSYSTEMS ENGINEERING*, 1: 174-190.

Zhang, D., 2009. *MATLAB/Simulink jian mo yu fang zhen*. China: PUBLISHING HOUSE OF ELECTRONICS INDUSTRY.

APPENDICES

APPENDIX A: Matlab code for simulation a pendulum system
(Adapted from Zhang 2009)

```
g=9.8;
T=780; %Simulation time
dt=0.0001; %Simulation stepping
t=0:dt:T;%The sequence of simulation time
L=0.7; %The cycloid length of pendulum
m=0.244; %Mass in Kg
K=0.006; %Air damping coefficient
v0=0; %Initial speed
theta0=30.1; %Initial angular setting
v=zeros(size(t));
theta=zeros(size(t));
v(1)=v0;
theta(1)=theta0;

%Start simulation
for i=1:length(t)
    v(i+1)=v(i)+(g*sin(theta(i))-K./m.*v(i)).*dt;
    theta(i+1)=theta(i)-1./L.*v(i).*dt;
end

[AX,H1,H2]=plotyy(t,v(1:length(t)),t,theta(1:length(t)),'plot')
;%2-D plots with y-axes on both LHD & RHS
set(H1,'LineStyle','--');
set(H2,'LineStyle','+');
set(get(AX(1),'Ylabel'),'string','linear velocity v(t) m/s');
set(get(AX(2),'Ylabel'),'string','angular displacement theta(t)
rad/s');
xlabel('time t/s');
legend(H1,'linear velocity v(t)',2);
legend(H2,'angular displacement theta(t)',1);
```

APPENDIX B: Arduino code for reading IMU sensor data via Serial connection

```
#include <FastSerial.h>
#include <AP_IMU.h>
#include <AP_ADC.h>
#include <AP_Math.h>
#include <AP_Common.h>
FastSerialPort(Serial, 0);
AP_ADC_ADS7844    adc;
AP_IMU_Oilpan     imu(&adc, 0);  // disable warm-start for now
unsigned long time;

void setup(void)
{
        Serial.begin(115200);
        Serial.println("Busy with IMU startup...");
        adc.Init();
        imu.init(IMU::COLD_START);
}
void loop(void)
{
        Vector3f        accel;
        Vector3f        gyro;

        delay(1000);
        imu.update();
        accel = imu.get_accel();
        gyro = imu.get_gyro();

      Serial.print("Time: ");
      time = millis();
      Serial.print(time );
Serial.printf("   AX: 0x%4.4f   AY: 0x%4.4f   AZ: 0x%4.4f   GX: 0x%4.4f   GY: 0x%4.4f
GZ: 0x%4.4f\n",  accel.x, accel.y, accel.z, gyro.x, gyro.y, gyro.z);

Serial.println("++++++++++++++++++++++++++++++++++++++++++++++++++++++++
++++++++++++++++++++++++++++++++++++++++++++++") ;
  }
```

APPENDIX C: Arduino code for reading IMU sensor data via XBee modules

```
// This is the code for Simple test for the AP_IMU Via XBee modules.
//

#include <FastSerial.h>
#include <AP_IMU.h>
#include <AP_ADC.h>
#include <AP_Math.h>
#include <AP_Common.h>



FastSerialPort(Serial, 3);

AP_ADC_ADS7844   adc;
AP_IMU_Oilpan        imu(&adc, 0);  // disable warm-start for now


unsigned long time;

char command = 's';

double R,theta_1;
double Est_Ax,Est_Ay,Est_Az;


void setup(void)
{
  Serial.begin(57600);
  Serial.println("Busy with IMU startup...");
  adc.Init();
  imu.init(IMU::COLD_START);
}

void loop(void)
{


  Vector3f      accel;
  Vector3f      gyro;

  int n=0;
  int s;


   delay(100);

  imu.update();
  accel = imu.get_accel();
  gyro = imu.get_gyro();


  Serial.print(" Time:");
```

```
 time = millis();
 Serial.print(time );

R=sqrt(pow(accel.x,2)+pow(accel.y,2)+pow(accel.z,2));

Est_Ax=accel.x/R;
Est_Ay=accel.y/R;
Est_Az=accel.z/R;

theta_1=(acos(Est_Az)* 180/PI);


if (accel.x>0){s=1; };
 if (accel.x<0){s=-1;};

  Serial.print("  Roll angle_1:");
  Serial.print(((theta_1-180)*-1)*(s));


    delay(100);


  Serial.printf("  AX: %4.4f  AY: %4.4f  AZ: %4.4f  GX: %4.4f  GY: %4.4f  GZ: %4.4f\n",
  accel.x, accel.y, accel.z, gyro.x, gyro.y, gyro.z);


// Serial.println("-----------------------------------------------------------------------------------------------------")
;

  //listen a pause command
  while (Serial.available()){
    command = Serial.read();
    while ((command == 's') | (command == 'S')){
      while (Serial.available()){
        command = Serial.read();
      }
      if (n<1){
        Serial.println("System Paused, Press any key to continue") ;
        n++;
      }
    }

  }
}
```

APPENDIX D: The setting up of “Putty”

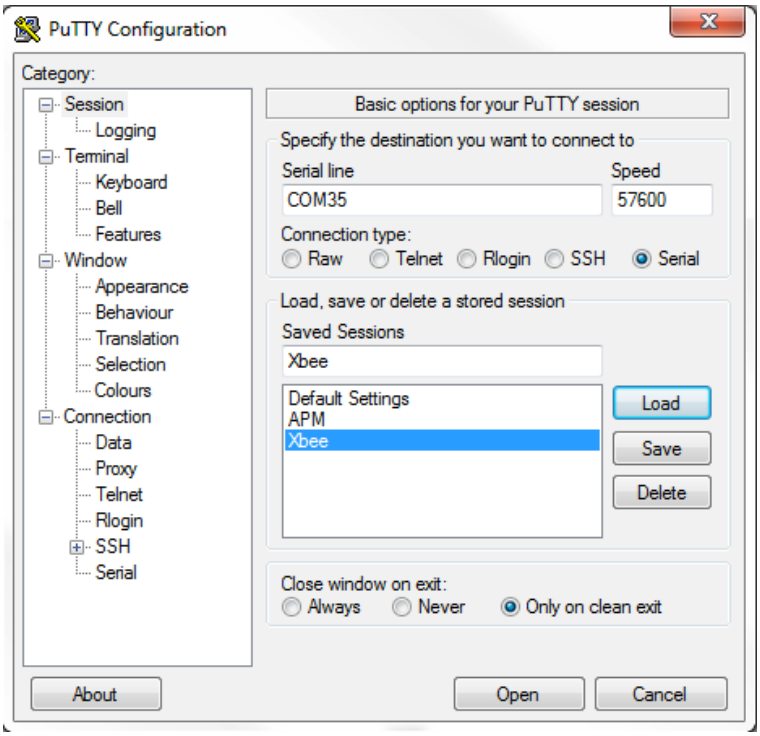

Figure B.1: Setting up the right serial port and baud rate for reading data via 2.4 GHz XBee module

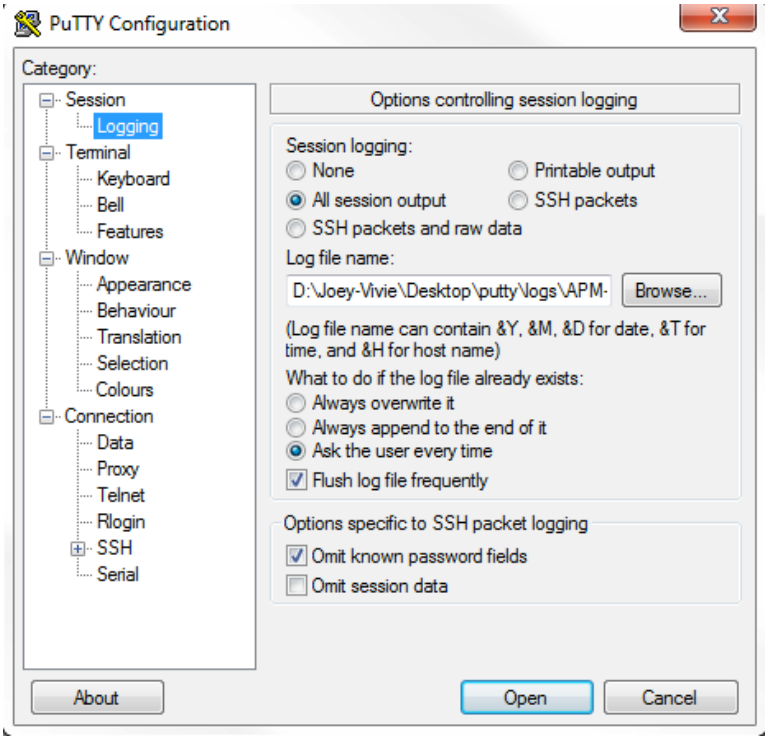

Figure B.2: Setting up the logging file path for raw sensor data reading

APPENDIX E: The ArduPilot Mega schematic

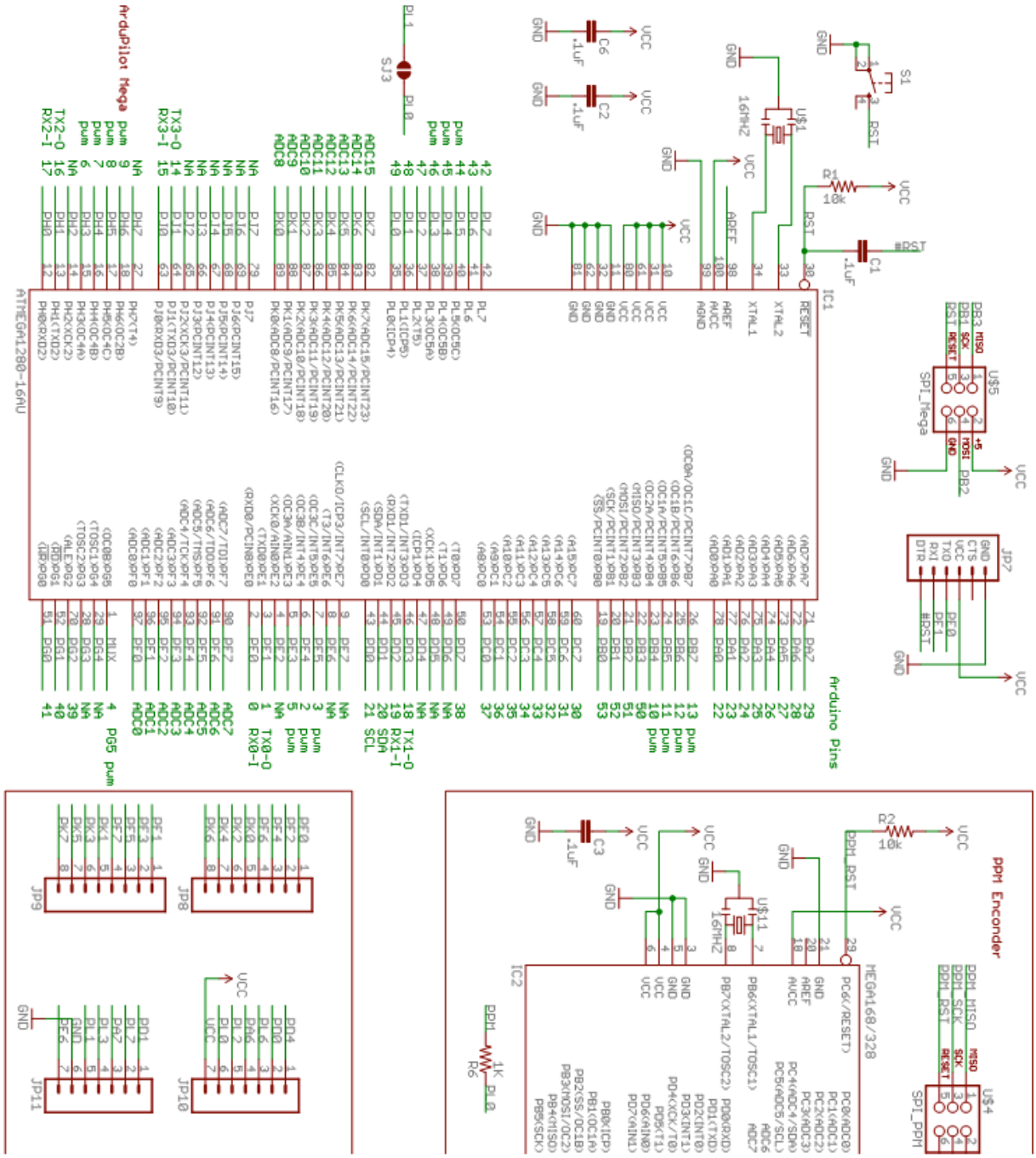

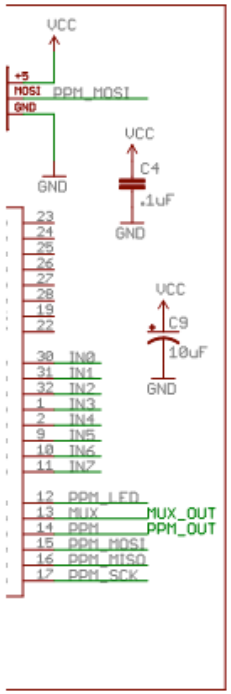
VCC
+5
MOSI PPM_MOSI
GND
C4
.1uF
C9
10uF
IN0
IN1
IN2
IN3
IN4
IN5
IN6
IN7
PPM_LED
MUX
PPM
PPM_MOSI
PPM_MISO
PPM_SCK
MUX_OUT
PPM_OUT

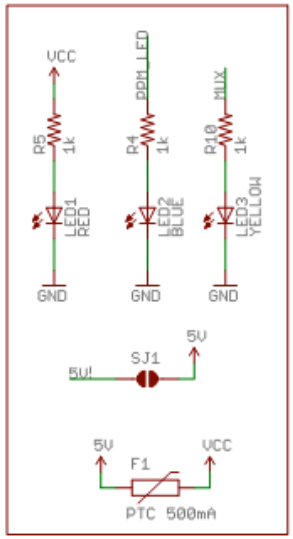
VCC
R5 1k
R4 1k
R10 1k
PPM_LED
MUX
LED1 RED
LED2 BLUE
LED3 YELLOW
SJ1
5V
5V!
F1
PTC 500mA

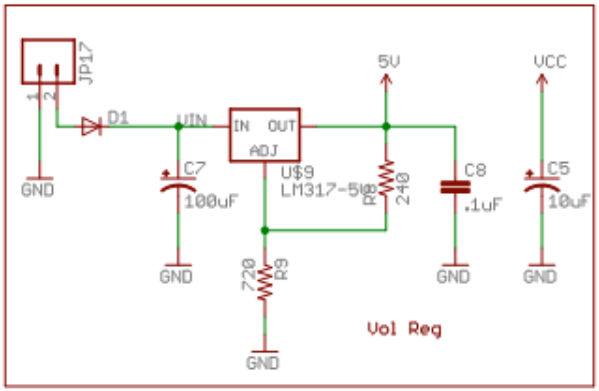
JP17
D1
VIN
IN OUT
ADJ
U$9
LM317-5V0
C7
100uF
C8
.1uF
C5
10uF
240
720
R9
5V
VCC
Vol Reg

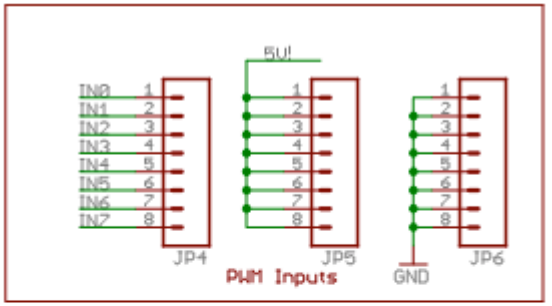
5V!
IN0
IN1
IN2
IN3
IN4
IN5
IN6
IN7
JP4
JP5
JP6
PWM Inputs

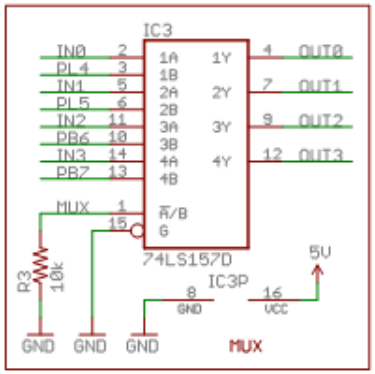
IC3
IN0
PL4
IN1
PL5
IN2
PB6
IN3
PB7
MUX
1A
1B
2A
2B
3A
3B
4A
4B
1Y
2Y
3Y
4Y
G
OUT0
OUT1
OUT2
OUT3
74LS157D
IC3P
R3 10k
MUX

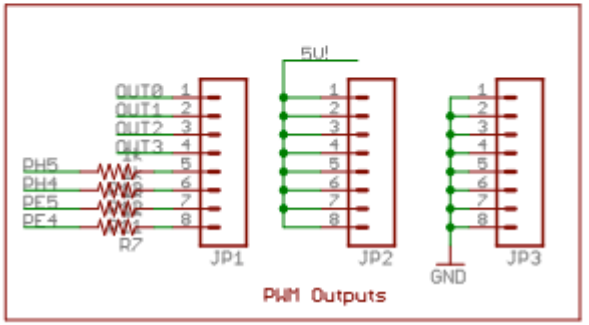
5V!
OUT0
OUT1
OUT2
OUT3
PH5
PH4
PE5
PE4
R7
JP1
JP2
JP3
PWM Outputs

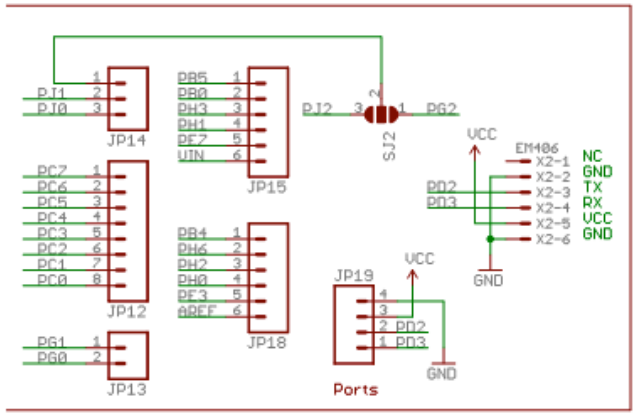
PJ1
PJ0
JP14
PC7
PC6
PC5
PC4
PC3
PC2
PC1
PC0
JP12
PG1
PG0
JP13
PB5
PB0
PH3
PH1
PE7
VIN
JP15
PB4
PH6
PH2
PH0
PE3
AREF
JP18
PJ2
PG2
SJ2
JP19
PD2
PD3
VCC
EM406
X2-1 NC
X2-2 GND
X2-3 TX
X2-4 RX
X2-5 VCC
X2-6 GND
Ports

APPENDIX F: The ArduPilot Mega IMU shield schematic

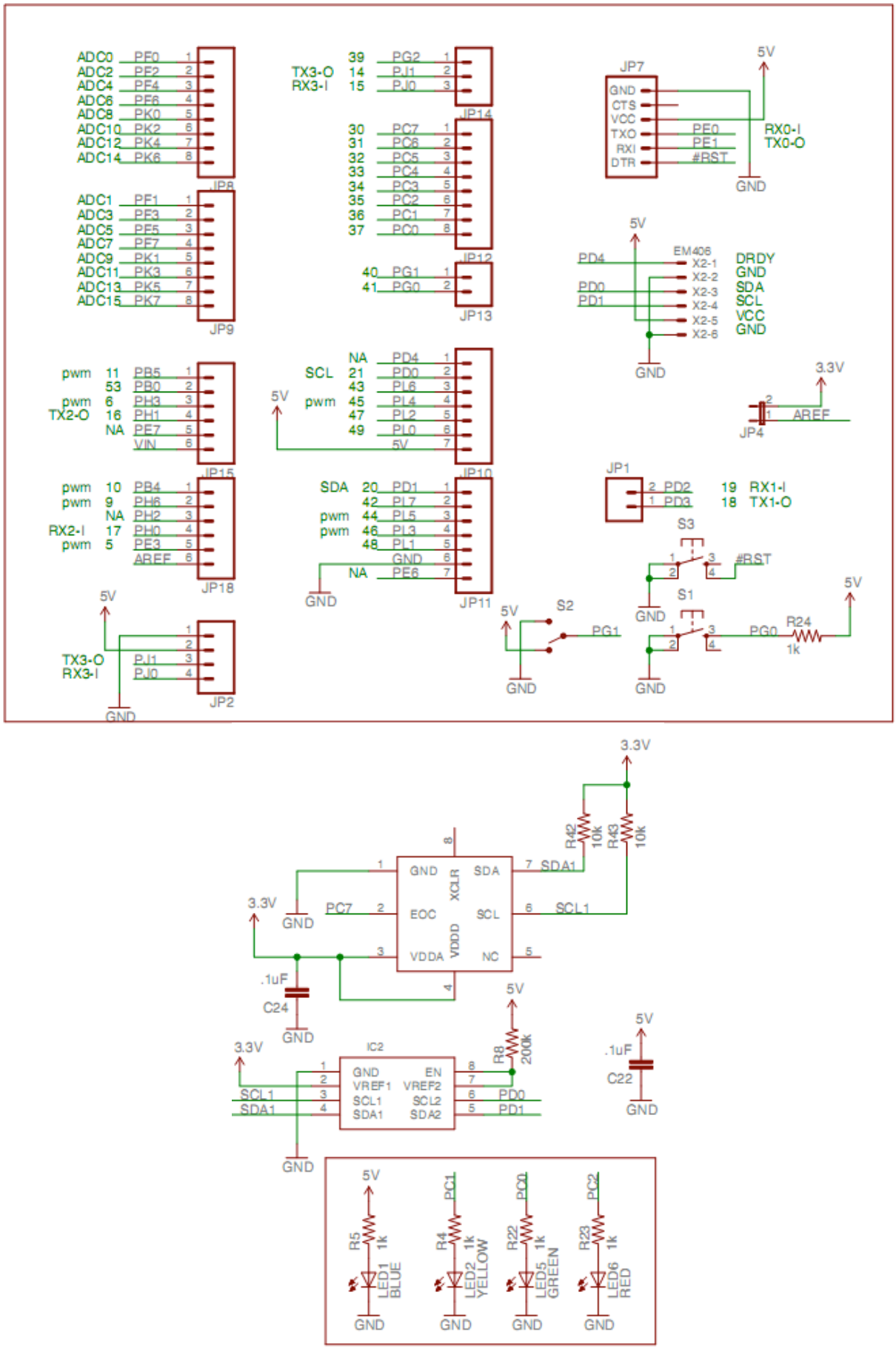

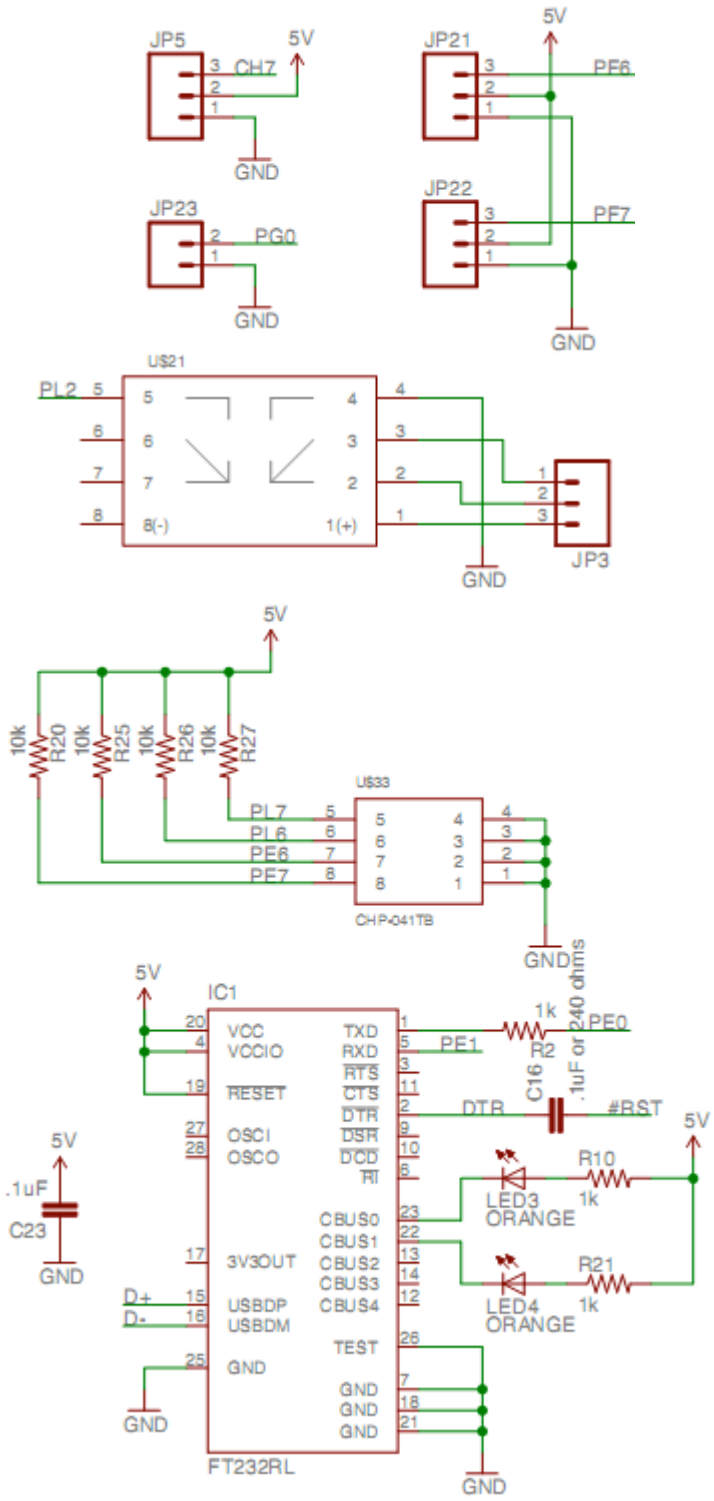
JP5
5V
3
CH7
2
1
GND
JP21
5V
3
PF6
2
1
JP22
3
PF7
2
1
GND
JP23
2
PG0
1
GND
U$21
PL2
5
6
7
8
8(-)
1(+)
4
3
2
1
JP3
GND
5V
10k
R20
10k
R25
10k
R26
10k
R27
U$33
PL7
PL6
PE6
PE7
CHP-041TB
GND
5V
IC1
VCC
VCCIO
RESET
OSCI
OSCO
3V3OUT
USBDP
USBDM
GND
TXD
RXD
RTS
CTS
DTR
DSR
DCD
RI
CBUS0
CBUS1
CBUS2
CBUS3
CBUS4
TEST
GND
GND
GND
FT232RL
D+
D-
1k
R2
PE1
PE0
C16
.1uF or 240 ohms
DTR
#RST
5V
R10
1k
LED3
ORANGE
R21
1k
LED4
ORANGE
5V
.1uF
C23
GND
GND
GND

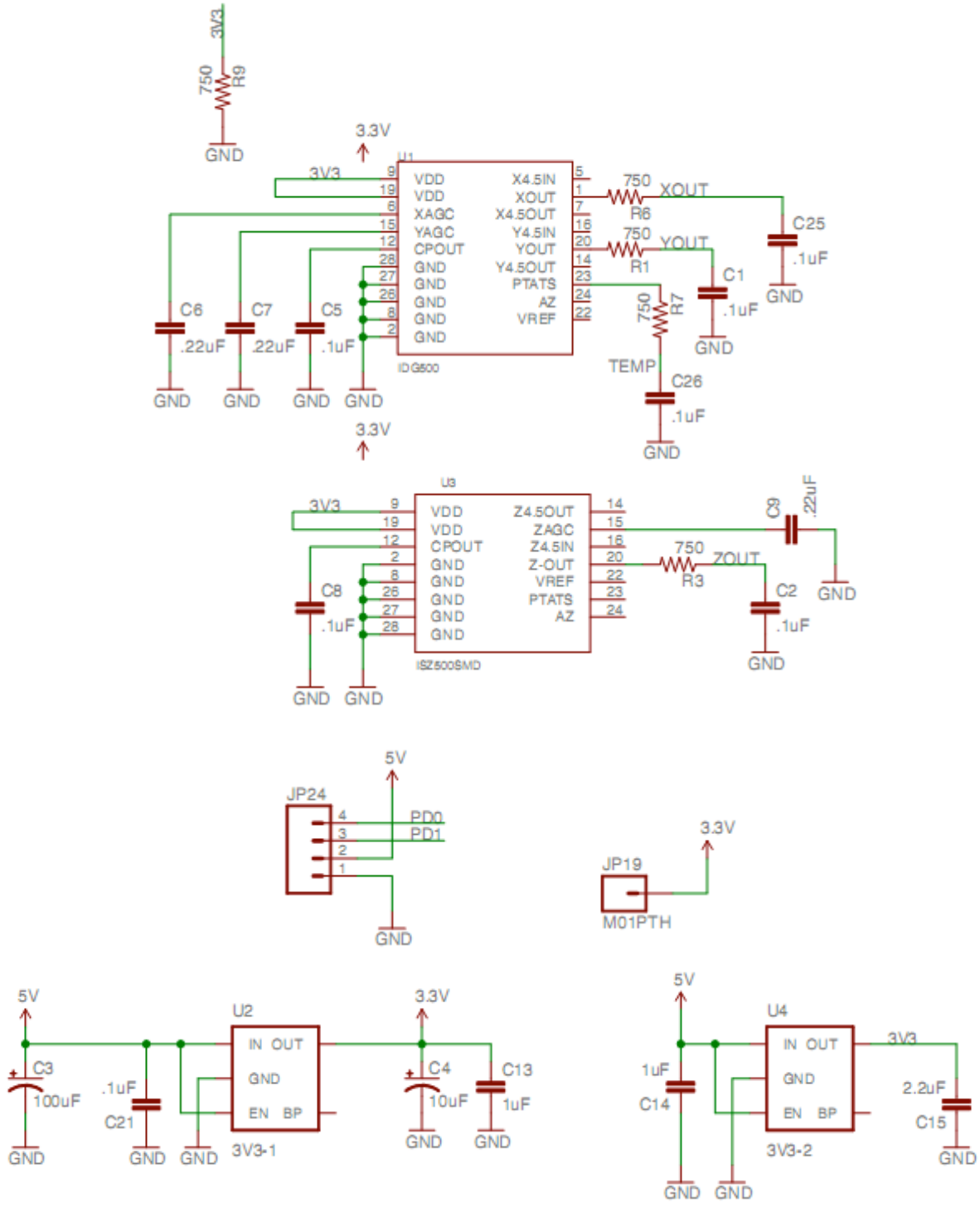
3V3
750
R9
GND
3.3V
U1
3V3
VDD
VDD
XAGC
YAGC
CPOUT
GND
GND
GND
GND
GND
X4.5IN
XOUT
X4.5OUT
Y4.5IN
YOUT
Y4.5OUT
PTATS
AZ
VREF
IDG500
750
R6
XOUT
C25
.1uF
750
R1
YOUT
C1
.1uF
750
R7
TEMP
C26
.1uF
C6
.22uF
C7
.22uF
C5
.1uF
U3
3V3
VDD
VDD
CPOUT
GND
GND
GND
GND
GND
Z4.5OUT
ZAGC
Z4.5IN
Z-OUT
VREF
PTATS
AZ
ISZ500SMD
C9
.22uF
750
R3
ZOUT
C2
.1uF
C8
.1uF
5V
JP24
PD0
PD1
JP19
3.3V
M01PTH
5V
U2
IN OUT
GND
EN BP
3V3-1
C3
100uF
.1uF
C21
3.3V
C4
10uF
C13
1uF
5V
U4
IN OUT
GND
EN BP
3V3-2
3V3
1uF
C14
2.2uF
C15
GND

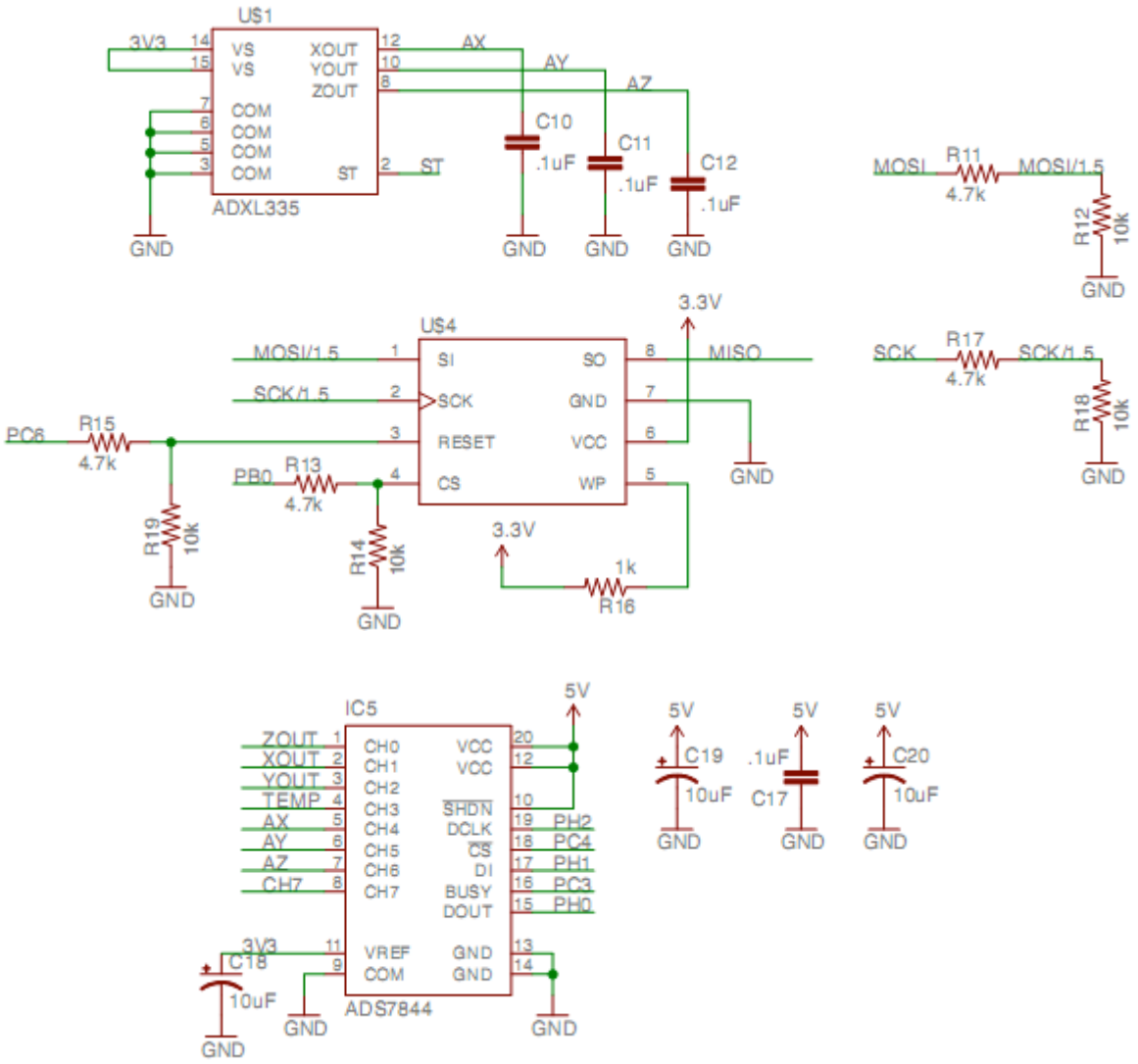
U$1
3V3
VS
VS
XOUT
YOUT
ZOUT
COM
COM
COM
COM
ST
ADXL335
AX
AY
AZ
ST
C10
.1uF
C11
.1uF
C12
.1uF
GND
MOSI
R11
4.7k
MOSI/1.5
R12
10k
U$4
MOSI/1.5
SCK/1.5
SI
SCK
RESET
CS
SO
GND
VCC
WP
MISO
3.3V
PC6
R15
4.7k
PB0
R13
4.7k
R19
10k
R14
10k
1k
R16
SCK
R17
4.7k
SCK/1.5
R18
10k
IC5
ZOUT
XOUT
YOUT
TEMP
AX
AY
AZ
CH7
CH0
CH1
CH2
CH3
CH4
CH5
CH6
CH7
VCC
VCC
SHDN
DCLK
CS
DI
BUSY
DOUT
VREF
COM
GND
GND
PH2
PC4
PH1
PC3
PH0
5V
3V3
C18
10uF
ADS7844
C19
10uF
C17
.1uF
C20
10uF

APPENDIX G: The ArduPilot Mega IMU shield circuit board layout